

Design, Synthesis and Biological Evaluation of Phenanthridine Amide and 1,2,3-Triazole Analogues against *Mycobacterium tuberculosis*

Adinarayana Nandikolla,^[a] Yogesh Mahadu Khetmalis,^[a] Boddupalli Venkata Siva kumar,^[a] Ala Chandu,^[b] Banoth Karan Kumar,^[b] Gauri Shetye,^[c] Rui Ma,^[c] Sankaranarayanan Murugesan,^[b] Scott G. Franzblau,^[c] Kondapalli Venkata Gowri Chandra Sekhar*^[a]

^a*Department of Chemistry, Birla Institute of Technology and Science, Pilani, Hyderabad Campus, Jawahar Nagar, Kapra Mandal, Hyderabad – 500078, Telangana, India.*

^b*Medicinal Chemistry Research Laboratory, Department of Pharmacy, Birla Institute of Technology and Science Pilani, Pilani Campus, Pilani-333031, Rajasthan. India.*

^c*Institute for Tuberculosis Research, College of Pharmacy, University of Illinois at Chicago, 833 South Wood Street, Chicago, IL 60612. USA*

Contents:	Page
1. Materials and methods	2
2. General procedure and analytical data	2
3. Biological Procedures	12
4. Molecular docking study	14
5. ¹ HNMR, ¹⁹ F NMR, ¹³ C NMR and Mass Spectras (including HRMS)	24
6. References	94

Experimental section:

*Corresponding author

Tel.: +91 40 66303527; E-mail: kvgc@hyderabad.bits-pilani.ac.in; kvgcs.bits@gmail.com

1. Materials and methods

All chemical reagents and solvents are purchased from Aldrich, Alfa Aesar, Finar. The solvents and reagents were of LR grade. All the solvents were dried and distilled before use. Thin-layer chromatography (TLC) was carried out on aluminium-supported silica gel plates (Merck 60 F254) with visualization of components by UV light (254 nm). Column chromatography was carried out on silica gel (Merck 100-200 mesh). ¹H NMR and ¹³C NMR spectra were recorded at 400 MHz and 101 MHz respectively using a Bruker AV 400 spectrometer (Bruker CO., Switzerland) in CDCl₃ and DMSO-*d*₆ solution with tetramethylsilane as the internal standard and chemical shift values (δ) were given in ppm. ¹H NMR spectra were recorded in CDCl₃ or DMSO-*d*₆. The following abbreviations are used to designate multiplicities: s = singlet, d = doublet, t = triplet, m = multiplet, br = broad. Melting points were determined on an electro thermal melting point apparatus (Stuart-SMP30) in open capillary tubes and are uncorrected. Elemental analyses were performed by ElementarAnalysensysteme GmbH vario MICRO cube CHN Analyzer. Mass spectra (ESI-MS) were recorded on Shimadzu MS/ESI mass spectrometer.

2. General procedure for preparation of intermediates

Compound **1** (1 eq) was taken in ethanol, water then Sodium acetate (2 eq), Hydroxylamine hydrochloride (2 eq) was added and stirred for 2h at 90 °C. The reaction was monitored by TLC. After completion of reaction, the formed solid was filtered off. Compound **2** with yielded 96% and confirmed with mass data (plae green). Compound **2** (1eq) was taken in polyphosphoric acid (10 V) then added Phosphorus pentoxide (0.5 eq) and stirred at 150 °C overnight. The reaction was monitored by TLC. After completion of reaction, the total reaction mixture was poured into ice cool water. The formed solid was filtered off. The formed solid was dissolved in ethyl acetate and workup with sodium bicarbonate after that organic layer was washed with brine solution then dried over anhydrous sodium sulphate. The organic layer was evaporated and yielded Compound **3** with 94% and confirmed with mass data (brown solid).

Compound **3** (1 eq) was taken in phosphorus oxychloride (6 eq) then added *N, N*-dimethylaniline (0.5 eq) at 0 °C and after that stirred at 100 °C overnight. The reaction was monitored by TLC. After completion of reaction, the total reaction mixture was evaporated under reduced pressure. The crude was dissolved in excesses ethyl acetate then added water. The organic layer was separated and washed with sodium bicarbonate and

brine solution then dried over anhydrous sodium sulphate and evaporated under reduced pressure. The crude was purified by silica gel column chromatography by eluting with 0-25% Ethyl acetate: petroleum ether. The compound **4** was yielded 96% and confirmed with mass data.

Compound **4** (1 eq) was taken in DMF then K_2CO_3 (5 eq) and 4-methoxy benzyl amine (3 eq) was added and stirred at 150 °C overnight. The reaction was monitored by TLC. After completion of reaction. The crude was dissolved in excesses ethyl acetate then added water. The organic layer was separated and washed with brine solution then dried over anhydrous sodium sulphate and evaporated under reduced pressure. The crude was purified by silica gel column chromatography by eluting with 0-15% Ethyl acetate: petroleum ether. The compound **5** was yield 90% and confirmed with mass data.

Compound **5** (1 eq) was taken in TFA (6 V) at 25 °C and overnight stirring. The reaction was monitored by TLC. After completion of reaction, the total reaction mixture was evaporated under reduced pressure. The crude was washed with pentane and dissolved in water then added saturated potassium carbonate. The compound was extracted with excesses ethyl acetate. The organic layer was washed with brine solution than the organic layer dried over anhydrous sodium sulphate and evaporated under reduced pressure. The compound **PA-01** was yielded 96% confirmed with mass data.

General procedure for the synthesis of titled compounds PA-02 to PA-14:

Alkyl / different substituted aryl acids (1.1 eq) were taken in DMF then DIPEA (3 eq) was added at 25 °C to this total reaction mixture was added HOBT (1.5 eq) and EDC.HCl (1.5 eq) and then added Compound **PA-01** (1 eq) at 25 °C and stirred for 5h. The reaction was monitored by TLC. After completion of reaction, the total reaction mixture was extracted with ethyl acetate and water. The organic layer was evaporated under reduced pressure. The crude was purified with silica gel column chromatography by eluting with 0-50% ethyl acetate: petroleum ether. The % yields of final compounds **PA-02 to PA-14** ranged from 60-80%.

General procedure for synthesis of compounds PT-01 to PT-11

Synthesis of compound 6:

Compound **PA-01** (1 equ.) was taken in dioxane then added ethyl 2-chloroacetoacetate (3 equ.) at 25 °C. The reaction mixture was heated to 100 °C and then allowed for overnight stirring. The reaction was monitored by TLC. After completion of reaction, the total reaction mixture was extracted with excess ethyl acetate. The organic layer was washed with brine solution, separated and dried over anhydrous sodium sulphate and evaporated under reduced pressure. The crude product was purified with silica gel column chromatography by eluting with 0- 20% ethyl acetate and pet ether. The compound **6** was obtained in 79% yield. T02 was confirmed with mass and NMR spectra's.

Synthesis of compound 7:

Compound **6** (1 equ.) was taken in ethanolic water mixture then LiOH (5 equ.) was added at 25 °C. The total reaction mixture was heated to 80 °C and stirred for 5 h. The reaction was monitored by TLC. After completion of reaction, the reaction mixture was evaporated under reduced pressure. The crude product was washed with ethyl acetate (2X). The obtained compound was dissolved in water, and pH was adjusted to 7 by the addition of saturated citric acid. The precipitated compound was filtered under vacuum. The compound **7** was obtained in 75% yield confirmed with mass and NMR spectra's.

Synthesis of compound PT-01:

Compound **7** (1 equ.) was taken in DMF then DIPEA (3 equ.) was added at 25 °C. To this reaction mixture HOBT (1.5 equ.), EDC.HCl (1.5 equ.) and then propargylamine (1.1 equ.) was added. The mixture was stirred at 25 °C for 5 h. The reaction was monitored by TLC. After completion of reaction, the reaction mixture was extracted with ethyl acetate. The organic layer was dried over anhydrous sodium sulphate and evaporated under reduced pressure. The crude product was purified with silica gel column chromatography by eluting with 0-50% ethylacetate: pet ether. The compound **PT-01** obtained in 80% yield and confirmed with mass and NMR spectra's.

Synthesis of Compounds PT-02 to PT-11:

Compound **PT-01** (1 equ.) was taken in DMF: t-BuOH: water then CuSO₄ (5 mol %), CuI (5 mol %), sodium ascorbate (1.5 equ.) was added at 25 °C. To this reaction mixture substituted azides (1.1 equ.) was added and stirred at 25 °C for 5 h. The reaction was monitored by TLC. After completion of reaction, the total reaction mixture was extracted with ethyl acetate. The organic layer was dried over anhydrous sodium sulphate

and evaporated under reduced pressure. The crude product was purified with silica gel column chromatography by eluting with 0-100% ethylacetate: pet ether. The triazoles **PT-02-PT-11** were confirmed with mass data and NMR data.

Analytical data for the titled compounds

Phenanthridin-6-amine (PA-01): Yellow solid (91 %), M.P.: 188-190 °C. ¹H NMR (400 MHz, DMSO-*d*₆) δ 9.53 (s, 2H), 8.80 (d, *J* = 8.0 Hz, 1H), 8.67 – 8.62 (dd, *J* = 8.3, 6.9 Hz, 2H), 8.14 – 8.08 (m, 1H), 7.91 – 7.85 (m, 1H), 7.75 – 7.69 (m, 2H), 7.56 (t, 1H).; ¹³C NMR (101 MHz, DMSO-*d*₆) δ 170.99, 162.78, 156.04, 145.51, 140.89, 133.87, 131.00, 129.19, 127.50, 126.07, 125.02, 122.89, 122.27, 120.67, 119.12, 117.83, 115.26, 113.50. ESI-MS: (*m/z*) calcd for C₁₃H₁₀N₂:194.24; found: 195 [M+H]⁺; HRMS: (*m/z*) calcd for C₁₃H₁₀N₂: 194.08 found 195.0814 (M+H)⁺; Anal. calcd for C₁₃H₁₀N₂: (%) C, 80.39; H, 5.19; N, 14.42; found: C, 80.34; H, 5.23; N, 14.37.

***N*-(phenanthridin-6-yl)-hexanamide (PA-02):**

Off-white solid (80 %), M.P.: 137-140 °C. ¹H NMR (400 MHz, DMSO-*d*₆) δ 10.61 (s, 1H), 8.91 (d, *J* = 8.3 Hz, 1H), 8.83 (d, *J* = 7.3 Hz, 1H), 8.19 (d, *J* = 7.8 Hz, 1H), 8.05 – 7.97 (m, 2H), 7.86 – 7.80 (m, 2H), 7.79 – 7.72 (m, 1H), 2.61 (t, *J* = 7.5 Hz, 2H), 1.79 – 1.68 (m, 2H), 1.49 – 1.35 (m, 4H), 0.99 – 0.92 (m, 3H).; ¹³C NMR (101 MHz, DMSO-*d*₆) δ 174.13, 150.52, 143.03, 134.18, 131.93, 131.72, 129.64, 129.01, 128.13, 127.34, 123.68, 123.11, 122.71, 36.11, 31.63, 28.85, 25.47, 22.51, 14.42.; ESI-MS: (*m/z*) calcd for C₁₉H₂₀N₂O: 292.16, found: 293[M+H]⁺; HRMS: (*m/z*) calcd for C₁₉H₂₀N₂O: 292.16,found 293.2018 (M+H)⁺; Anal. calcd for C₁₉H₂₀N₂O: (%) C, 78.05; H, 6.90; N, 9.58; found: C, 78.00; H, 6.86; N, 9.53.

***N*-(phenanthridin-6-yl)-octanamide (PA-03):**

Off-white solid (75 %), M.P.: 113-116 °C. ¹H NMR (400 MHz, DMSO-*d*₆) δ 10.61 (s, 1H), 8.91 (d, *J* = 8.3 Hz, 1H), 8.84 (d, *J* = 7.4 Hz, 1H), 8.19 (d, *J* = 8.0 Hz, 1H), 8.03 (dd, *J* = 2.2, 1.3 Hz, 1H), 8.02 – 8.00 (m, 1H), 7.85 – 7.80 (m, 2H), 7.78 – 7.73 (m, 1H), 2.62 (t, *J* = 7.5 Hz, 2H), 1.79 – 1.68 (m, 2H), 1.43 – 1.39 (m, 2H), 1.37 – 1.32 (m, 4H), 1.31 (d, *J* = 6.7 Hz, 2H), 0.94 (dd, *J* = 9.1, 4.9 Hz, 3H).; ¹³C NMR (101 MHz, DMSO-*d*₆) δ 174.10, 150.56, 143.01, 134.15, 131.91, 129.64, 129.05, 128.10, 127.31, 123.71, 123.08, 122.68, 36.07, 31.60, 28.87, 25.44, 22.49, 14.39. ESI-MS: (*m/z*) calcd for C₂₁H₂₄N₂O: 320.19, found: 321 [M+H]⁺; Anal. calcd for C₂₁H₂₄N₂O: (%) C, 78.71; H, 7.55; N, 8.74; found: C, 78.66; H, 7.58; N, 8.71.

***N*-(phenanthridin-6-yl)-pyrazine-2-carboxamide (PA-04):**

Pale brown solid (70 %), M.P.: 115-118 °C. ¹H NMR (400 MHz, DMSO-*d*₆) δ 11.46 (s, 1H), 9.40 (s, 1H), 9.03 (d, *J* = 2.4 Hz, 1H), 8.96 (d, *J* = 8.2 Hz, 1H), 8.93 (dd, *J* = 2.5, 1.5 Hz, 1H), 8.89 (d, *J* = 7.6 Hz, 1H), 8.40 – 8.25 (m, 1H), 8.09 – 8.05 (m, 2H), 7.86 (dd, *J* = 11.1, 8.5, Hz, 3H).; ¹³C NMR (101 MHz, DMSO-*d*₆) δ 176.82, 167.06, 165.01, 160.97, 158.72, 153.00, 152.26, 148.38, 144.56, 144.16, 134.23, 132.27, 129.83, 128.50, 127.81, 127.13, 123.29, 123.09. ESI-MS: (*m/z*) calcd for C₁₈H₁₂N₄O: 300.10, found: 301 [M+H]⁺; Anal. calcd for C₁₈H₁₂N₄O: (%) C, 71.99; H, 4.03; N, 18.66; found: C, 71.95; H, 4.09; N, 18.60.

***N*-(phenanthridin-6-yl)-pent-4-ynamide (PA-05):**

Off-white solid (82 %), M.P.: 160-163 °C. ¹H NMR (400 MHz, DMSO-*d*₆) δ 10.72 (s, 1H), 8.91 (d, *J* = 8.3 Hz, 1H), 8.84 (d, *J* = 7.7 Hz, 1H), 8.28 (d, *J* = 8.1 Hz, 1H), 8.02 (dd, *J* = 9.5, 6.5, Hz, 2H), 7.87 – 7.74 (m, 3H), 2.96 (t, *J* = 2.6 Hz, 1H), 2.85 (dd, *J* = 9.2, 5.3 Hz, 2H), 2.61 (dd, *J* = 7.2, 2.6 Hz, 2H).; ¹³C NMR (101 MHz, DMSO-*d*₆) δ 172.01, 156.03, 150.48, 143.05, 134.19, 131.83, 130.06, 129.33, 128.01, 127.53, 127.24, 126.01, 125.04, 123.77, 123.13, 122.91, 122.58, 122.40, 84.29, 72.07, 35.14, 14.53. ESI-MS: (*m/z*) calcd for C₁₈H₁₄N₂O: 274.11, found: 275 [M+H]⁺; HRMS: (*m/z*) calcd for, C₁₈H₁₄N₂O: 274.11, found 275.1321 (M+H)⁺; Anal. calcd for C₁₈H₁₄N₂O: (%) C, 78.81; H, 5.14; N, 10.21; found: C, 78.78; H, 5.19; N, 10.25.

***4*-amino-*N*-(phenanthridin-6-yl)-benzamide (PA-06):**

Pale Yellow solid (78 %), M.P.: 83-86 °C. ¹H NMR (400 MHz, DMSO-*d*₆) δ 10.66 (s, 1H), 8.71 (d, *J* = 8.0 Hz, 3H), 8.52 (d, *J* = 7.9 Hz, 2H), 8.40 (d, *J* = 7.5 Hz, 2H), 7.10 (d, *J* = 8.3 Hz, 3H), 6.70 (d, *J* = 8.4 Hz, 3H), 5.92 (s, 3H).; ¹³C NMR (101 MHz, DMSO-*d*₆) δ 167.81, 149.74, 142.87, 140.62, 139.76, 134.25, 132.02, 131.64, 129.71, 129.18, 128.95, 128.58, 128.22, 127.48, 127.24, 123.79, 123.25, 123.05, 122.53, 93.72.; ESI-MS: (*m/z*) calcd for C₂₀H₁₅N₃O: 313.12, found: 314 [M+H]⁺; Anal. calcd for C₂₀H₁₅N₃O: (%) C, 76.66; H, 4.83; N, 13.41; found: C, 76.63; H, 4.87; N, 13.37.

***3*-chloro-*N*-(phenanthridin-6-yl)-benzamide (PA-07)**

Off-white solid (86 %), M.P.: 163-166 °C. ¹H NMR (400 MHz, DMSO-*d*₆) δ 11.31 (s, 1H), 8.87 (s, 3H), 8.38 – 8.35 (m, 1H), 8.10 – 8.03 (m, 2H), 7.87 (dd, *J* = 13.7, 6.8 Hz, 2H), 7.79 – 7.74 (m, 2H), 7.68 (dd, *J* = 14.3, 6.5 Hz, 2H).; ¹³C NMR (101 MHz, DMSO-*d*₆) δ 164.14, 158.59, 156.23,

134.22, 133.37, 132.67, 131.35, 131.10, 130.00, 129.16, 128.51, 127.54, 126.92, 125.87, 125.07, 124.28, 123.72, 123.33, 123.16, 122.98, 122.29, 120.65, 119.11, 118.98. ESI-MS: (m/z) calcd for $C_{20}H_{13}ClN_2O$: 332.07, found: 333 $[M+H]^+$; Anal. calcd for $C_{20}H_{13}ClN_2O$: (%) C, 72.18; H, 3.94; Cl, 10.65; N, 8.42; found: C, 72.14; H, 3.97; Cl, 10.62; N, 8.46.

2-iodo-N-(phenanthridin-6-yl)-benzamide (PA-08):

Off-white solid (80 %), M.P.: 188-191 °C. 1H NMR (400 MHz, DMSO- d_6) δ 11.27 (s, 1H), 8.95 (d, $J = 8.3$ Hz, 1H), 8.85 (d, $J = 7.9$ Hz, 1H), 8.55 (d, $J = 8.3$ Hz, 1H), 8.04 (dd, $J = 16.3, 7.8$ Hz, 2H), 7.95 (d, $J = 7.8$ Hz, 1H), 7.88 (t, $J = 7.6$ Hz, 1H), 7.82 (t, $J = 7.3$ Hz, 1H), 7.80 – 7.74 (m, 1H), 7.74 – 7.68 (m, 1H), 7.62 – 7.54 (m, 1H), 7.30 (t, $J = 7.8, 4.0$ Hz, 1H).; ^{13}C NMR (101 MHz, DMSO- d_6) δ 167.86, 149.72, 142.90, 140.58, 139.73, 134.23, 132.06, 131.63, 129.68, 129.13, 128.97, 128.55, 128.27, 127.50, 127.20, 123.75, 123.21, 123.09, 122.51, 93.83.; ESI-MS: (m/z) calcd for $C_{20}H_{13}IN_2O$: 424.01, found: 425 $[M+H]^+$; Anal. calcd for $C_{20}H_{13}IN_2O$: (%) C, 56.62; H, 3.09; I, 29.91; N, 6.60; found: C, 56.64; H, 3.04; I, 30.03; N, 6.65.

N-(phenanthridin-6-yl)-cinnamamide (PA-09):

Pale Yellow solid (87 %), M.P.: 183-187 °C. 1H NMR (400 MHz, DMSO- d_6) δ 10.95 (s, 1H), 8.92 (t, $J = 10.0$ Hz, 1H), 8.86 (d, $J = 8.0$ Hz, 1H), 8.25 (d, $J = 8.1$ Hz, 1H), 8.03 (t, $J = 8.0$ Hz, 2H), 7.87 – 7.82 (m, 2H), 7.78 (t, $J = 5.7$ Hz, 1H), 7.76 – 7.71 (m, 3H), 7.55 – 7.50 (m, 3H), 7.19 (d, $J = 15.8$ Hz, 1H).; ^{13}C NMR (101 MHz, DMSO- d_6) δ 166.05, 150.58, 143.13, 141.55, 138.05, 135.19, 134.24, 131.88, 130.43, 129.59, 129.09, 128.61, 128.23, 127.48, 127.34, 125.05, 123.78, 123.33, 123.18, 122.54, 122.01. ESI-MS: (m/z) calcd for $C_{22}H_{16}N_2O$: 324.13, found: 325 $[M+H]^+$; Anal. calcd for $C_{22}H_{16}N_2O$: (%) C, 81.46; H, 4.97; N, 8.64; found: C, 81.50; H, 4.94; N, 8.60.

4-(1H-indol-3-yl)-N-(phenanthridin-6-yl)-butanamide (PA-10):

Off-white solid (75 %), M.P.: 180-183 °C. 1H NMR (400 MHz, DMSO- d_6) δ 10.85 (s, 1H), 10.64 (s, 1H), 8.91 (d, $J = 8.3$ Hz, 1H), 8.83 (d, $J = 7.4$ Hz, 1H), 8.21 (t, $J = 8.3$ Hz, 1H), 8.06 – 7.96 (m, 2H), 7.85 – 7.79 (m, 2H), 7.78 – 7.71 (m, 1H), 7.61 (d, $J = 8.0$ Hz, 1H), 7.40 (d, $J = 8.1$ Hz, 1H), 7.23 (d, $J = 2.2$ Hz, 1H), 7.12 (t, $J = 4.3, 2.1$ Hz, 1H), 7.05 – 7.00 (m, 1H), 2.91 – 2.84 (m, 2H), 2.71 (t, $J = 7.4$ Hz, 2H), 2.15 – 2.10 (m, 2H).; ^{13}C NMR (101 MHz, DMSO- d_6) δ 172.24, 155.69, 145.21, 136.59, 133.91, 131.72, 131.04, 129.41, 129.04, 127.89, 127.54, 125.92, 125.01,

124.64, 122.95, 122.31, 120.68, 119.09, 111.91, 108.80, 33.49, 20.08; ESI-MS: (m/z) calcd for $C_{25}H_{21}N_3O$: 379.17, found: 380 $[M+H]^+$; Anal. calcd for $C_{25}H_{21}N_3O$: (%) C, 79.13; H, 5.58; N, 11.07; found: C, 79.17; H, 5.48; N, 11.12.

2-(1H-indol-3-yl)-N-(phenanthridin-6-yl)-acetamide (PA-11):

Brown solid (60 %), M.P.: 163-164 °C. 1H NMR (400 MHz, DMSO- d_6) δ 11.00 (s, 1H), 10.76 (s, 1H), 8.85 (dd, $J = 25.8, 8.1$ Hz, 2H), 8.71 (d, $J = 8.2$ Hz, 1H), 8.52 (d, $J = 8.0$ Hz, 1H), 8.39 (s, 1H), 7.97 (t, $J = 7.4$ Hz, 1H), 7.88 (d, $J = 7.5$ Hz, 1H), 7.82 (t, $J = 7.4$ Hz, 1H), 7.58 (t, $J = 7.5$ Hz, 3H), 7.14 (s, 2H), 4.06 (s, 2H).; ^{13}C NMR (101 MHz, DMSO- d_6) δ 172.27, 155.66, 145.25, 136.62, 133.88, 131.75, 131.02, 129.37, 129.07, 127.92, 127.55, 125.90, 125.06, 124.60, 122.99, 122.29, 120.65, 119.07, 111.88, 108.77, 33.47. ESI-MS: (m/z) calcd for $C_{23}H_{17}N_3O$: 351.14, found: 352 $[M+H]^+$; Anal. calcd for $C_{23}H_{17}N_3O$: (%) C, 78.61; H, 4.88; N, 11.96; found: C, 78.66; H, 4.83; N, 11.92.

N-(phenanthridin-6-yl)-2-phenylacetamide (PA-12):

Pale Yellow gummy solid (68 %). 1H NMR (400 MHz, DMSO- d_6) δ 8.75 – 8.68 (m, 1H), 8.53 (d, $J = 7.7$ Hz, 1H), 8.39 (t, $J = 7.5$ Hz, 1H), 7.96 – 7.87 (m, 2H), 7.76 – 7.70 (m, 1H), 7.68 – 7.63 (m, 1H), 7.58 (d, $J = 1.5$ Hz, 1H), 7.49 – 7.44 (m, 1H), 7.37 (dd, $J = 2.9, 1.8$ Hz, 1H), 7.35 (t, $J = 2.0$ Hz, 1H), 7.32 (d, $J = 2.1$ Hz, 2H), 7.30 (d, $J = 2.9$ Hz, 1H), 7.14 (s, 1H), 3.62 (s, 2H).; ^{13}C NMR (101 MHz, DMSO- d_6) δ 173.47, 155.81, 135.40, 131.79, 129.76, 129.50, 128.76, 127.94, 127.10, 125.59, 125.17, 125.09, 124.37, 123.08, 122.94, 118.80, 111.08, 42.82. ESI-MS: (m/z) calcd for $C_{21}H_{16}N_2O$: 312.13, found: 313 $[M+H]^+$; Anal. calcd for $C_{21}H_{16}N_2O$: (%) C, 80.75; H, 5.16; N, 8.97; found: C, 80.80; H, 5.19; N, 8.95.

2-(4-bromophenyl)-N-(phenanthridin-6-yl)-acetamide (PA-13):

Pale Yellow gummy solid (75 %). 1H NMR (400 MHz, DMSO- d_6) δ 10.91 (s, 1H), 8.91 (d, $J = 8.2$ Hz, 1H), 8.84 (d, $J = 8.0$ Hz, 1H), 8.72 (d, $J = 7.9$ Hz, 1H), 8.52 (d, $J = 8.0$ Hz, 1H), 8.40 (d, $J = 7.5$ Hz, 1H), 7.64 – 7.62 (m, 1H), 7.61 (d, $J = 2.0$ Hz, 2H), 7.57 (s, 1H), 7.55 (s, 1H), 7.29 (s, 1H), 7.27 (s, 1H), 3.97 (s, 2H).; ^{13}C NMR (101 MHz, DMSO- d_6) δ 174.32, 158.30, 151.09, 142.88, 134.38, 131.90, 129.71, 128.43, 127.51, 125.34, 124.33, 122.50, 119.65, 119.30, 110.78, 56.13, 37.59, 36.10, 31.76, 29.41. ESI-MS: (m/z) calcd for $C_{21}H_{15}BrN_2O$: 390.04, found: 391 $[M+H]^+$; Anal. calcd for $C_{21}H_{15}BrN_2O$: (%) C, 64.47; H, 3.86; Br, 20.42; N, 7.16; found: (%) C, 64.42; H, 3.91; Br, 20.45; N, 7.20.

3-amino-N-(phenanthridin-6-yl)-benzamide (PA-14):

Brown gummy solid (80 %). ¹H NMR (400 MHz, DMSO-*d*₆) δ 10.36 (s, 1H), 8.71 (d, *J* = 8.0 Hz, 2H), 8.52 (d, *J* = 7.9 Hz, 1H), 8.41 – 8.36 (m, 1H), 7.88 (dd, *J* = 8.2, 7.1, 1.2 Hz, 2H), 7.72 (dd, *J* = 8.2, 7.1, 1.1 Hz, 2H), 7.33 (d, *J* = 8.2, 6.3, 2.0 Hz, 2H), 7.07 (s, 1H), 5.39 (s, 2H).; ¹³C NMR (101 MHz, DMSO-*d*₆) δ 174.02, 155.77, 151.10, 146.05, 143.25, 137.58, 134.38, 133.72, 132.54, 131.25, 131.01, 129.75, 128.42, 127.13, 126.04, 125.03, 123.80, 123.21, 122.55, 121.31, 119.37, 118.54, 116.52, 114.56, 112.02, 45.71, 36.28, 27.16, 24.94. ESI-MS: (*m/z*) calcd for C₂₀H₁₅N₃O: 313.12, found: 314 [M+H]⁺; Anal. calcd for C₂₀H₁₅N₃O: (%) C, 76.66; H, 4.83; N, 13.41; found: C, 76.69; H, 4.87; N, 13.45.

2-methyl-N-(prop-2-yn-1-yl)-imidazo-[1,2-*f*]-phenanthridine-3-carboxamide (PT-01): Off-white solid (90 %), M.P.: 254-256 °C. ¹H NMR (400 MHz, DMSO-*d*₆) δ 9.37 (t, *J* = 5.6 Hz, 1H), 8.74 (dd, *J* = 8.1, 1.5 Hz, 1H), 8.67 (dd, *J* = 8.2, 0.9 Hz, 1H), 8.56 – 8.51 (m, 1H), 7.96 (dd, *J* = 8.4, 1.1 Hz, 1H), 7.79 – 7.70 (m, 2H), 7.68 – 7.57 (m, 2H), 4.21 (dd, *J* = 5.7, 2.5 Hz, 2H), 3.32 (t, *J* = 2.0 Hz, 1H), 2.46 (s, 3H). ¹³C NMR (101 MHz, DMSO-*d*₆) δ 162.42, 142.20, 131.76, 129.85, 129.37, 127.95, 125.82, 125.12, 124.39, 123.52, 122.84, 121.90, 121.31, 118.15, 81.00, 73.89, 29.08, 14.27. ESI-MS: (*m/z*) calcd for C₂₀H₁₅N₃O: 313.12; HRMS: (*m/z*) calcd for C₂₀H₁₅N₃O: 313.12; found 314.0895 (M+H)⁺; Anal. calcd for C₂₀H₁₅N₃O: (%) C, 76.66; H, 4.83; N, 13.41; found: C, 76.63; H, 4.85; N, 13.44.

N-((1-(4-ethylphenyl)-1H-1,2,3-triazol-4-yl)-methyl)-2-methylimidazo-[1,2-*f*]-phenanthridine-3-carboxamide (PT-02): Off-white solid (70 %), M.P.: 232-234 °C. ¹H NMR (400 MHz, DMSO-*d*₆) δ 9.40 (t, *J* = 5.2 Hz, 1H), 8.72 (dd, *J* = 8.1, 1.4 Hz, 1H), 8.66 – 8.64 (m, 1H), 8.54 (d, *J* = 1.2 Hz, 1H), 8.52 (d, *J* = 1.6 Hz, 1H), 7.93 (dd, *J* = 8.3, 1.2 Hz, 1H), 7.79 – 7.69 (m, 4H), 7.68 – 7.54 (m, 4H), 4.19 (dd, *J* = 5.7, 2.5 Hz, 2H), 3.26 (t, *J* = 2.5 Hz, 2H), 2.42 (s, 3H), 2.08 (s, 3H). ¹³C NMR (101 MHz, DMSO-*d*₆) δ 166.13, 162.54, 152.63, 146.14, 142.38, 137.59, 131.82, 129.83, 129.28, 127.96, 126.14, 125.14, 125.03, 124.29, 122.72, 122.59, 122.04, 121.64, 119.73, 118.38, 117.04, 35.09, 14.48. ESI-MS: (*m/z*) calcd for C₂₈H₂₄N₆O: 460.20; found: 461 [M+H]⁺; HRMS: (*m/z*) calcd for C₂₈H₂₄N₆O: 460.20; found 461.2315 (M+H)⁺; Anal. calcd for C₂₈H₂₄N₆O: (%) C, 73.02; H, 5.25; N, 18.25; found: C, 73.07; H, 5.29; N, 18.21.

2-methyl-N-((1-(4-(trifluoromethyl)-phenyl)-1H-1,2,3-triazol-4-yl)-methyl)-imidazo[1,2-*f*]-phenanthridine-3-carboxamide (PT-03): Off-white solid (75 %), M.P.: 216-218 °C. ¹H NMR (400 MHz, DMSO-*d*₆) δ 9.52 (s, 1H), 9.06 (s, 1H), 8.68 (dd, *J* = 22.6, 6.9 Hz, 2H), 8.34 (s, 2H), 8.25 (d, *J* = 10.8 Hz, 2H), 7.97 (t, *J* = 12.2 Hz, 2H), 7.72 (dd, *J* = 15.2, 7.4 Hz, 2H), 7.55 (s, 2H), 4.78 (s, 2H), 2.45 (s, 3H). ¹⁹F NMR (377 MHz, DMSO-*d*₆) δ - 61.26. ¹³C NMR (101 MHz, DMSO-*d*₆) δ 162.71, 153.06, 144.64, 142.95, 135.28, 132.10, (d, *J* = 272.7 Hz), 131.84, 131.64, 131.09, 129.02,

128.80, 128.04, 127.90, 125.92, 125.12, 124.65, 124.39, 123.46, 122.87, 121.73, 119.70, 118.35, 34.82, 14.88. ESI-MS: (m/z) calcd for $C_{27}H_{19}F_3N_6O$: 500.16; found: 501 $[M+H]^+$; Anal. calcd for $C_{27}H_{19}F_3N_6O$: (%) C, 64.80; H, 3.83; F, 11.39; N, 16.79; found: C, 64.83; H, 3.87; F, 11.35; N, 16.74.

N-((1-(2-chlorophenyl)-1H-1,2,3-triazol-4-yl)-methyl)-2-methylimidazo-[1,2-f]-phenanthridine-3-carboxamide (PT-04): Pale Brown solid (79 %), M.P.: 221-222 °C. 1H NMR (400 MHz, DMSO- d_6) δ 9.44 (t, 1H), 8.65 (dd, $J = 6.3, 3.4$ Hz, 1H), 8.59 (d, $J = 7.5$ Hz, 1H), 8.48 (s, 1H), 8.46 (dd, $J = 7.7, 1.4$ Hz, 1H), 7.95 – 7.91 (m, 1H), 7.73 (dd, $J = 7.8, 1.5$ Hz, 1H), 7.68 (d, $J = 1.4$ Hz, 1H), 7.66 (d, $J = 1.5$ Hz, 1H), 7.65 (d, $J = 1.8$ Hz, 1H), 7.63 (d, $J = 2.0$ Hz, 1H), 7.58 – 7.55 (m, 1H), 7.52 – 7.48 (m, 2H), 4.72 (d, $J = 5.7$ Hz, 2H), 2.37 (s, 3H). ^{13}C NMR (101 MHz, DMSO- d_6) δ 165.94, 162.56, 159.60, 144.83, 142.40, 142.12, 135.07, 132.09, 131.80, 131.08, 129.80, 129.76, 129.00, 127.95, 125.75, 125.03, 124.38, 123.51, 122.87, 121.87, 121.65, 118.34, 35.02, 14.44. ESI-MS: (m/z) calcd for $C_{26}H_{19}ClN_6O$: 466.13; found: 467 $[M+H]^+$; Anal. calcd for $C_{26}H_{19}ClN_6O$: (%) C, 66.88; H, 4.10; Cl, 7.59; N, 18.00; found: C, 66.83; H, 4.14; Cl, 7.63; N, 18.04.

2-methyl-N-((1-(3-nitrophenyl)-1H-1,2,3-triazol-4-yl)-methyl)-imidazo-[1,2-f]-phenanthridine-3-carboxamide (PT-05): Brown solid (85 %), M.P.: 201-203 °C. 1H NMR (400 MHz, DMSO- d_6) δ 9.43 (t, 1H), 8.96 (s, 1H), 8.64 – 8.59 (m, 1H), 8.56 (d, $J = 7.2$ Hz, 1H), 8.45 (d, $J = 8.5$ Hz, 1H), 8.25 (s, 1H), 7.90 – 7.85 (m, 1H), 7.89 – 7.83 (m, 2H), 7.61 (d, $J = 8.2$ Hz, 2H), 7.51 (dd, $J = 8.4, 1.9$ Hz, 3H), 4.73 (d, $J = 7.8$ Hz, 2H), 2.35 (s, 3H). ^{13}C NMR (101 MHz, DMSO- d_6) δ 162.53, 146.09, 142.37, 137.61, 133.763, 131.84, 131.22, 130.25, 130.04, 127.94, 125.73, 125.05, 124.33, 123.62, 122.81, 122.26, 121.90, 118.41, 117.83, 35.05, 14.51. ESI-MS: (m/z) calcd for $C_{26}H_{19}N_7O_3$: 477.15; found: 478 $[M+H]^+$; Anal. calcd for $C_{26}H_{19}N_7O_3$: (%) C, 65.40; H, 4.01; N, 20.53; found: C, 65.43; H, 3.98; N, 20.50,

N-((1-(4-methoxy-2-nitrophenyl)-1H-1,2,3-triazol-4-yl)-methyl)-2-methylimidazo-[1,2-f]-phenanthridine-3-carboxamide (PT-06): Brown solid (80 %), M.P.: 212-213 °C. 1H NMR (400 MHz, DMSO- d_6) δ 9.46 (t, $J = 5.4$ Hz, 1H), 8.64 (dd, $J = 10.6, 7.1$ Hz, 1H), 8.59 (d, $J = 7.8$ Hz, 1H), 8.53 (s, 1H), 8.46 (d, $J = 7.4$ Hz, 1H), 7.95 – 7.87 (m, 1H), 7.74 – 7.62 (m, 4H), 7.55 – 7.47 (m, 2H), 7.44 (dd, $J = 8.8, 2.5$ Hz, 1H), 4.69 (d, $J = 5.5$ Hz, 2H), 3.87 (d, $J = 6.9$ Hz, 3H), 2.35 (s, 3H). ^{13}C NMR (101 MHz, DMSO- d_6) δ 162.56, 160.69, 145.58, 145.32, 142.49, 142.15, 131.79, 129.81, 129.30, 127.97, 125.75, 125.08, 124.39, 123.50, 122.86, 122.53, 121.85, 121.45, 119.95, 118.39, 111.06, 105.31, 57.08, 34.96, 14.45. ESI-

MS: (m/z) calcd for $C_{27}H_{21}N_7O_4$: 507.17; found: 508 $[M+H]^+$; Anal. calcd for $C_{27}H_{21}N_7O_4$: (%) C, 63.90; H, 4.17; N, 19.32; found: C, 63.87; H, 4.14; N, 19.35.

2-methyl-N-((1-(3-(trifluoromethyl)-phenyl)-1H-1,2,3-triazol-4-yl)-methyl)-imidazo-[1,2-f]-phenanthridine-3-carboxamide (PT-07): Off-white solid (81 %), M.P.: 214-216 °C. 1H NMR (400 MHz, DMSO- d_6) δ 9.45 (t, $J = 5.3$ Hz, 1H), 8.99 (s, 1H), 8.67 – 8.62 (m, 1H), 8.58 (d, $J = 7.8$ Hz, 1H), 8.49 (d, $J = 7.2$ Hz, 1H), 8.27 (s, 1H), 7.95 – 7.89 (m, 1H), 7.84 – 7.79 (m, 2H), 7.65 (d, $J = 7.9$ Hz, 2H), 7.48 (dd, $J = 8.9, 5.9$ Hz, 3H), 4.71 (d, $J = 5.5$ Hz, 2H), 2.38 (s, 3H). ^{19}F NMR (377 MHz, DMSO- d_6) δ - 61.26. ^{13}C NMR (101 MHz, DMSO- d_6) δ 162.56, 146.12, 142.36, 137.59, 133.73, 131.82, 131.25, 131.76-132.07 (d, $J = 32.32$ Hz), 130.27, 130.00, 127.97, 125.71, 125.02-122.49 (d, $J = 273$ Hz), 124.36, 123.58, 122.77, 122.22, 121.88, 118.38, 117.80, 35.09, 14.49. ESI-MS: (m/z) calcd for $C_{27}H_{19}F_3N_6O$: 500.16; found: 501 $[M+H]^+$; Anal. calcd for $C_{27}H_{19}F_3N_6O$: (%) C, 64.80; H, 3.83; F, 11.39; N, 16.79; found: C, 64.84; H, 3.81; F, 11.42; N, 16.75.

N-((1-(3,5-dimethylphenyl)-1H-1,2,3-triazol-4-yl)-methyl)-2-methylimidazo-[1,2-f]-phenanthridine-3-carboxamide (PT-08): Brown solid (69 %), M.P.: 83-84 °C. 1H NMR (400 MHz, DMSO- d_6) δ 9.40 (t, $J = 5.4$ Hz, 1H), 9.01 (s, 1H), 8.70 (s, 1H), 8.63 (t, $J = 7.1$ Hz, 1H), 8.58 (d, $J = 7.5$ Hz, 1H), 8.47 (d, $J = 7.1$ Hz, 1H), 7.94 – 7.88 (m, 1H), 7.69 – 7.63 (m, 2H), 7.53 – 7.48 (m, 3H), 7.07 (s, 1H), 4.68 (d, $J = 5.5$ Hz, 2H), 2.37 (s, 3H), 2.09 (s, 5H). ^{13}C NMR (101 MHz, DMSO- d_6) δ 162.55, 157.67, 145.58, 142.31, 139.91, 138.80, 137.07, 132.68, 131.09, 130.32, 130.06, 127.94, 125.76, 125.04, 124.38, 123.57, 122.85, 121.81, 120.97, 118.36, 118.00, 113.46, 35.15, 21.32, 14.44. ESI-MS: (m/z) calcd for $C_{28}H_{24}N_6O$: 460.20; found: 461 $[M+H]^+$; Anal. calcd for $C_{28}H_{24}N_6O$: (%) C, 73.02; H, 5.25; N, 18.25; found: C, 73.05; H, 5.24; N, 18.21.

N-((1-(3,4-dimethylphenyl)-1H-1,2,3-triazol-4-yl)-methyl)-2-methylimidazo-[1,2-f]-phenanthridine-3-carboxamide (PT-09): Brown solid (75 %), M.P.: 158-160 °C. 1H NMR (400 MHz, DMSO- d_6) δ 9.40 (t, $J = 5.4$ Hz, 1H), 8.68 (s, 1H), 8.64 (d, $J = 6.5$ Hz, 1H), 8.58 (d, $J = 7.4$ Hz, 1H), 8.47 (d, $J = 7.6$ Hz, 1H), 7.92 – 7.87 (m, 1H), 7.67 (d, $J = 8.1$ Hz, 2H), 7.57 (dd, $J = 8.1, 2.1$ Hz, 1H), 7.52 – 7.43 (m, 3H), 7.28 (t, $J = 6.5$ Hz, 1H), 4.68 (d, $J = 5.5$ Hz, 2H), 2.37 (s, 3H), 2.26 (s, 3H), 2.23 (s, 3H). ^{13}C NMR (101 MHz, DMSO- d_6) δ 162.53, 142.29, 138.67, 137.47, 135.09, 131.78, 131.09, 129.83, 129.24, 127.94, 125.76, 125.00, 124.37, 123.57, 122.85, 121.87, 121.67, 121.25, 118.35, 117.64, 35.15, 19.90, 14.44. ESI-MS: (m/z) calcd for $C_{28}H_{24}N_6O$: 460.20; found: 461 $[M+H]^+$; HRMS: (m/z) calcd for $C_{28}H_{24}N_6O$: 460.20; found 461.1326 ($M+H$) $^+$; Anal. calcd for $C_{28}H_{24}N_6O$: (%) C, 73.02; H, 5.25; N, 18.25; found: C, 72.98; H, 5.30; N, 18.27.

N-((1-(2-bromo-4-nitrophenyl)-1H-1,2,3-triazol-4-yl)-methyl)-2-methylimidazo-[1,2-f]-phenanthridine-3-carboxamide (PT-10): Off-white solid (70 %), M.P.: 262-263°C. ¹H NMR (400 MHz, DMSO-*d*₆) δ 9.55 (t, *J* = 5.6 Hz, 1H), 8.71 (s, 2H), 8.66 (d, *J* = 7.7 Hz, 1H), 8.53 (d, *J* = 8.2 Hz, 2H), 8.21 (d, *J* = 7.7 Hz, 1H), 7.97 (d, *J* = 3.3 Hz, 1H), 7.85 (d, *J* = 8.5 Hz, 1H), 7.78 – 7.69 (m, 2H), 7.60 – 7.53 (m, 2H), 4.77 (d, *J* = 5.2 Hz, 2H), 2.44 (s, 3H). ¹³C NMR (101 MHz, DMSO-*d*₆) δ 162.59, 145.70, 144.92, 142.53, 142.18, 137.52, 131.77, 129.83, 129.57, 128.71, 127.97, 125.77, 124.96, 124.40, 123.50, 122.84, 121.95, 121.72, 118.37, 34.92, 14.45. ESI-MS: (*m/z*) calcd for C₂₆H₁₈BrN₇O₃: 555.07; found: 556 [M+H]⁺; Anal. calcd for C₂₆H₁₈BrN₇O₃: (%) C, 56.13; H, 3.26; Br, 14.36; N, 17.62; found: C, 56.16; H, 3.30; Br, 14.32; N, 16.99.

N-((1-(3,4-dichloro-2-nitrophenyl)-1H-1,2,3-triazol-4-yl)-methyl)-2-methylimidazo-[1,2-f]-phenanthridine-3-carboxamide (PT-11): Off-white solid (67 %), M.P.: 264-265 °C. ¹H NMR (400 MHz, DMSO-*d*₆) δ 9.47 (t, *J* = 5.8 Hz, 1H), 8.65 (s, 1H), 8.65 – 8.61 (m, 1H), 8.57 (d, *J* = 7.8 Hz, 2H), 8.44 (dd, *J* = 7.7, 1.4 Hz, 1H), 8.29 (s, 1H), 7.92 – 7.87 (m, 1H), 7.70 – 7.59 (m, 2H), 7.48 (d, *J* = 10.2, 2H), 4.68 (d, *J* = 5.8 Hz, 2H), 2.36 (s, 3H). ¹³C NMR (101 MHz, DMSO-*d*₆) δ 162.62, 145.71, 143.12, 142.58, 142.20, 137.24, 133.79, 131.78, 129.83, 129.35, 128.96, 127.98, 127.73, 125.76, 125.10, 124.40, 123.51, 122.84, 121.71, 118.40, 34.91, 14.49. ESI-MS: (*m/z*) calcd for C₂₆H₁₇Cl₂N₇O₃: 545.08; found: 546 [M+H]⁺; Anal. calcd for C₂₆H₁₇Cl₂N₇O₃: (%) C, 57.16; H, 3.14; Cl, 12.98; N, 17.95; found: C, 57.19; H, 3.16; Cl, 13.02; N, 17.98.

3. Biological Procedures

MIC versus replicating *M. tuberculosis*

All experiments with *M. tuberculosis* were conducted within a biosafety level 3 (BSL3) laboratory. Samples were dissolved in dimethyl sulfoxide (DMSO) prior to addition to the assay plate containing 7H12 medium (4.7 g 7H9 broth, 1 g casitone (Bacto), 5 g bovine serum albumin (BSA), 4 mg catalase and 5.6 mg palmitic acid for 1 L media). Twofold serial dilution of the compounds was performed. Plates were inoculated with *M. tuberculosis* strain H₃₇Rv (ATCC 27294) to get the final inoculum of 3 to 5 X10⁵ cells/mL and incubated for 7 days at 37°C. Wells containing drug only were used to detect auto fluorescence of compounds. Additional control wells consisted of bacteria only (B) and medium only (M). Then the redox dye (20 µl of 0.6 mM resazurin dye and 12 µl of 20% Tween 80) was added to each well, and the plates were incubated for an additional 18 to 24 h at 37°C. Final fluorescence was measured after 24 h at 530 nm excitation and 590 nm emission using a CLARIOstar (BMG LABTECH,

Ortenberg, Germany) plate reader. The MIC was defined as the minimum concentration of the compound required to achieve a reduction in fluorescence of 90% relative to untreated bacterial controls.

MIC versus non-replicating *M. tuberculosis*

In this method, the *M. tuberculosis* strain H₃₇Rv carrying auto-luminescent plasmid LuxABCDE was first adapted to low oxygen conditions and then exposed to test compounds under hypoxia; this is followed by a period of outgrowth in aerobic conditions and growth is measured using luminescence. Initially the cultures were thawed, diluted in Middlebrook 7H12 broth (Middlebrook 7H9 broth containing 1 mg/ml Casitone, 5.6 µg/ml palmitic acid, 5 mg/ml bovine serum albumin, and 4 µg/ml filter-sterilized catalase), and sonicated for 15s. The cultures were diluted to obtain a final inoculum of 5 x 10⁵ to 2 x 10⁶ CFU/mL. Two fold serial dilutions of test compounds were prepared in a volume 100 µl in white 96-well microtiter plates, and 100 µl of the cell suspension was added. The microplate cultures were placed under anaerobic conditions (oxygen concentration, less than 0.16%) by using an Anoxomat model WS-8080 (MART Microbiology) and three cycles of evacuation and filling with a mixture of 10% H₂, 5% CO₂, and the balance N₂ (7, 32). An anaerobic indicator strip was placed inside the chamber to confirm the removal of oxygen visually. The plates were incubated at 37°C for 10 days and then transferred to an ambient gaseous condition (5% CO₂-enriched air) incubator for a 28 h “recovery.” On day 11 (after the 28 h aerobic recovery) luminescence of the plate was read on CLARIOstar (BMG LABTECH, Ortenberg, Germany) plate reader. The MIC was defined as the minimum concentration of the compound required to achieve a reduction in fluorescence of 90% relative to untreated bacterial controls.

Cytotoxicity assay

The safety of the compounds was tested both on primary cultures of murine splenocytes and on human hepatocarcinoma cell HepG2 line (ATCC HB-8065) as a suitable *in vitro* toxicity model system of human hepatocytes. HepG2 cells and splenocyte cells were seeded in 96-well plates at 37°C under 5% CO₂ atmosphere. For HepG2 cells was used The Glutamax Dulbecco’s Modified Eagle’s Medium (DMEM, Gibco), supplemented with 10% (v/v) FBS, and antibiotic mix. Viability of splenocytes and hepatocarcinoma cells were measured using the Almar Blue staining method, according to manufacturer’s recommendations (Invitrogen). Selectivity index for each compound was calculated as the ratio between the CC₅₀

value obtained for non-infected murine splenocytes or CC_{50} value obtained for HepG2 cells and the EC_{50} values for promastigotes/amastigotes obtained with ex vivo murine splenic explant cultures.

4. Computation studies

In-silico prediction of ADME and Toxicity (ADMET) parameters

The ADMET parameters of the titled compounds were *in silico* predicted using Qikprop module of Schrodinger. The diverse parameters predicted were molecular weight (M.Wt.), total solvent accessible surface area (SASA), number of hydrogen bond donor (HBD), number of hydrogen bond acceptor (HBA), octanol / water partition coefficient (log P), aqueous solubility (Log S), predicted apparent Caco-2 cell permeability in nm/sec (P Caco) and number of rotatable bonds (Rot) (Schrödinger Release 2019-1: QikProp, Schrödinger, LLC, New York, NY, 2019., (n.d.). SMILES format of the compounds was generated by using OSIRIS DataWarrior. All the related toxicity parameters were also predicted by the same software.

Materials and methods

Molecular docking:

Computational sources: Xenon W3565 processor, Ubuntu 18.04

Software and version: Schrodinger software, version 2019-1.¹

Retrieval of the protein: RCSB protein data bank.²

(PDB-4BAE, <https://www.rcsb.org/structure/4BAE>).

Docking method: Extra precession mode.

Results analysis: XP visualizer (Schrodinger)

Molecular Dynamics:

Computational sources: Tyrone workstation (NVIDIA RTX 2040), Ubuntu 18.04

Software and version: Desmond software, D.E Shaw research group (Academic license, Version 2020-1; *Schrödinger Release 2020-4: Desmond Molecular Dynamics System, D. E. Shaw Research, New York, NY, 2020. Maestro-Desmond Interoperability Tools, Schrödinger, New York, NY, 2020., n.d.*)

Docking workflow: To perform docking studies, ChemDraw 16.0 was used to sketch the ligand. Then, the Ligprep module of the software (Version 2019-1, Schrodinger) (Schrodinger, n.d.) was used to minimize the energy with Optimized Potentials for Liquid Simulations (OPLS3e) force field. The minimization process enables the allocation of bond orders, addition of hydrogens to ligands and the conversion of 2D into 3D structures to improve docking. Further, docking studies were conducted using the output file (Best conformations of the ligands).³

In Schrodinger, the protein preparation wizard (version 2019-1, Schrodinger; *Schrödinger Release 2019-1: Schrödinger Suite 2019-1 Protein Preparation Wizard; Epik, Schrödinger, LLC, New York, NY, 2019., n.d.*) is the primary application for preparing proteins and minimizing their energy content. It adds hydrogen atoms to proteins and assigns charges to them. The Het states were generated using Epik at pH 7.0 ± 2.0 . Using workspace analysis, the protein was refined, modified and the heteroatoms in the water were removed. The crucial water molecules stayed the same, but all other molecules apart from the water were removed except the co-crystal ligand. The OPLS3 force field was then used to minimize the protein. An active site grid was generated by considering co-crystal ligands, which are included in the active site of the selected protein target (PDB-4BAE). Root mean square deviation (RMSD) was calculated using the overlay view of the X-ray native pose of co-crystal ligand and its docked pose in XP mode to validate the protein.

Molecular dynamics workflow: Simulation of Molecular Dynamics (MD) helps visualize the action of Protein-Ligand complexes (PLC) at the target's binding site region under physiological conditions. MD was performed using Desmond module of Schrödinger developed by D.E Shaw research group (Academic license, Version 2020-1; *Schrödinger Release 2020-4: Desmond Molecular Dynamics System, D. E. Shaw Research, New York, NY, 2020. Maestro-Desmond Interoperability Tools, Schrödinger, New York, NY, 2020., n.d.*) through the system's builder panel; the orthorhombic simulation box was prepared with the Simple Point-Charge (SPC) explicit water model in such a way that the minimum distance between the protein surface and the solvent surface is 10 Å. Complexes docked with receptors were solvated with the orthorhombic TIP3P water

model.⁴ Neutralization of the solvated system was accomplished by using counterions and limiting the salt concentration in the physiological system to 0.15 M. The receptor-ligand complex system was designated with the OPLS AA force field.⁵

Two seconds of relaxation time was used for the Reversible reference system Propagator Algorithms (RESPA) integrator.⁶ Nose-Hoover chain thermostat,⁷ and Martyna-Tobias-Klein barostat. The final production of MD simulations was performed using the equilibrated system. This MD simulation was set to run for 100 ns with 310 K temperatures at 1.0 bar pressure, with the NPT (Isothermal-Isobaric ensemble, constant temperature, constant pressure, constant number of particles) ensemble at default settings for relaxation before simulation. The MD simulation was performed with MD simulation tool, with the simulation time set to 100 ns. Furthermore, the .out file was used to view the trajectories and create a movie. The out.cms file was imported and the movie was exported at higher resolution (1280x1024) with better quality. The trajectories were written with 1000 frames during MD simulation. The protein backbone frames were aligned to the backbone of the initial frame to better understand the complex's stability during MD simulation. Finally, after loading the .out file and selected the Root Mean Square Deviation (RMSD) and Root Mean Square Fluctuation (RMSF) in the analysis type to oblique, the simulation interaction diagram and the results were analysed.^{8,9}

Annexure I

Molecular docking analysis

The docking studies was performed to explore the binding interaction of the potential compound within the active site of the receptor using Schrodinger Glide module (Version 2019-1). Mycobacterial GyrB ATPase (PDB-4BAE) crystal structure was retrieved from the protein data bank with resolution of 2.35 Å.^{10,11} The protocol was validated by checking the RMSD of the docked pose of the co-crystal ligand with its X-ray pose of the co-crystal ligand. The RMSD was found to be 0.83 Å (**Figure 1**). Based on the results of RMSD, the docking study was initiated for the test compound.

From the docked pose view of the co-crystal ligand (**Figure 2**), the binding residues like ARG141, ASP79, H₂O formed hydrogen bonds. The amino acid residue ASN52, is involved in the halogen bond at the active site of the target protein with docking score of -8.77 kcal/mol (**Table 1**). Similarly, the test compound **PA-01** showed hydrogen bond interaction with the H₂O (**Figure 3**) at the active site with the docking score value -

4.94 kcal/mol. No hydrogen bond, halogen bond and salt bridge interactions were observed at the active site amino acid residues of the target protein. This could be the possible reason for its low docking score of the significantly active compound. **Table 1** shows the docking score and amino acid residues involved in the interaction with the potent compound **PT-09** at the active site of DNA gyrase (PDB: 4BAE). The docking score of the biologically active compound PT09 was found to be -2.6 kcal/mol. The results of docking analysis showed three water-mediated hydrogen bond interactions with GLY83 (2.18 Å), THR169 (2.06 Å) and ASP79 (1.79 Å) at the binding site of 4BAE. In addition, a pair of residues ASP79 (2.18 Å) and ASP55 (2.5 Å) are actively involved in connection with PT09 via an aromatic hydrogen bond at the binding pocket (**Figure 4**). Since there is no direct hydrogen bond contact, halogen bond and salt bridge interactions were observed at the active site of the target protein, which were seen with the co-crystal ligand. This could be the probable reason for the low docking score of the significantly active compound.

Table 1: Molecular docking results of co-crystal ligand and compound **PA-01** at the active site of target protein (PDB: 4BAE)

Comp. code	Binding residues	Bond distances (Å)	Type of interaction	Glide score (kcal/mol)
Co-crystal ligand	ARG141	1.93	Hydrogen bond	-8.77
	ARG141	4.36	Salt bridge	
	ASN52	2.63	Halogen bond	
	ASP79	1.92	Hydrogen bond	
	H ₂ O	1.81	Hydrogen bond	
PA-01	H ₂ O	2.08	Hydrogen bond	-4.94
PT09	H ₂ O			-2.6
	GLY83	2.18	Hydrogen bond	
	THR169	2.06	Hydrogen bond	

ASP79	1.79	Hydrogen bond
ASP79	2.18	Aromatic H-bond
ASP55	2.5	Aromatic H-bond

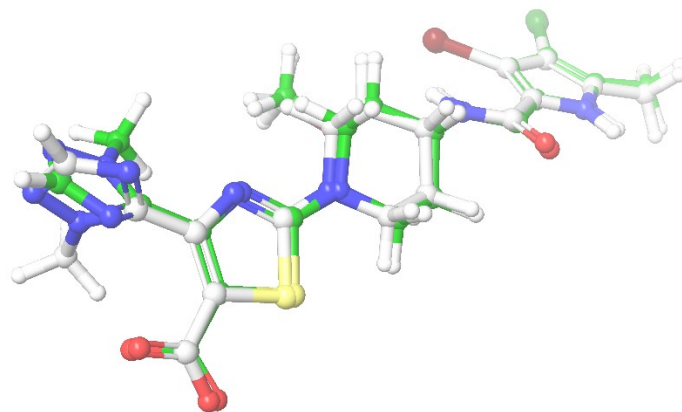


Figure 1. Super-imposed re-docked view of the X-ray native pose of co-crystal ligand (Green) and its docked pose (Blue) in the active site of target protein **4BAE** (RMSD 0.83 Å)

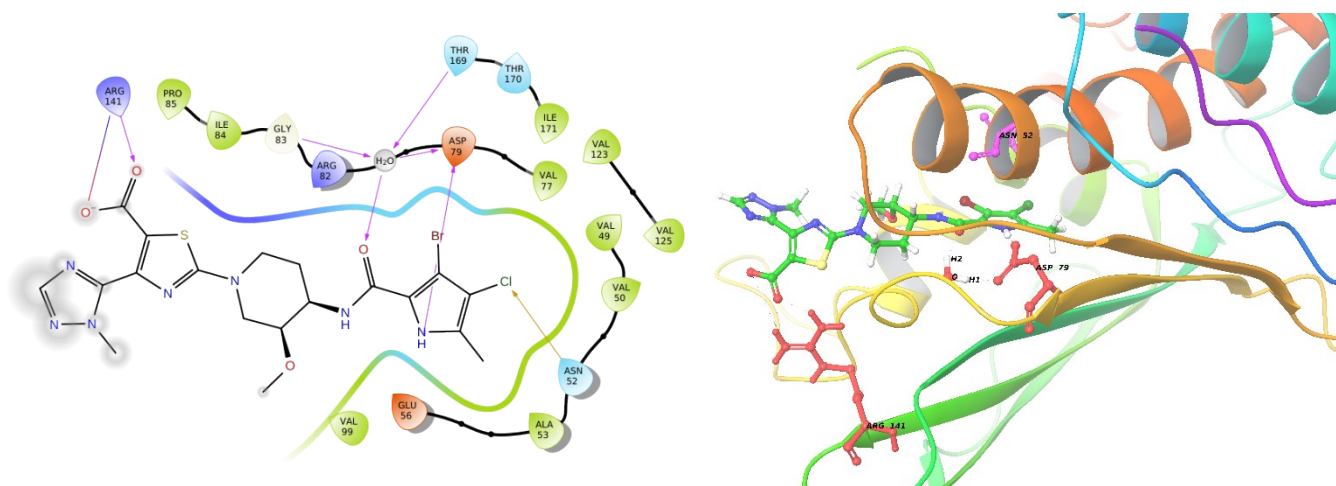


Figure 2. Docked pose appearance of the co-crystal ligand in the active site of target protein **4BAE** (3D- Right, 2D- Left)

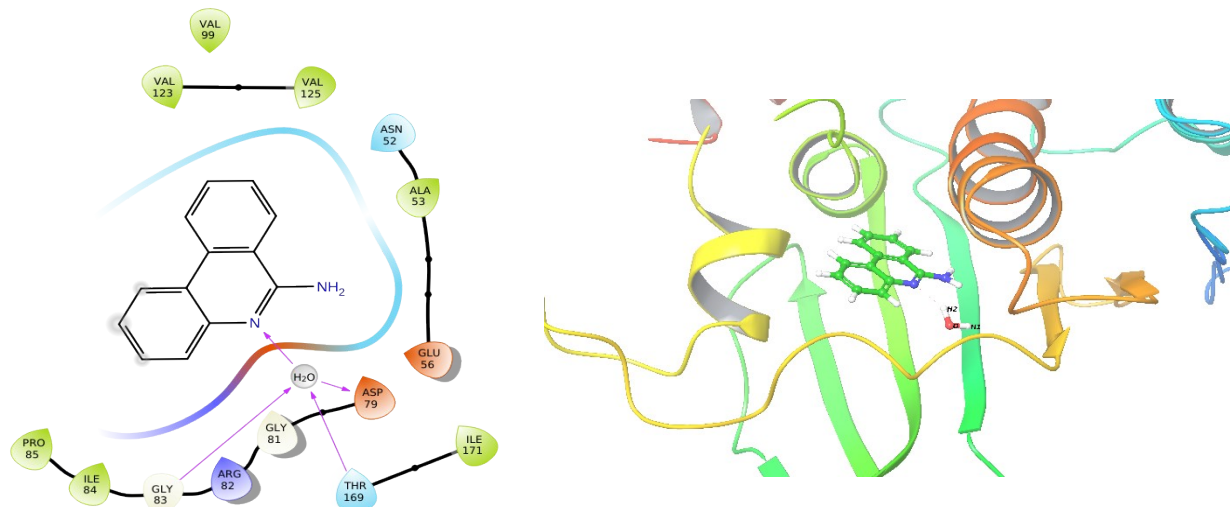
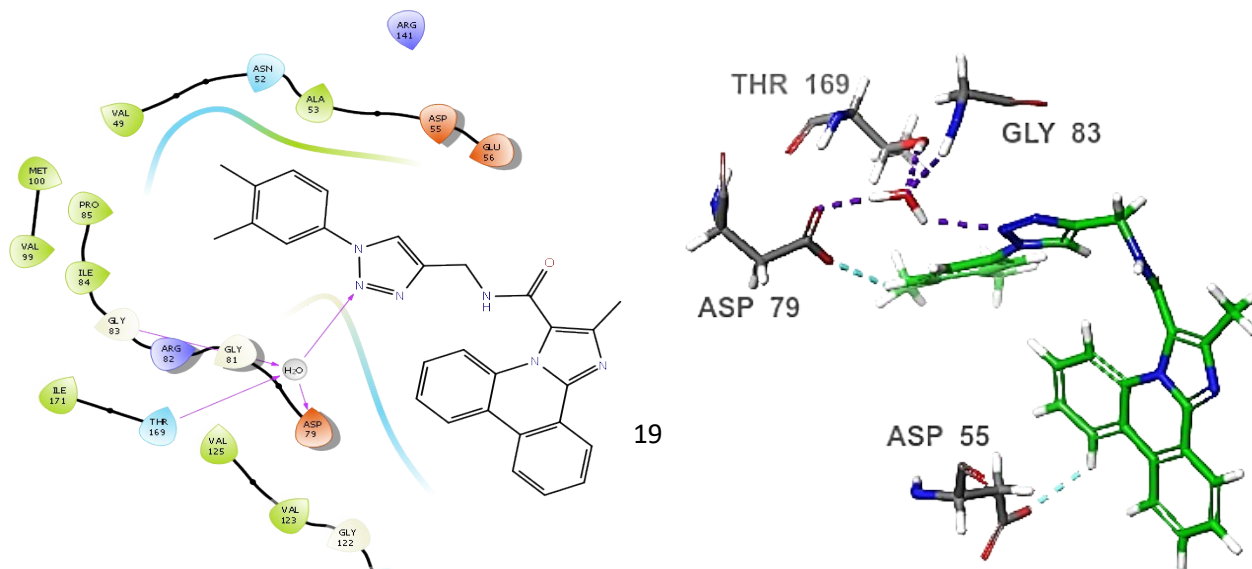


Figure 3. Docked pose appearance of the significantly active compound **PA-01** in the active site of target protein 4BAE (3D- Right, 2D- Left)



Molecular dynamics studies

Molecular dynamics study helps in assessing the stability and integrity of the ligand within the active site of the target protein. MD studies was performed with the docked complex co-crystal ligand in the protein and **PA-01** ligand. Root Mean Square Deviation (RMSD) was generated (**Figure 5**), to perceive the structural changes of the ligands in the active stie of the target during MD simulation for 100 ns. **Figure 5** shows a high

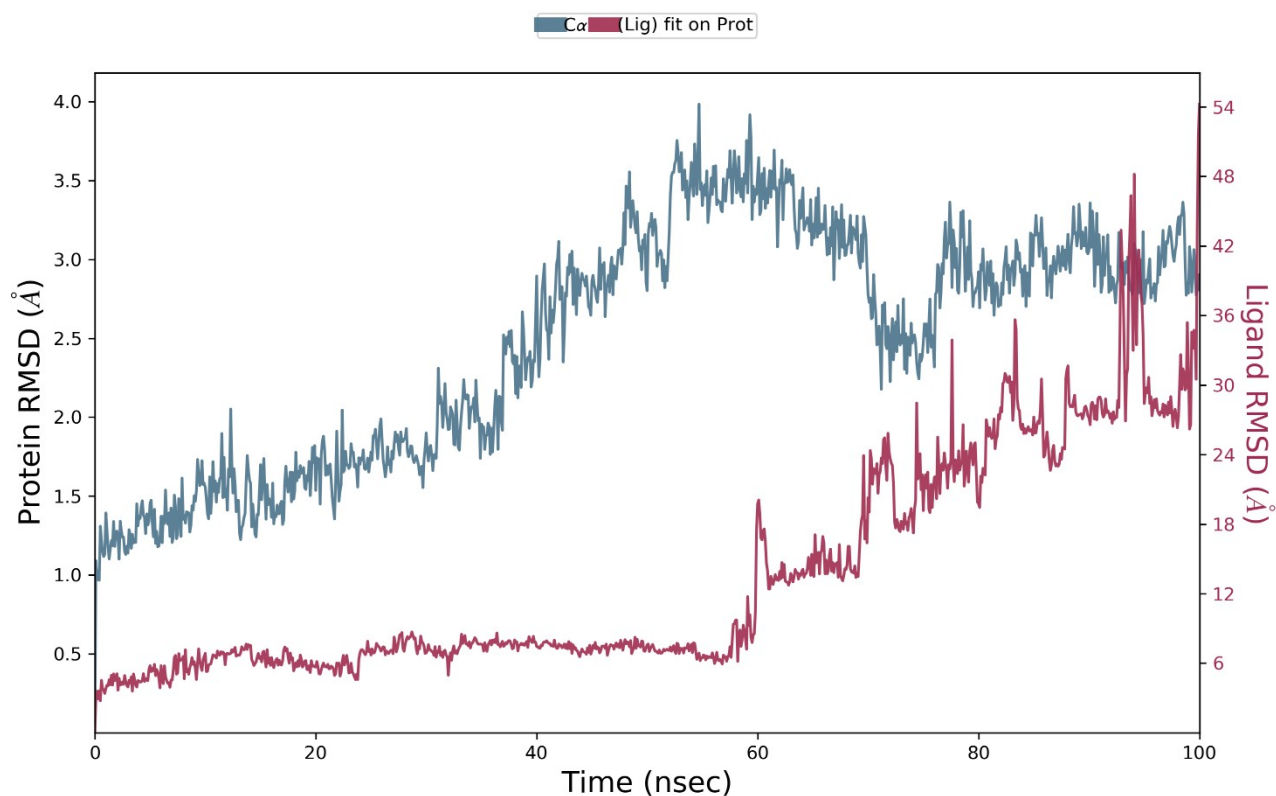


Figure 5. MD simulation Root mean square deviation (RMSD) graph of protein- compound **PA-01** complex

All the interacting residues were below 2.4 Å except Phe173, as can be seen in **Figure 6**, this indicates no significant change in the active site groove and hence, the ligand fits within the target protein.

From ligand-protein contacts showed in **Figure 7**, hydrophobic interactions seen to be predominant, followed by H-bonds and water bridges. However, the interacting residues from the dynamics vary with our docking analysis. The primary amine, which was free in docking result, tend

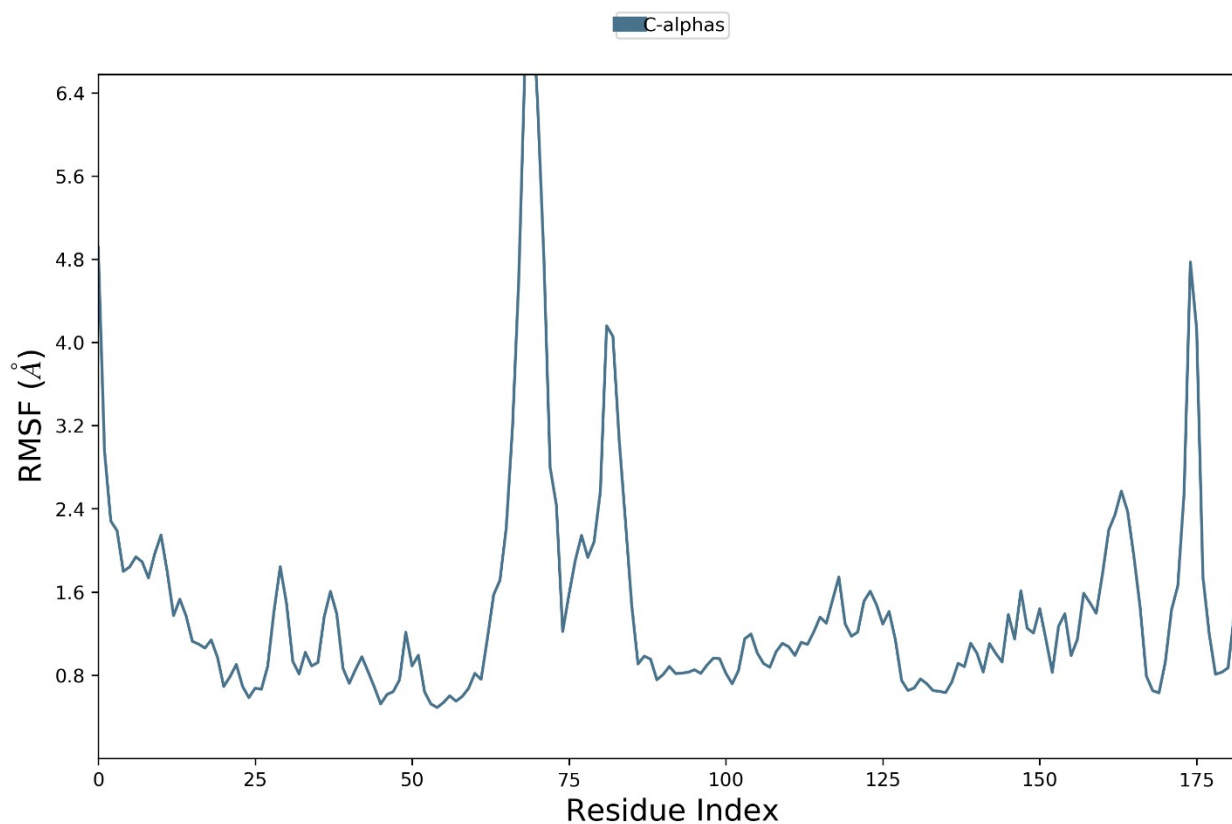


Figure 6. MD simulation Root mean square fluctuation (RMSF) graph of protein- compound **PA-01** complex

to participate in hydrophobic interactions with Val49 and Val99 (6% and 16%, respectively) (**Figure 8**) while the benzene ring of the quinoline shows hydrophobic interaction with Phe173 (5%) via pi-pi stacking.

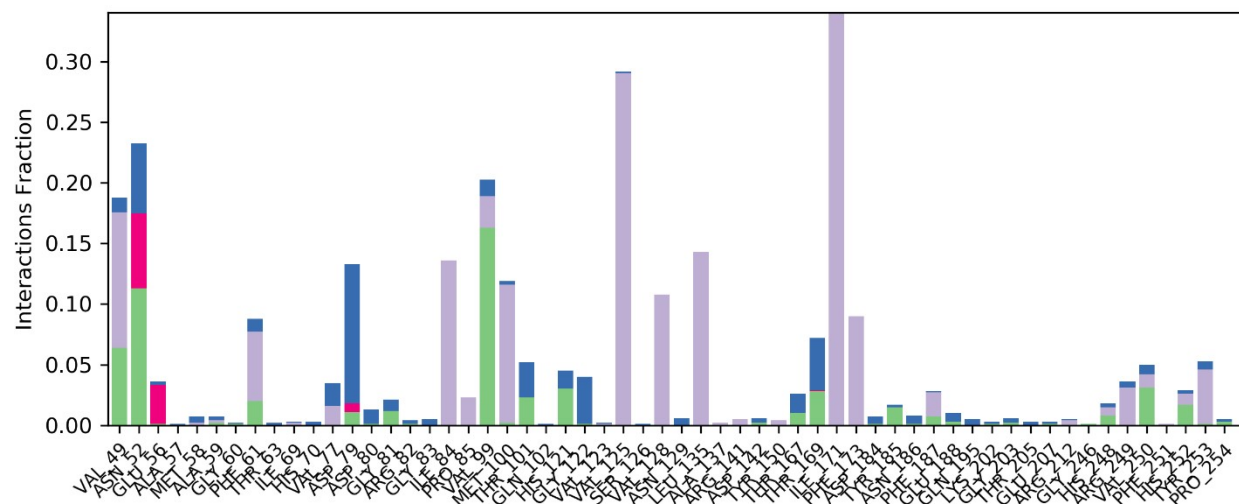


Figure 7. Different amino acid interactions plot of the protein with the ligand **PA-01**

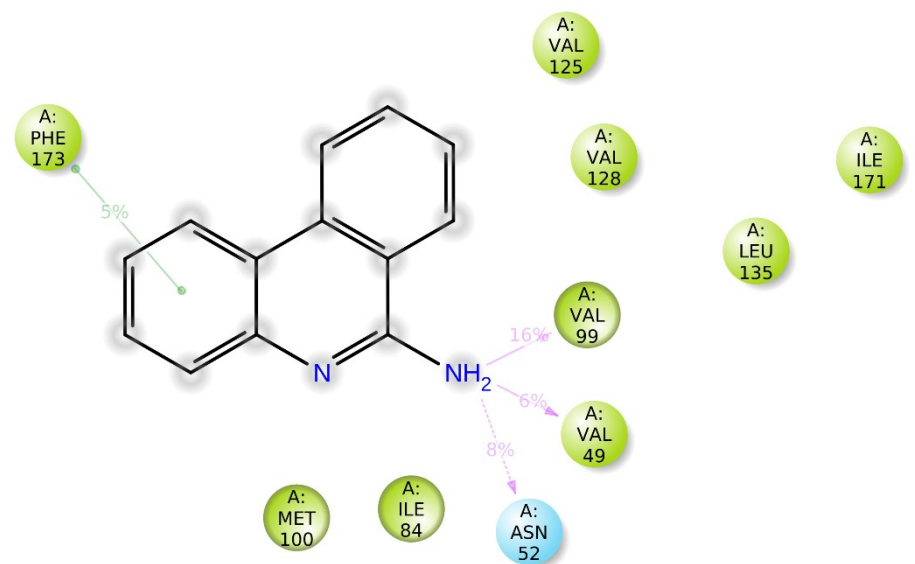
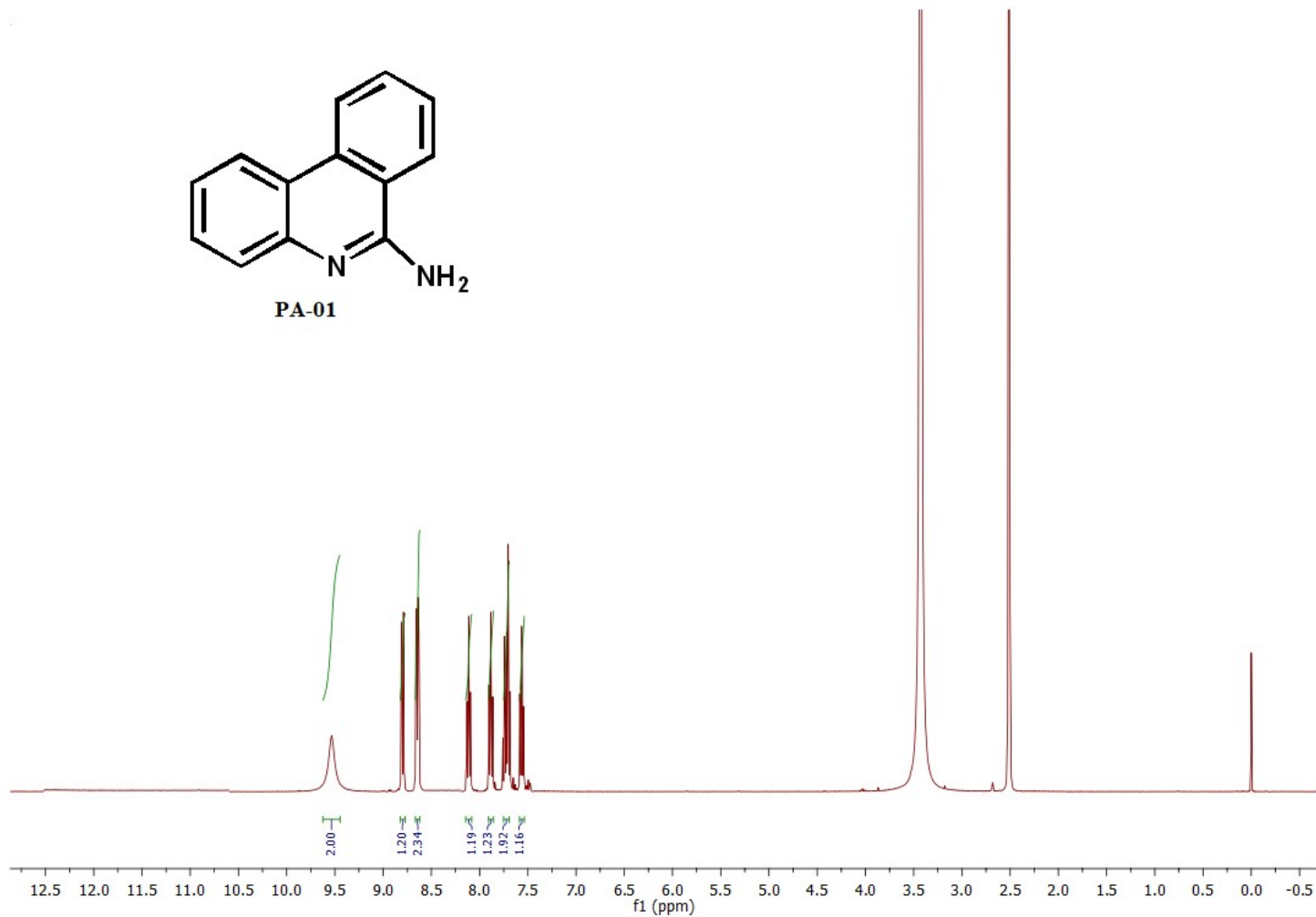
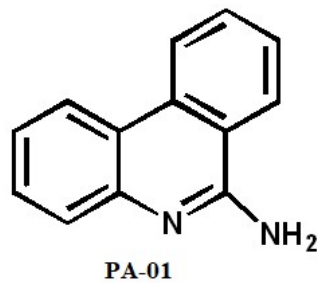


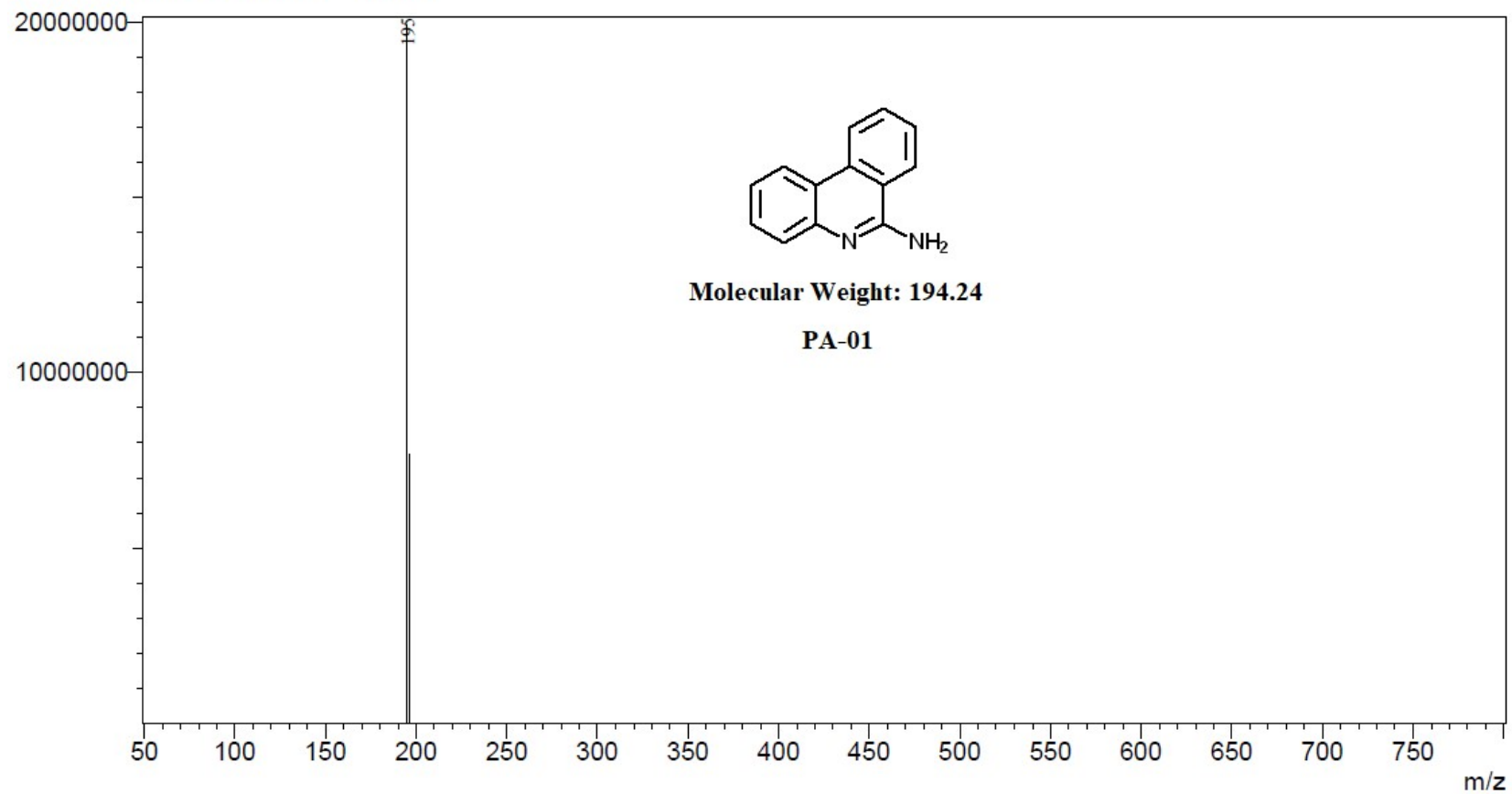
Figure 8. 2D interaction view of PA-01 ligand contacts in the active site of target protein

5. ^1H NMR, ^{19}F NMR, ^{13}C NMR spectras and mass spectras of intermediate compounds and final compounds

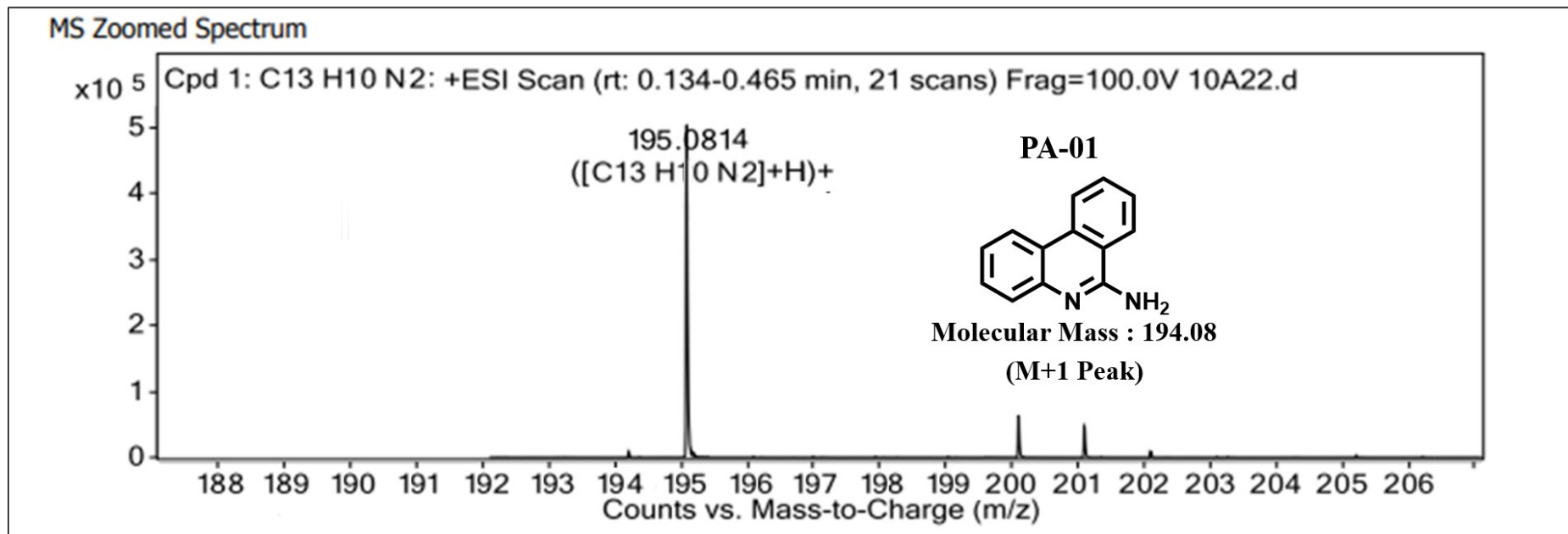


^1H NMR (400 MHz, $\text{DMSO-}d_6$) of PA-01

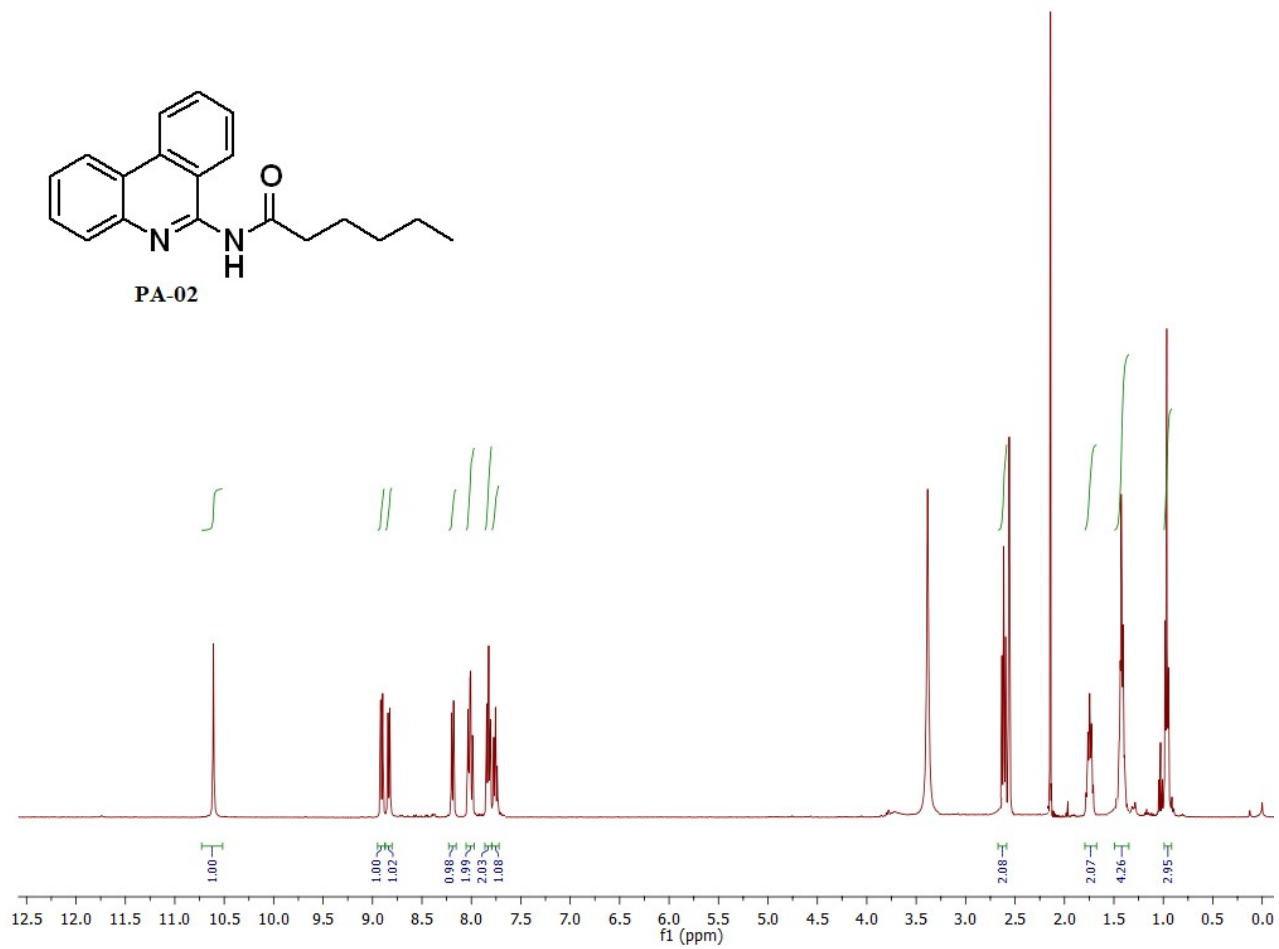
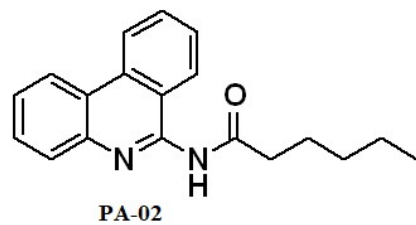
RawMode:Averaged 0.20-0.50(83-207) BasePeak:195(19928757)
BG Mode:None Segment 1 - Event 1



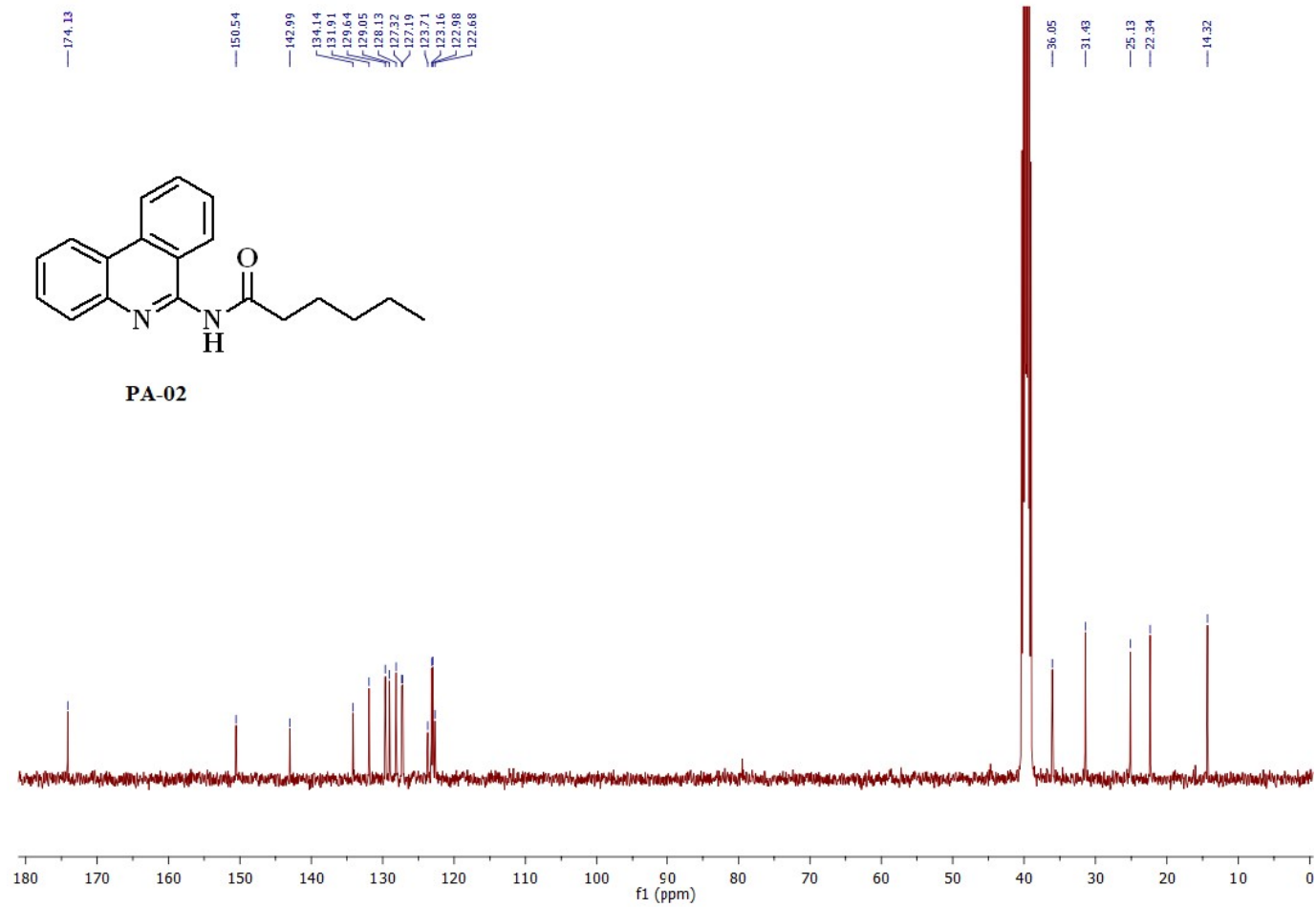
Mass spectra of compound PA-01



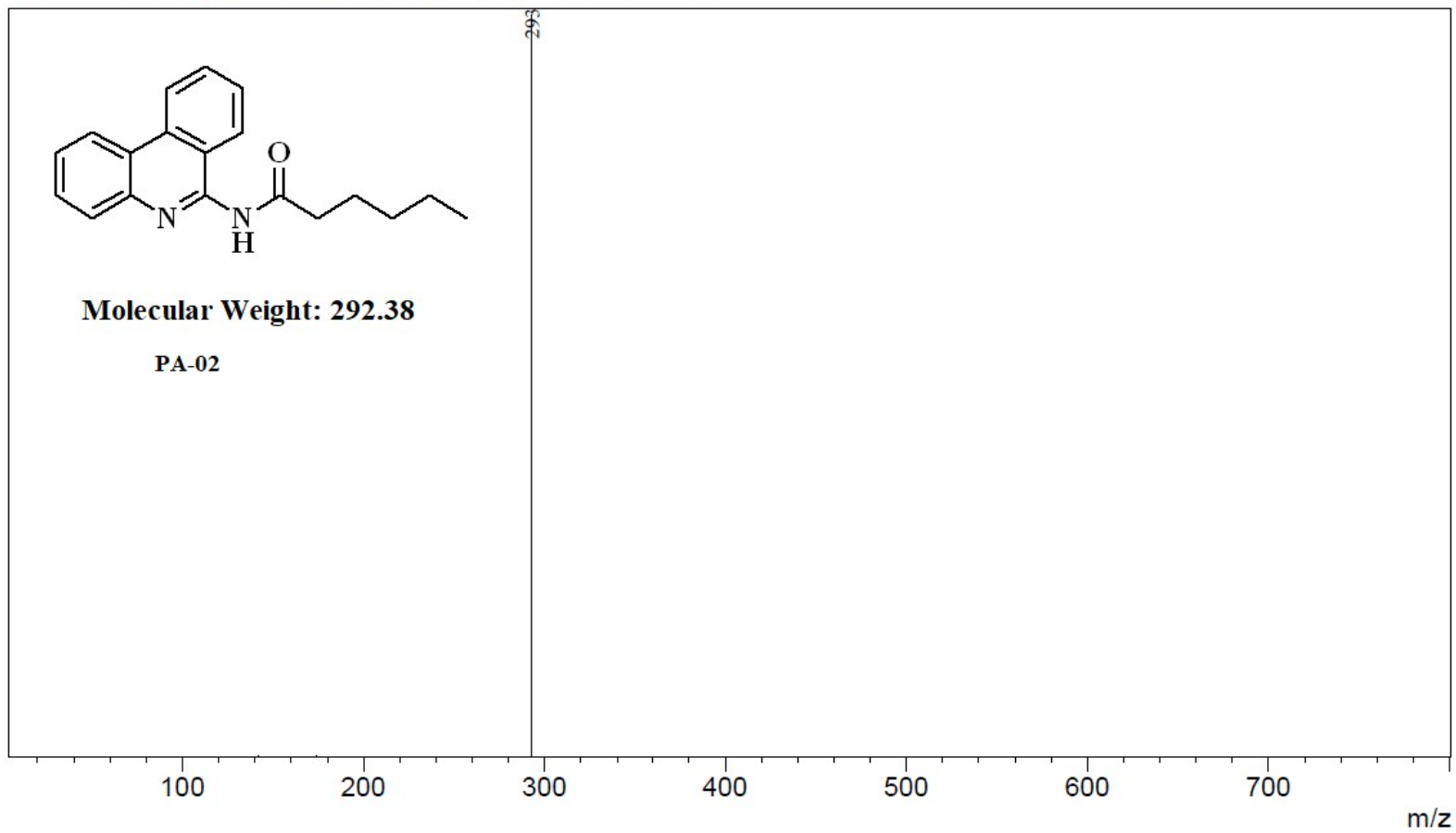
HRMS Mass spectra of compound PA-01



^1H NMR (400 MHz, $\text{DMSO-}d_6$) of PA-02

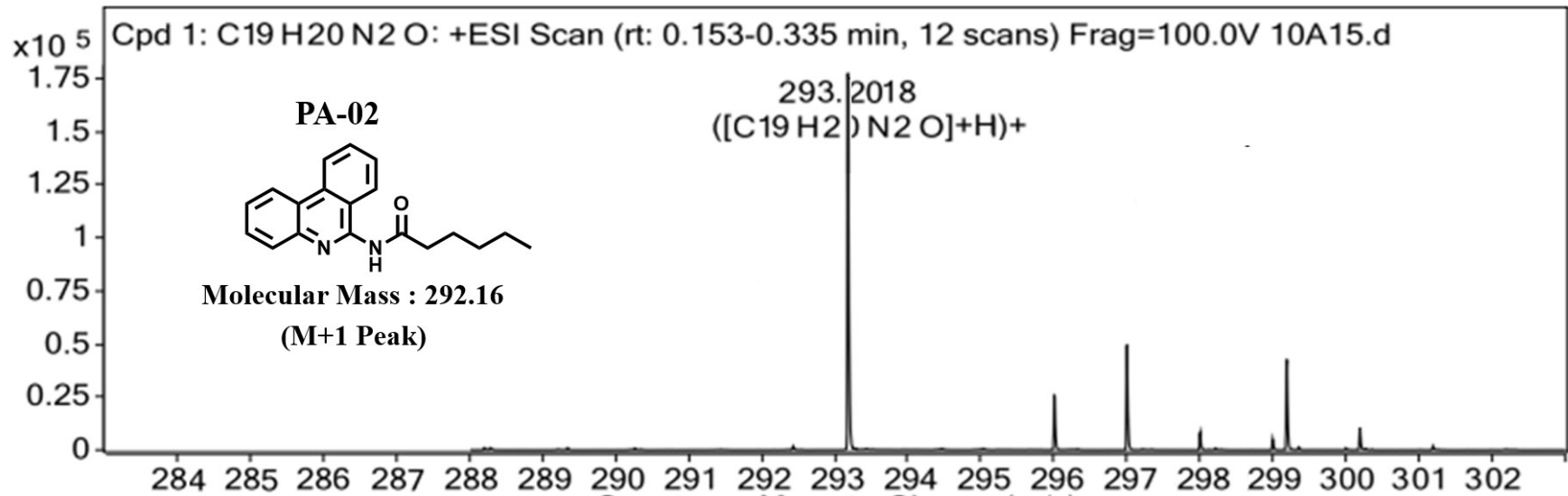


RawMode:Averaged 0.14-0.50(65-221) BasePeak:293(17614819)
BG Mode:Averaged 0.00-0.14(1-63) Segment 1 - Event 1

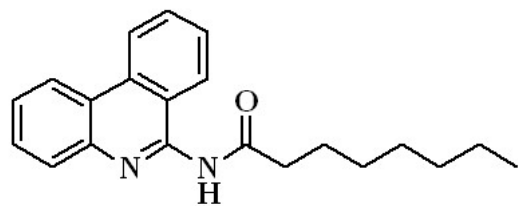


Mass spectra of compound PA-02

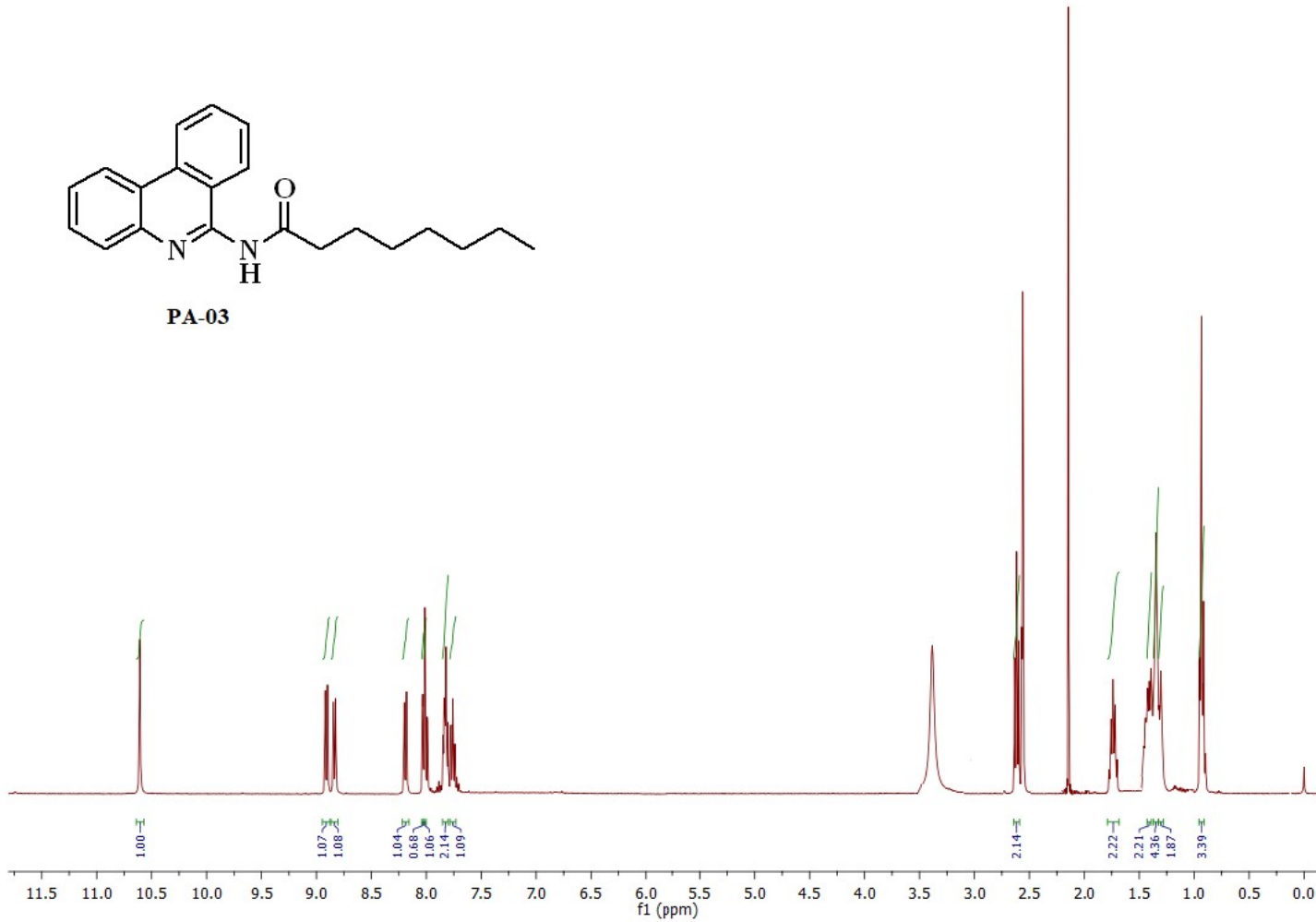
MS Zoomed Spectrum



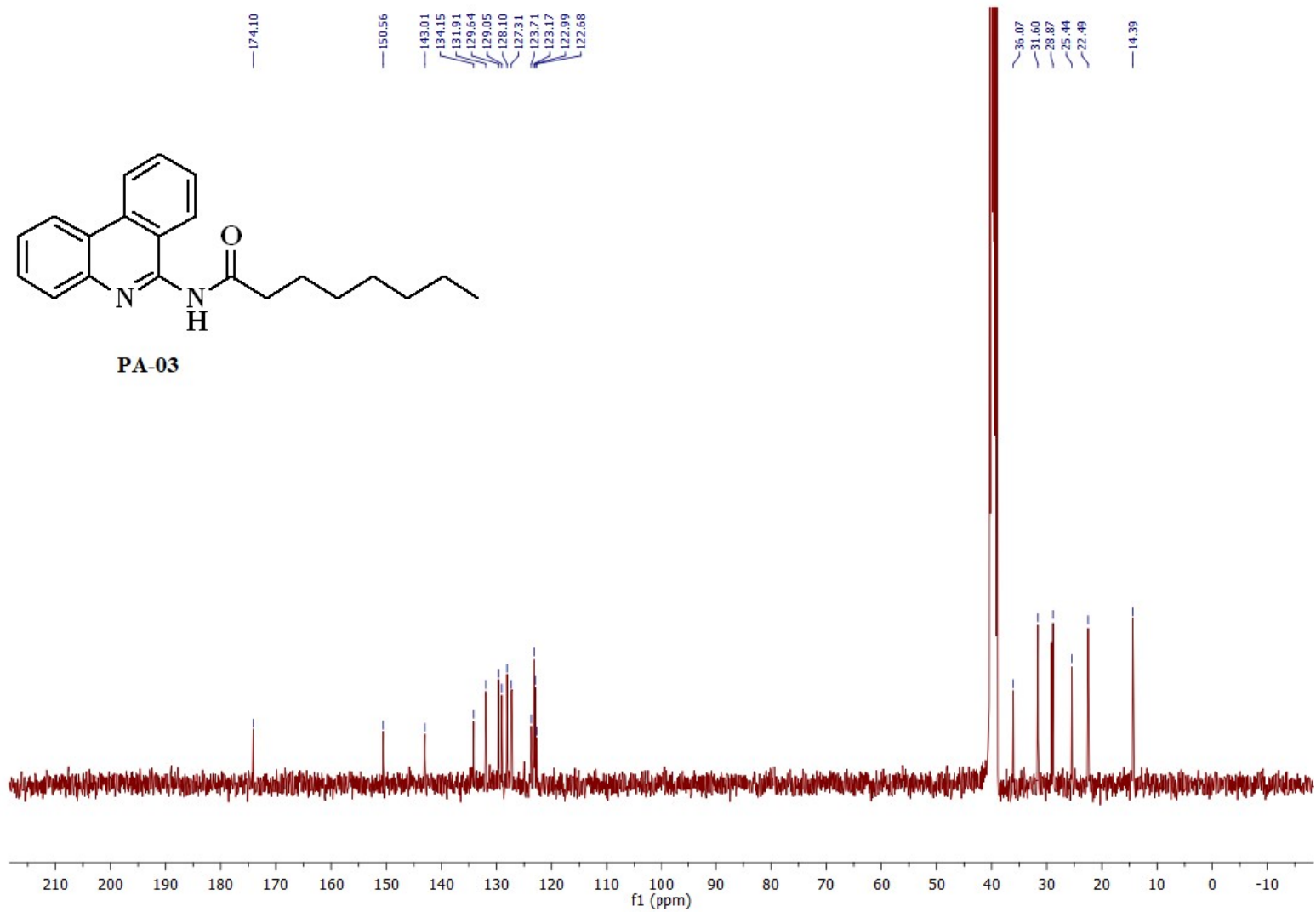
HRMS Mass spectra of compound PA-02



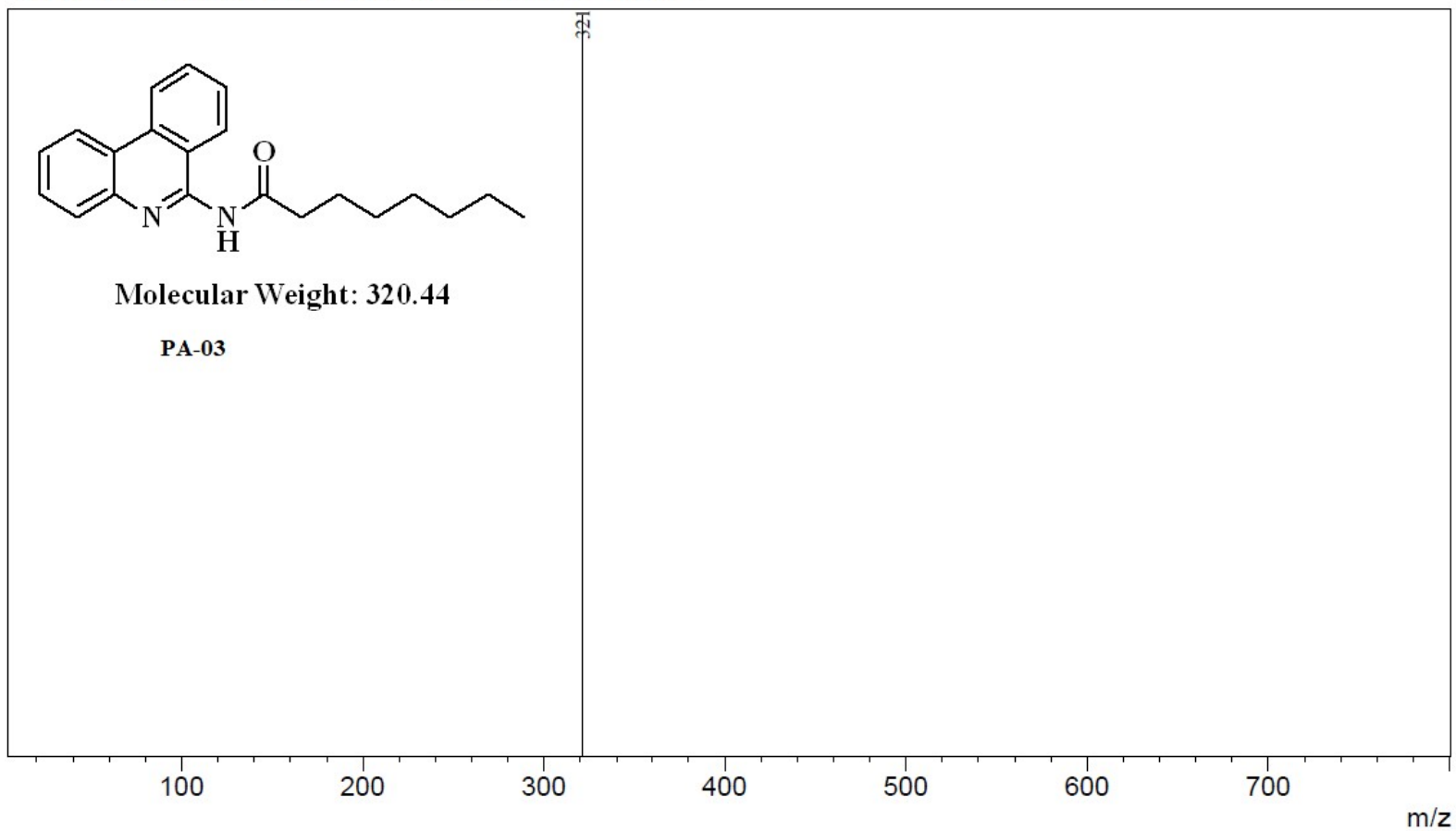
PA-03



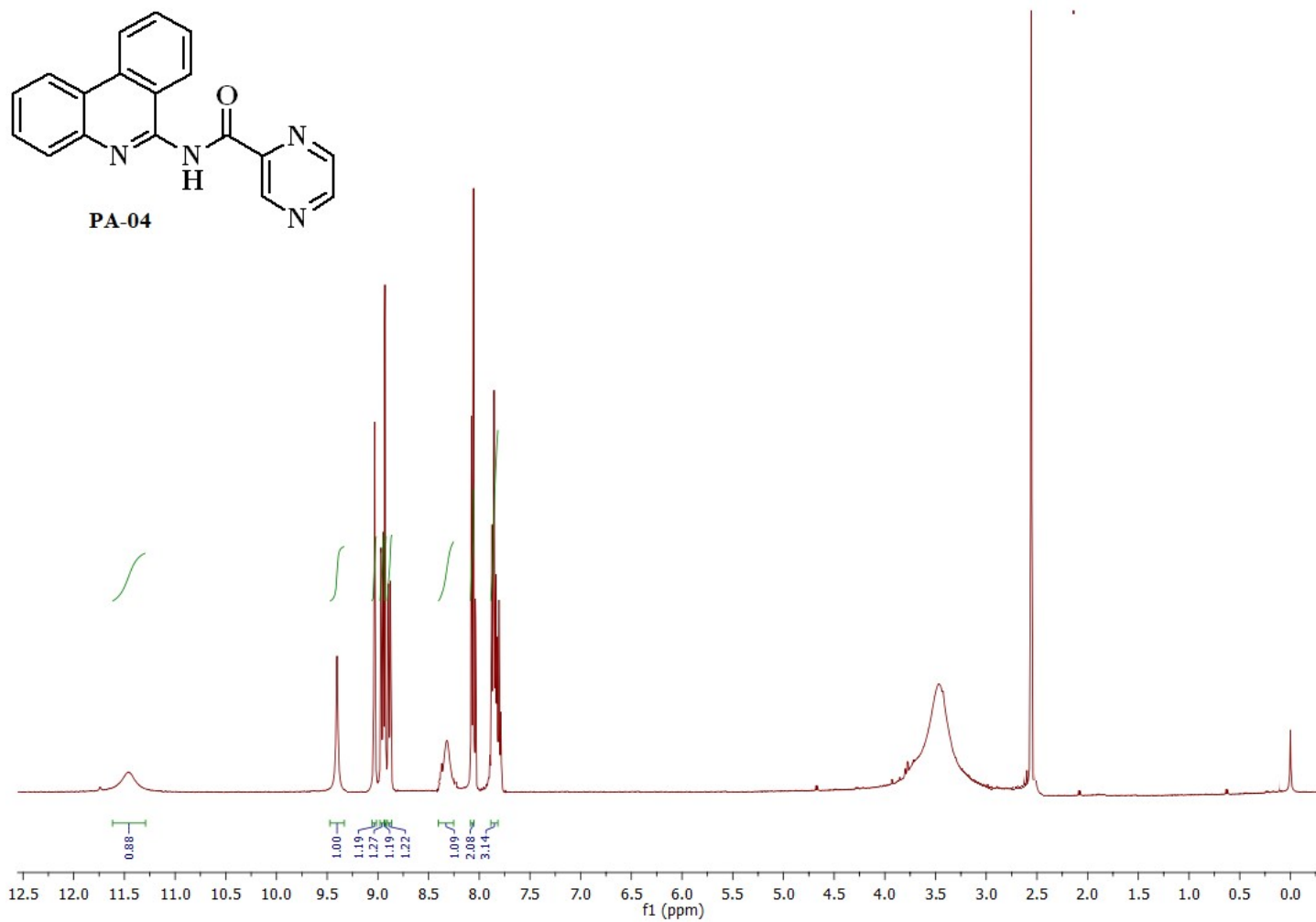
^1H NMR (400 MHz, $\text{DMSO-}d_6$) of PA-03



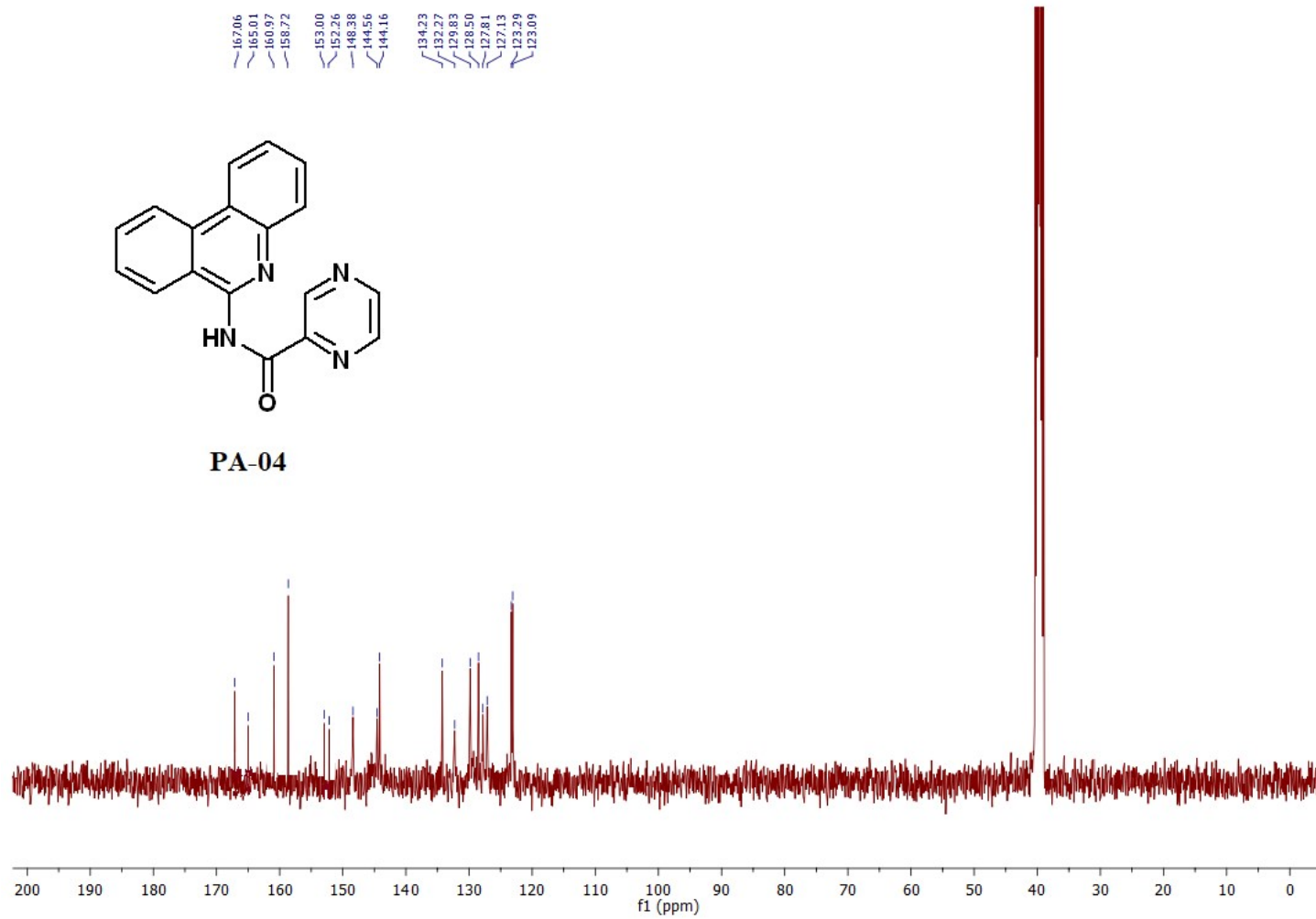
RawMode:Averaged 0.14-0.50(65-221) BasePeak:321(15849090)
BG Mode:Averaged 0.00-0.15(1-67) Segment 1 - Event 1



Mass spectra of compound PA-03

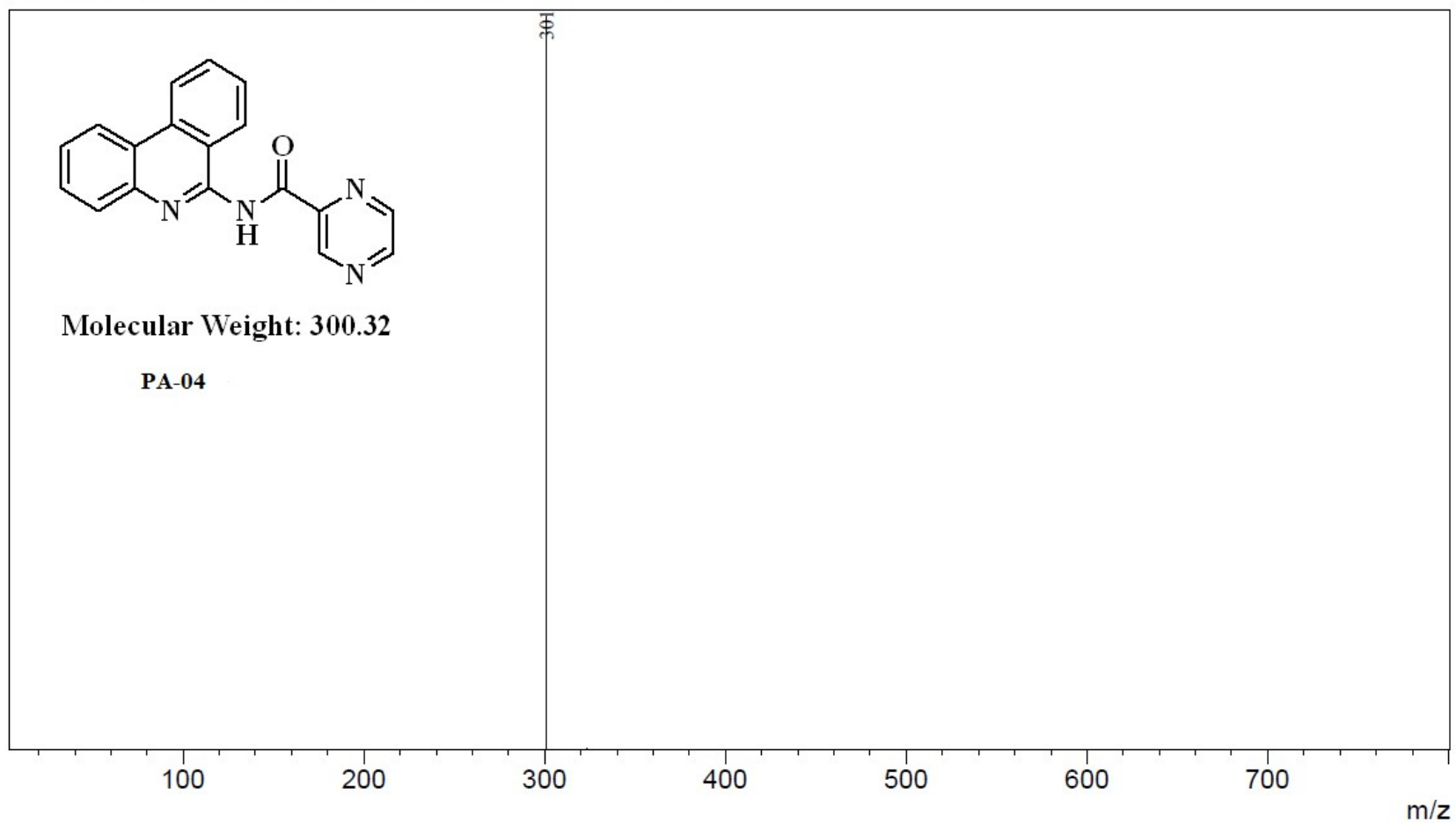


¹H NMR (400 MHz, DMSO-*d*₆) of PA-04

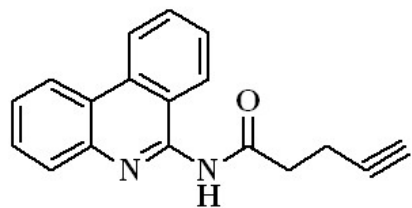


^{13}C NMR (101 MHz, $\text{DMSO-}d_6$) of PA-04

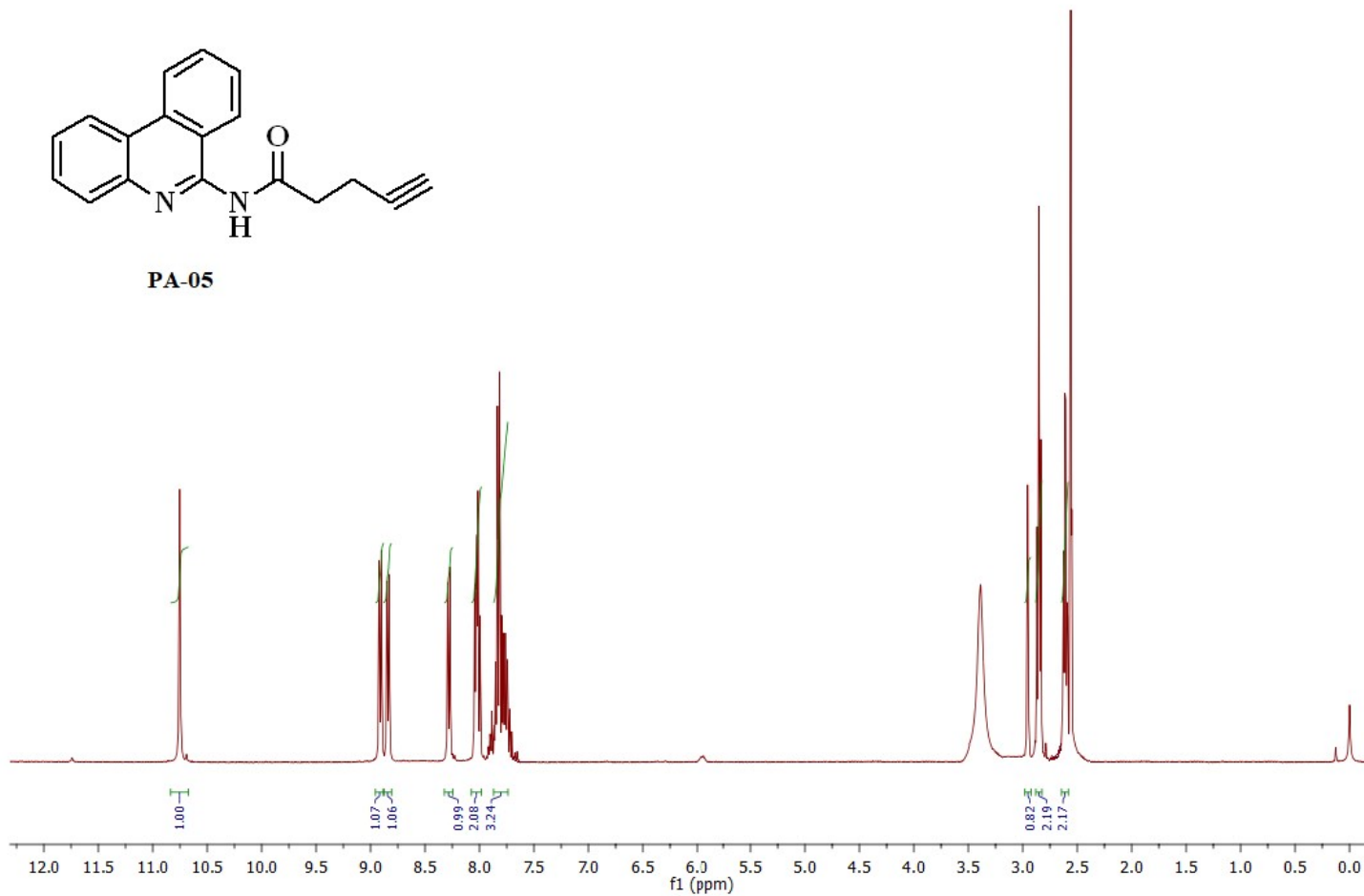
RawMode:Averaged 0.14-0.50(63-221) BasePeak:301(9722840)
BG Mode:Averaged 0.00-0.14(1-65) Segment 1 - Event 1



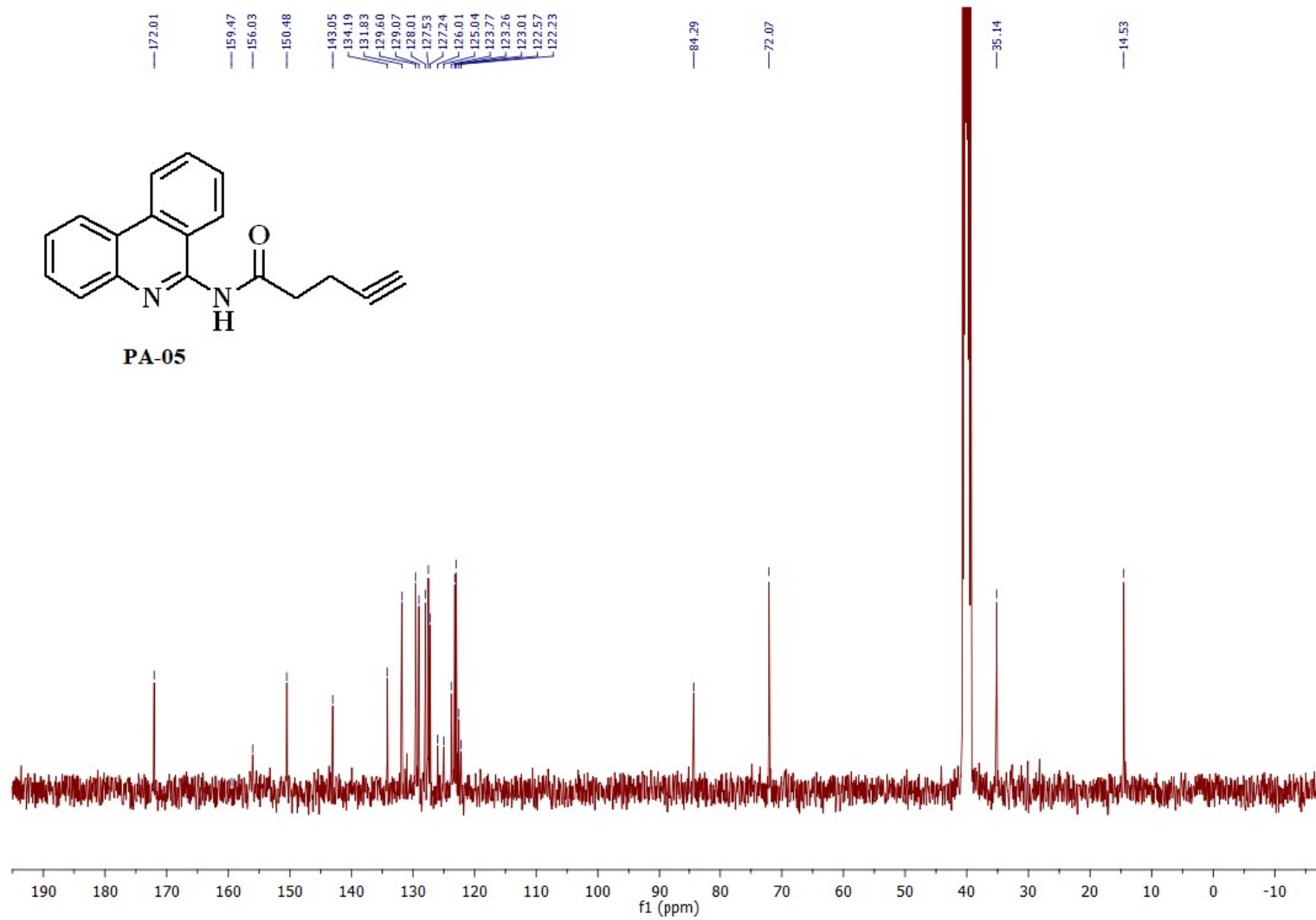
Mass spectra of compound PA-04



PA-05

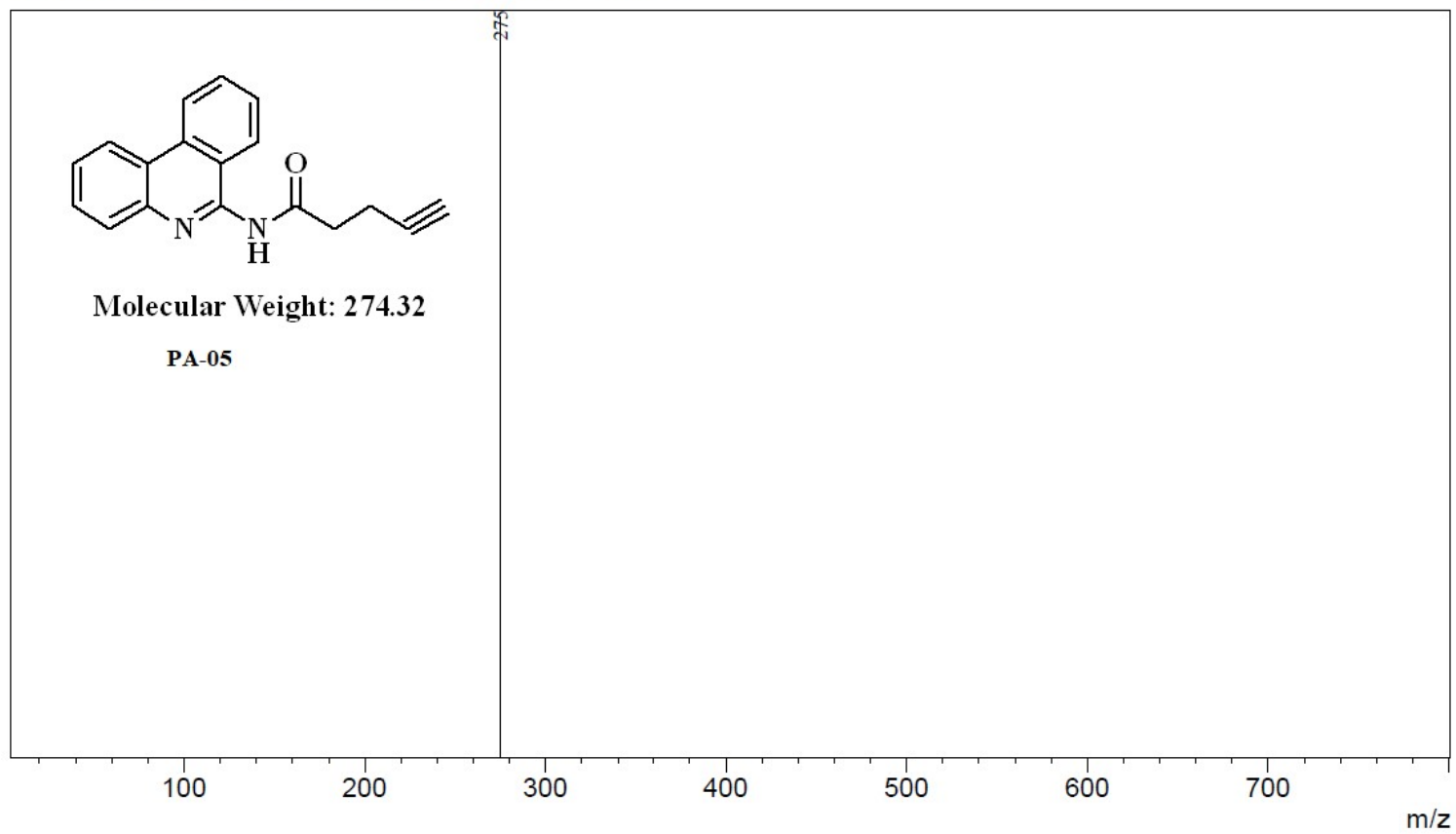


^1H NMR (400 MHz, $\text{DMSO-}d_6$) of PA-05



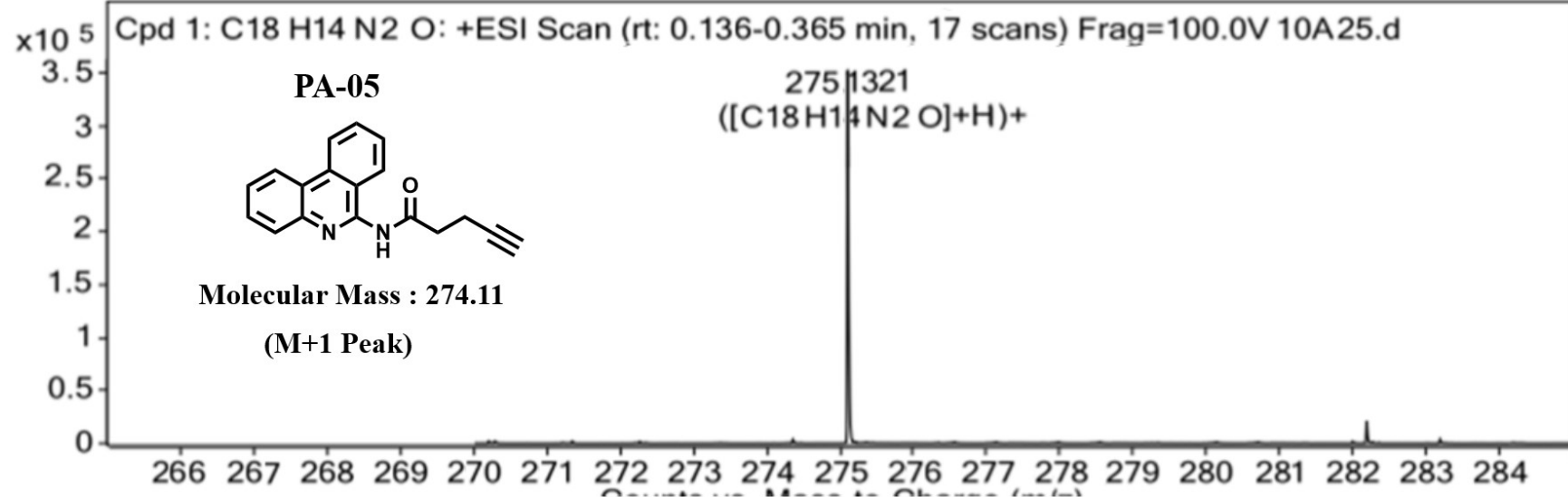
¹³C NMR (101 MHz, DMSO-*d*₆) of PA-05

RawMode:Averaged 0.14-0.50(61-221) BasePeak:275(13927489)
BG Mode:Averaged 0.00-0.14(1-63) Segment 1 - Event 1

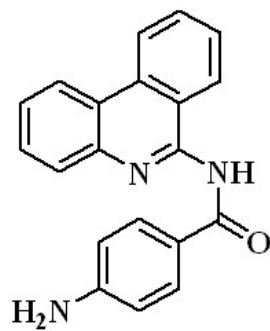


Mass spectra of compound PA-05

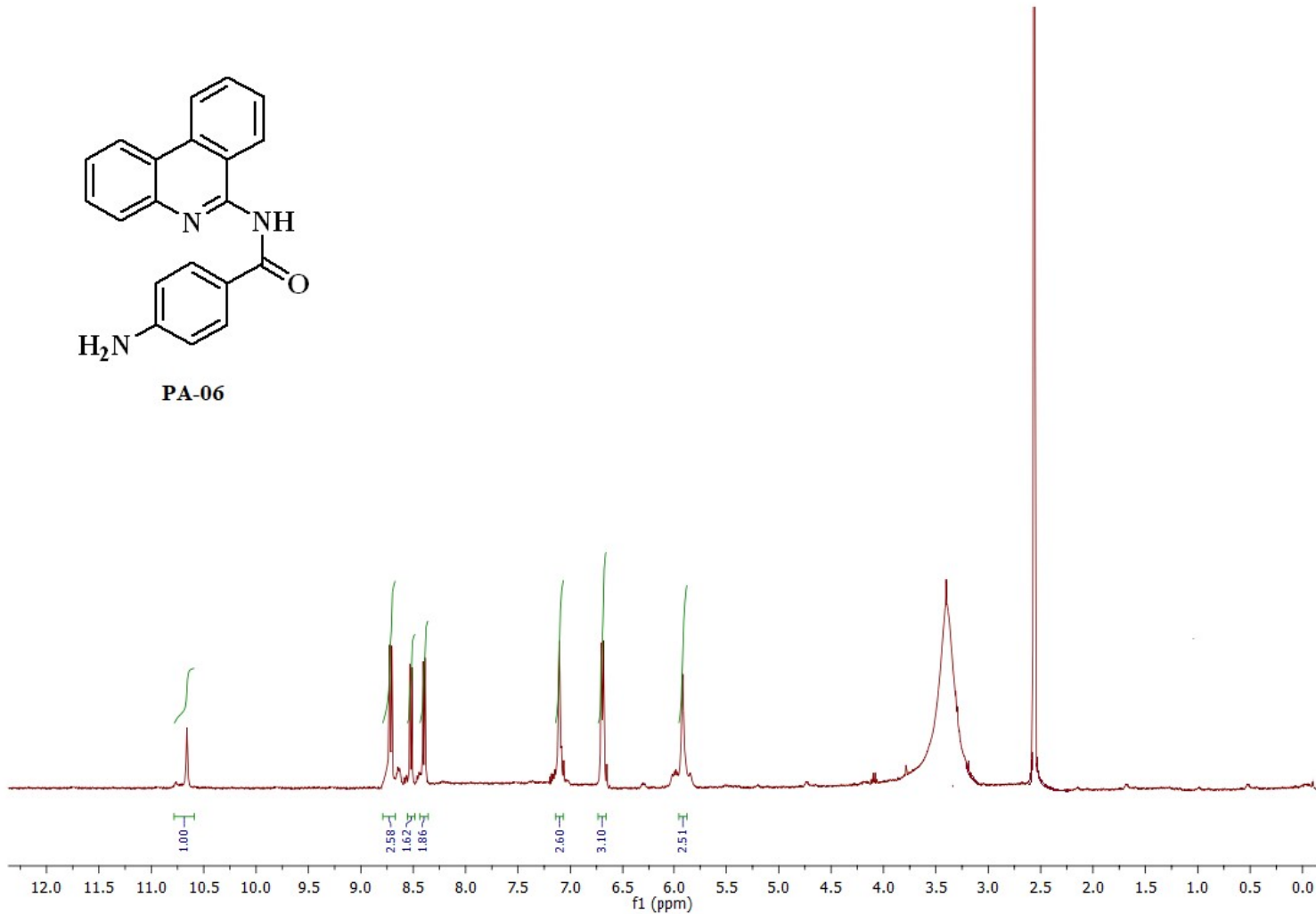
MS Zoomed Spectrum



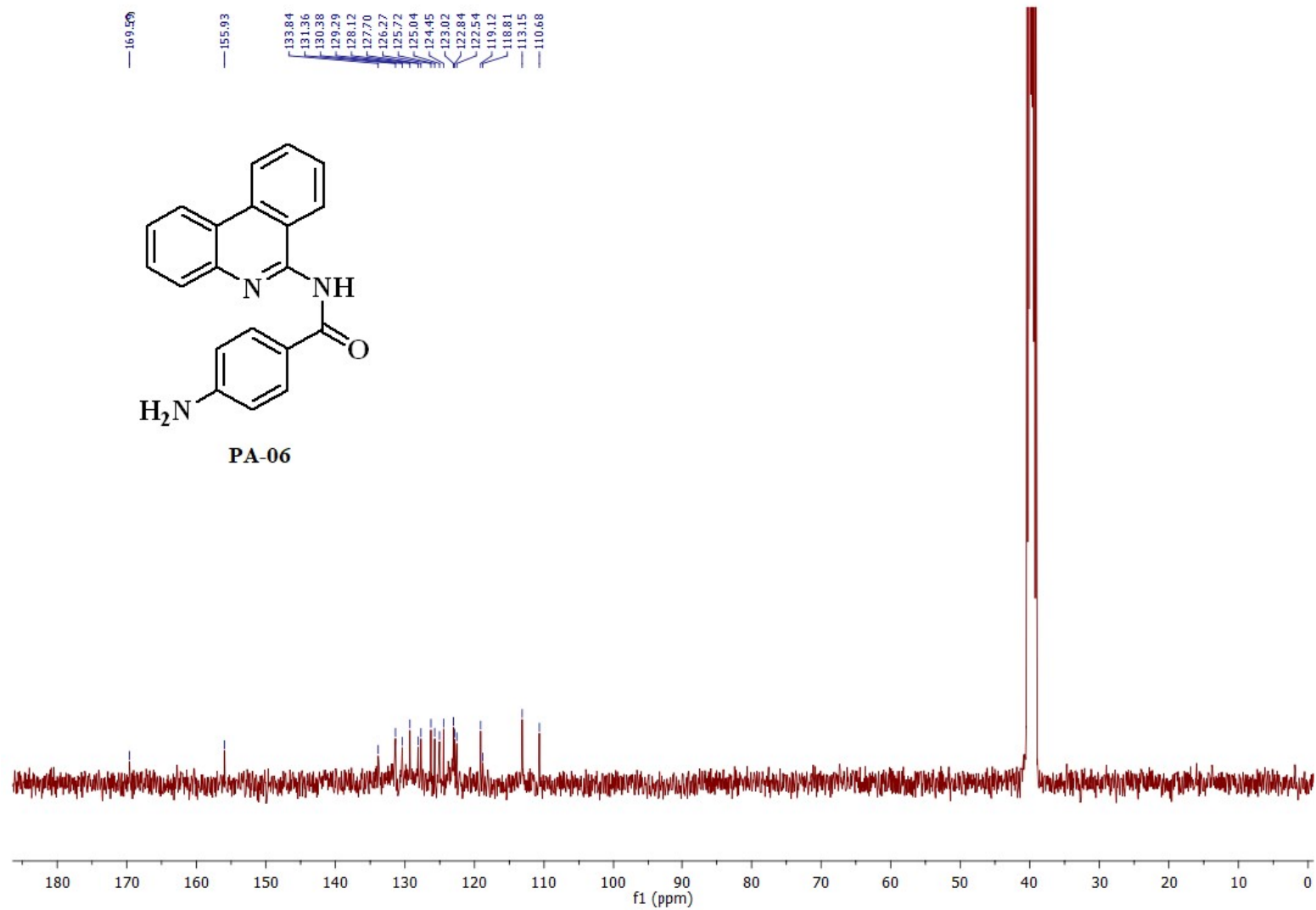
HRMS Mass spectra of compound PA-05



PA-06

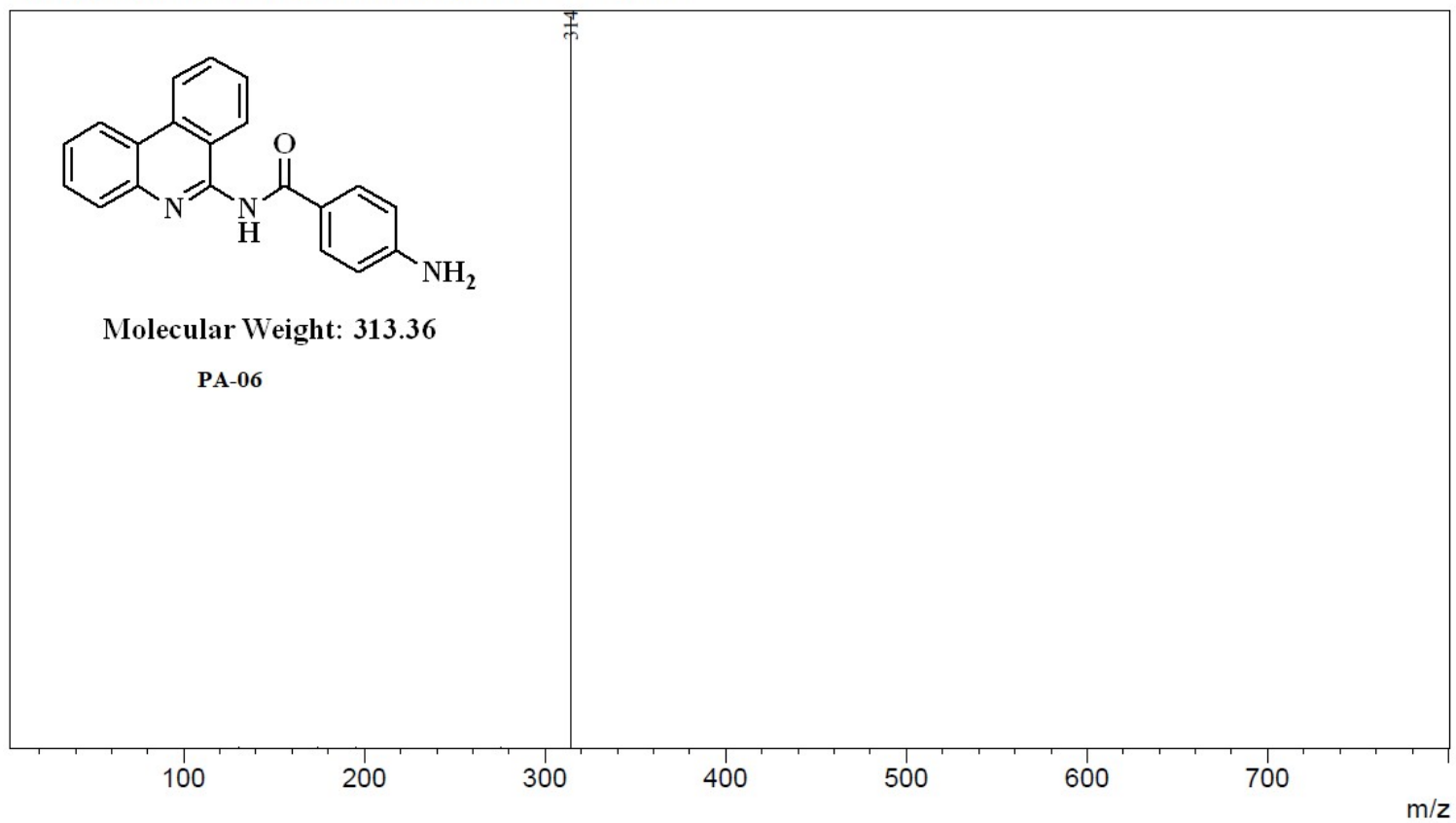


¹H NMR (400 MHz, DMSO-*d*₆) of PA-06

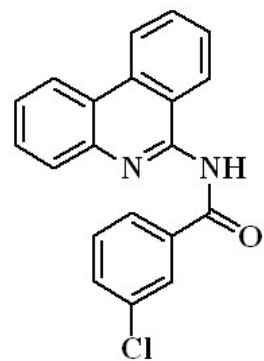


¹³C NMR (101 MHz, DMSO-*d*₆) of PA-06

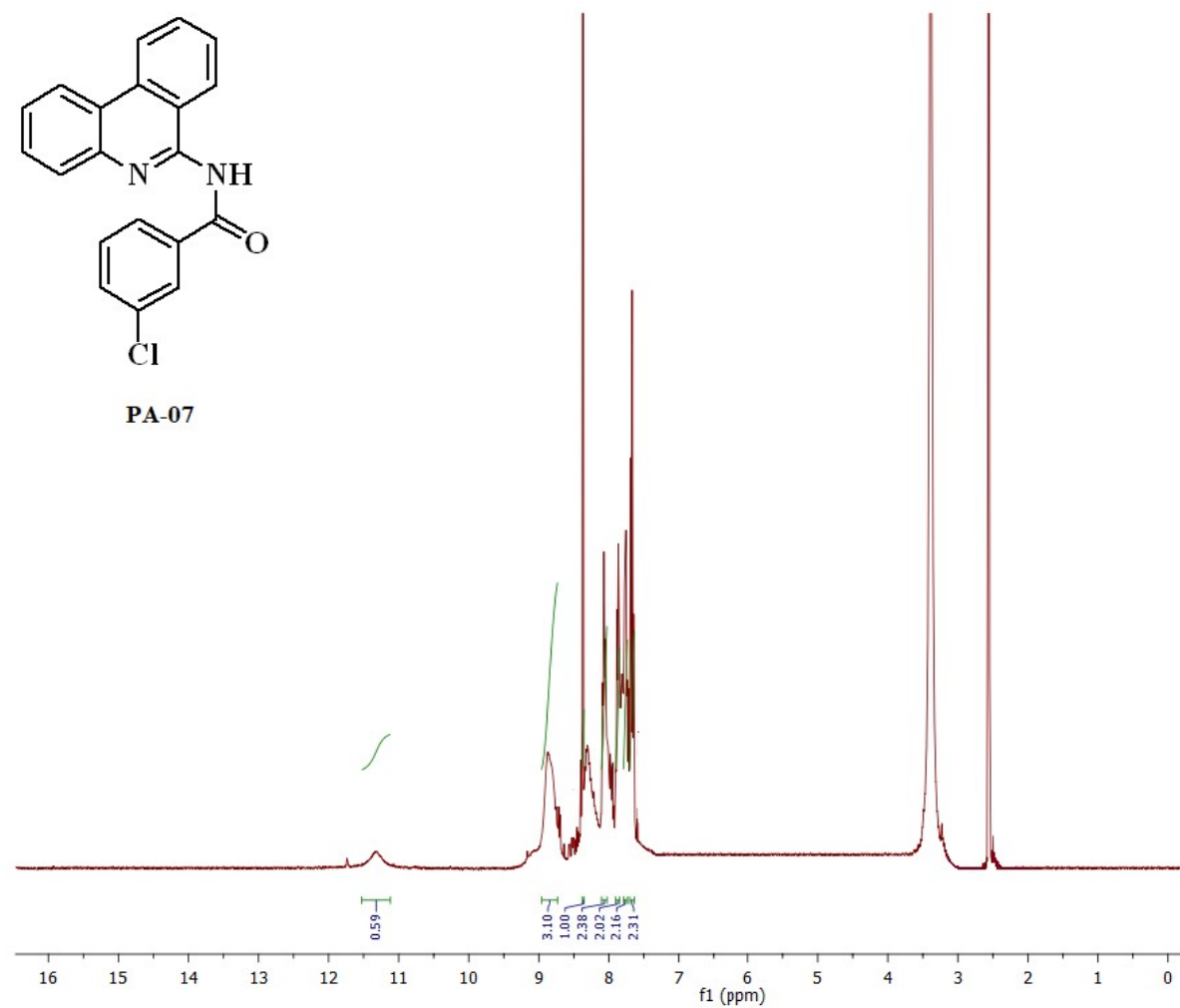
RawMode:Averaged 0.15-0.50(67-223) BasePeak:314(7547289)
BG Mode:Averaged 0.00-0.14(1-63) Segment 1 - Event 1



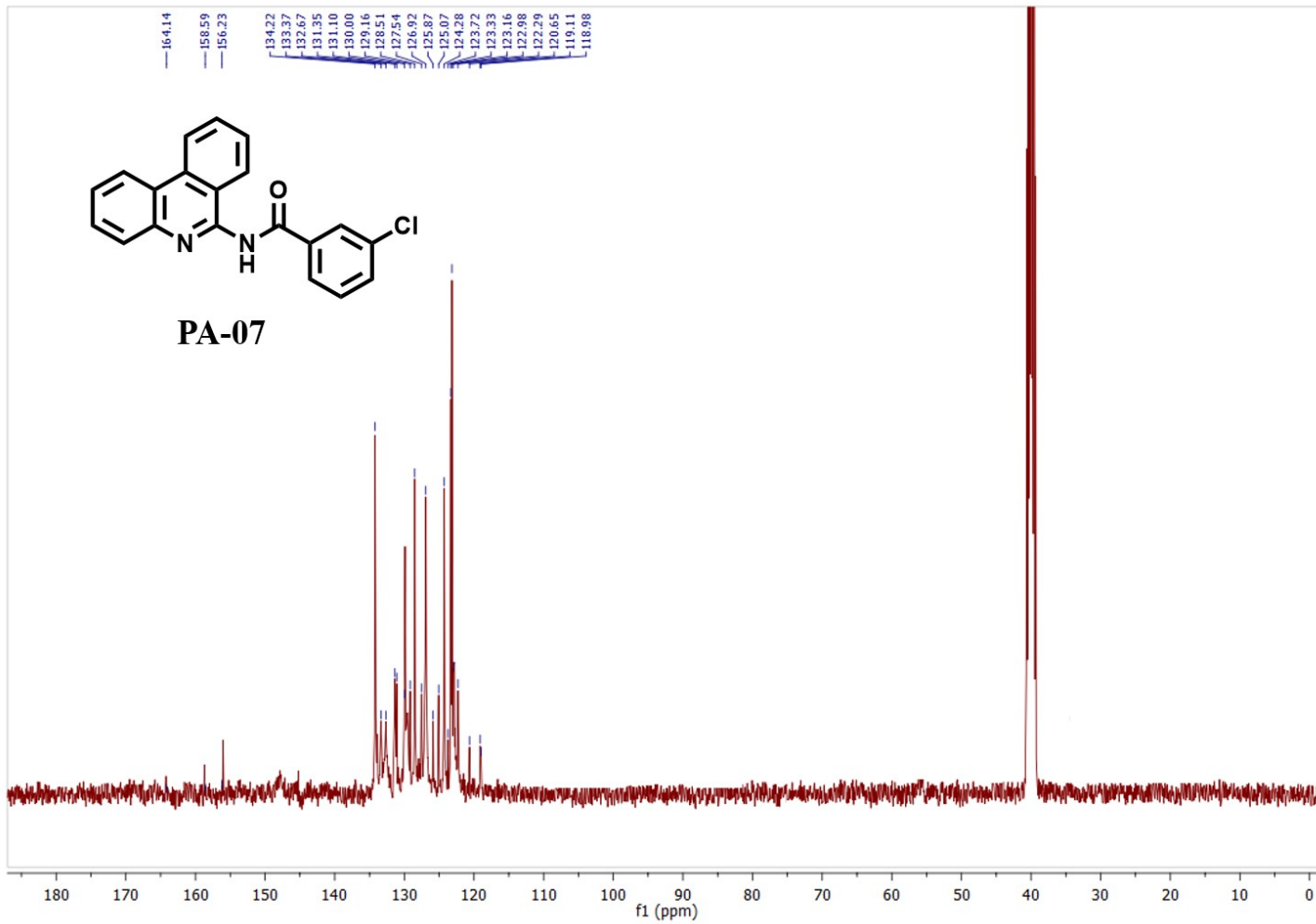
Mass spectra of compound PA-06



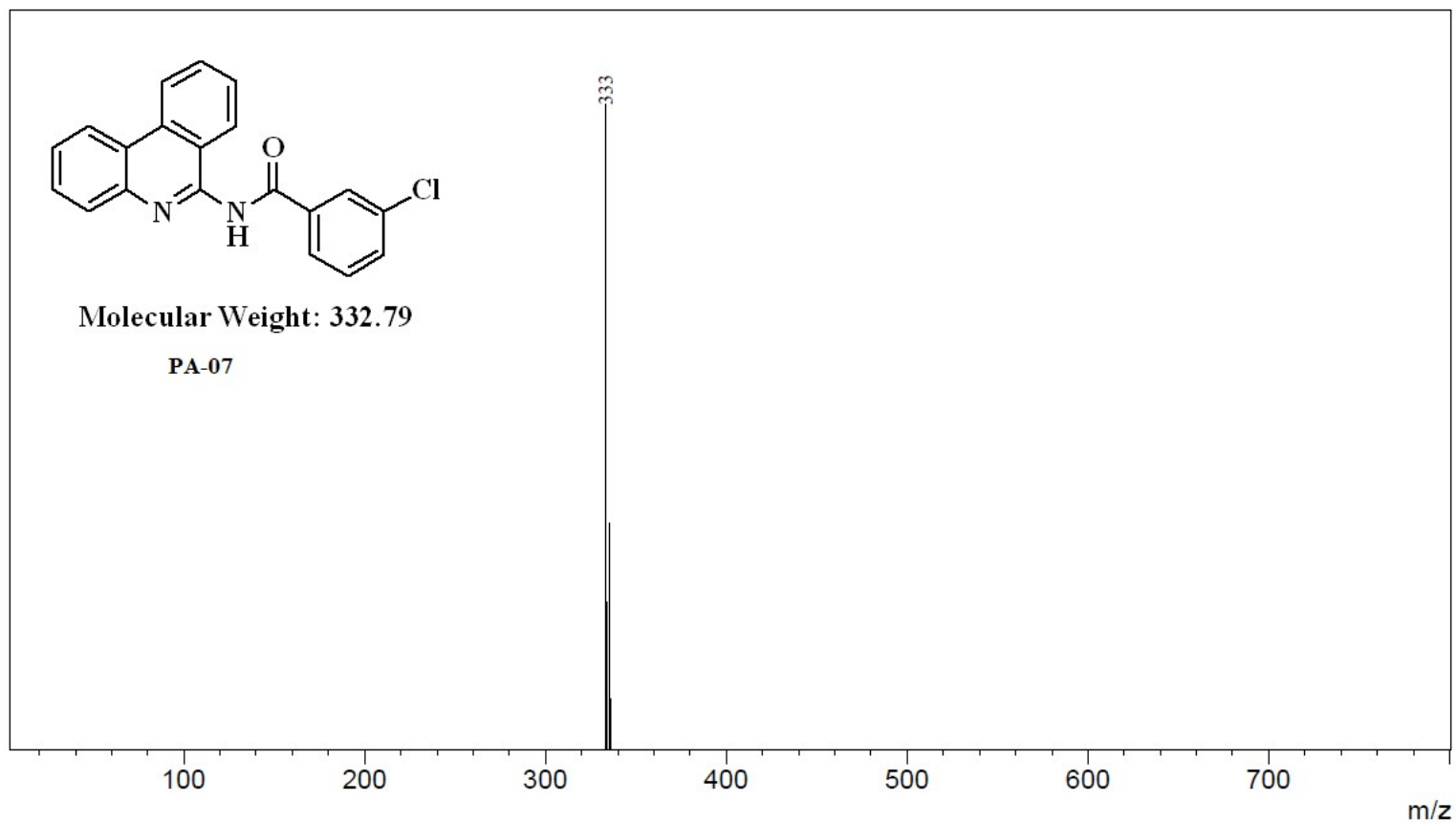
PA-07



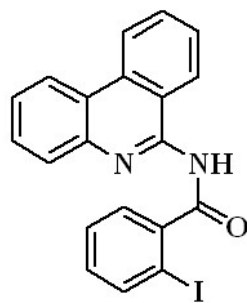
^1H NMR (400 MHz, DMSO- d_6) of PA-07



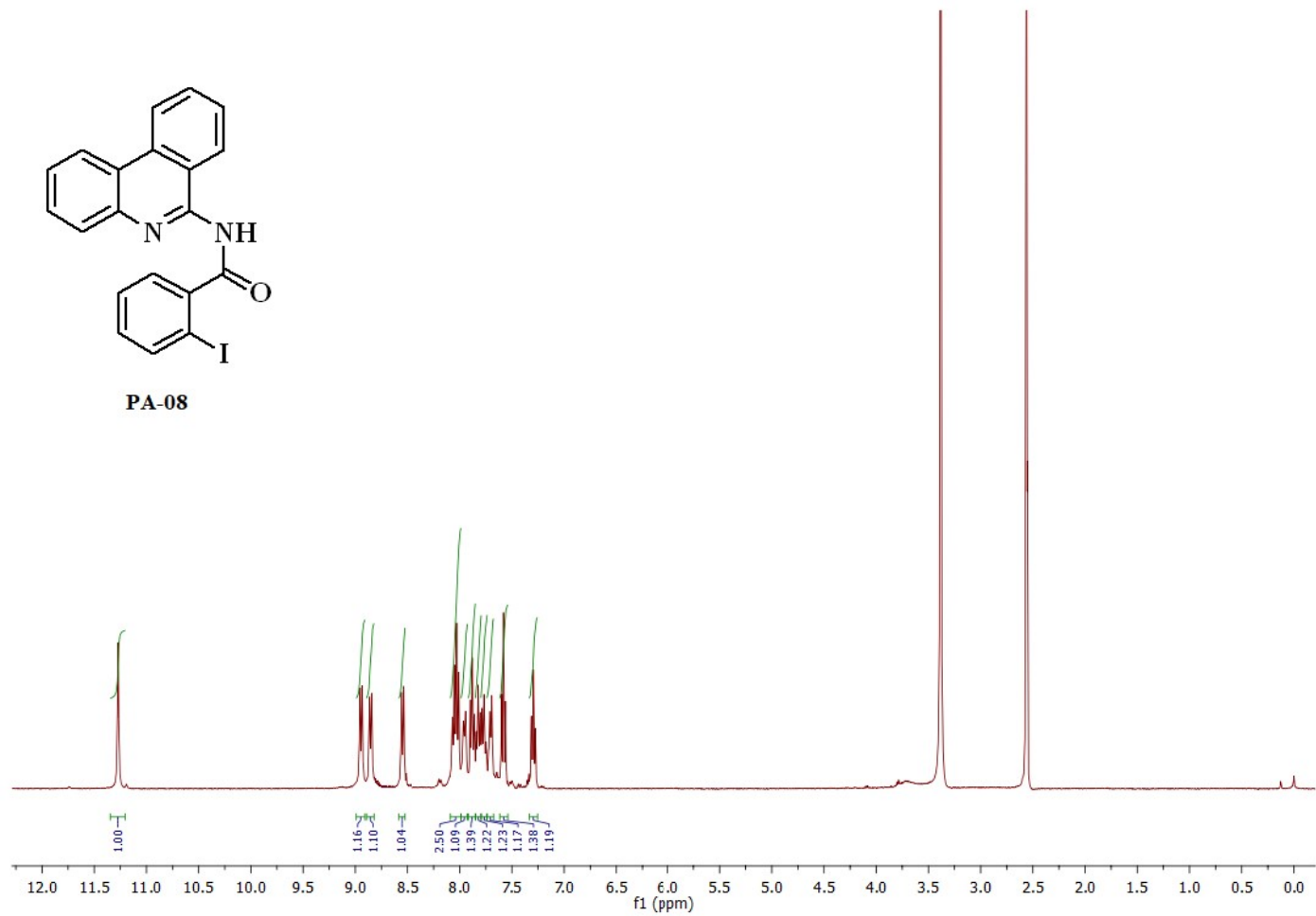
RawMode:Averaged 0.16-0.50(71-221) BasePeak:333(3697555)
BG Mode:Averaged 0.00-0.15(1-67) Segment 1 - Event 1



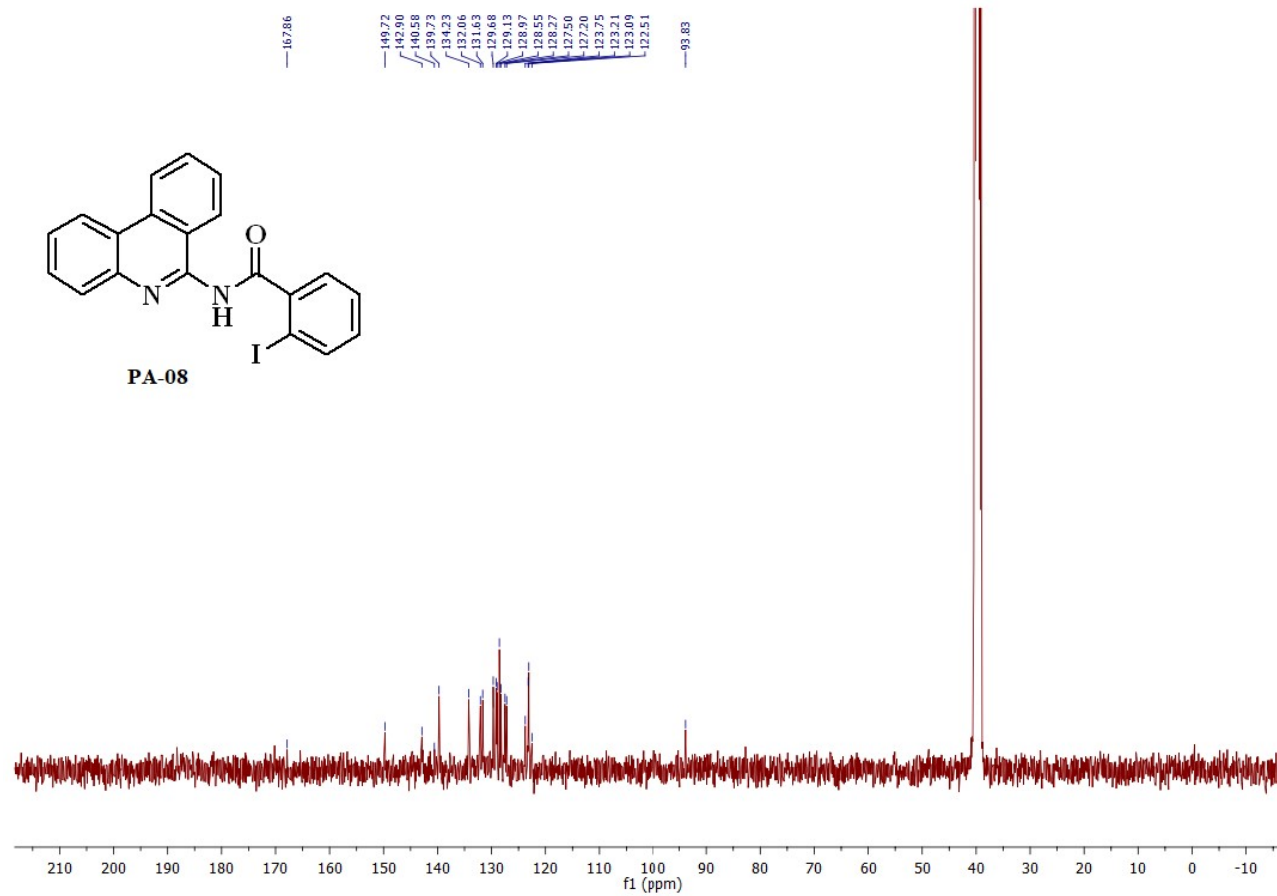
Mass spectra of compound PA-07



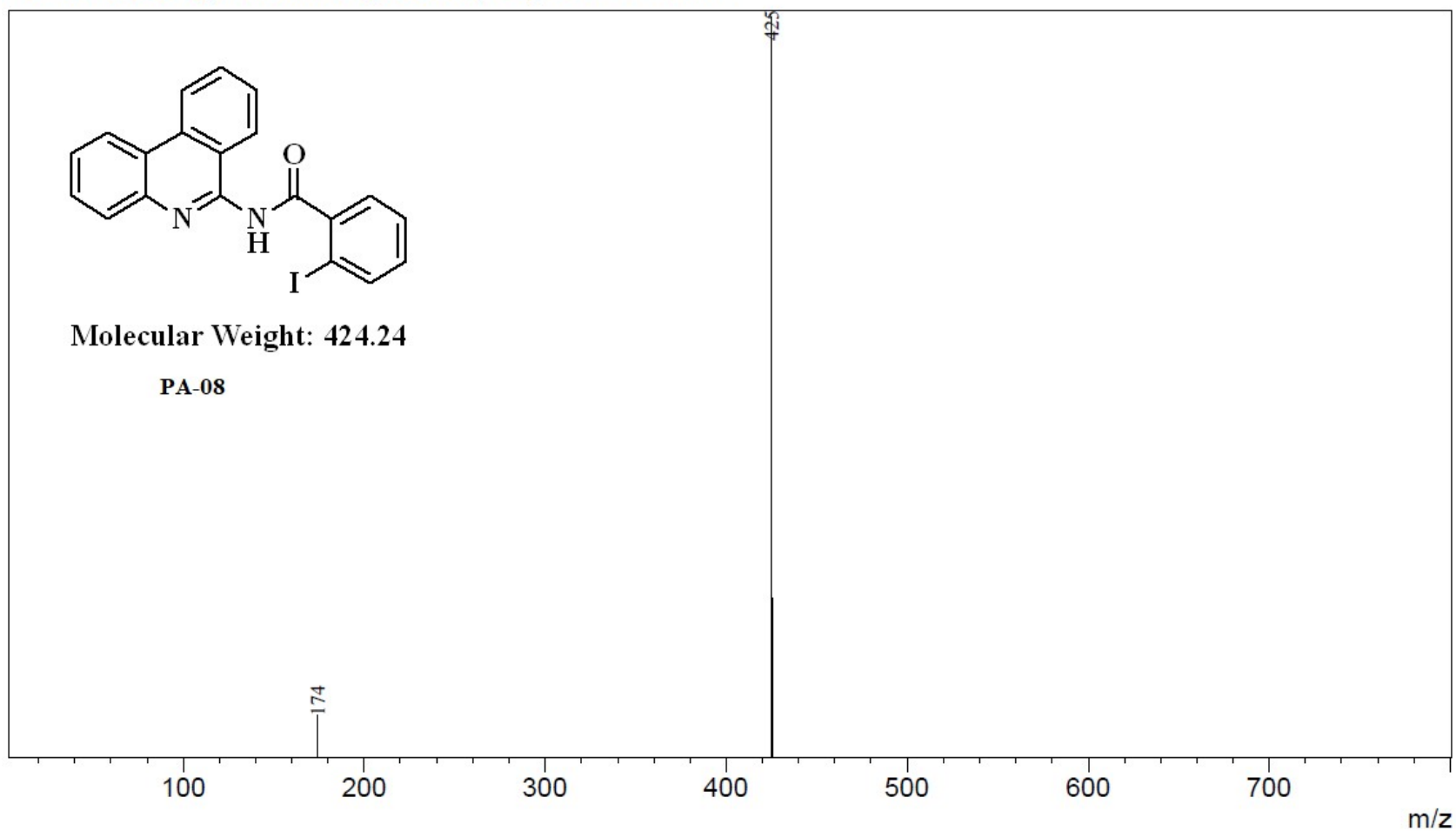
PA-08



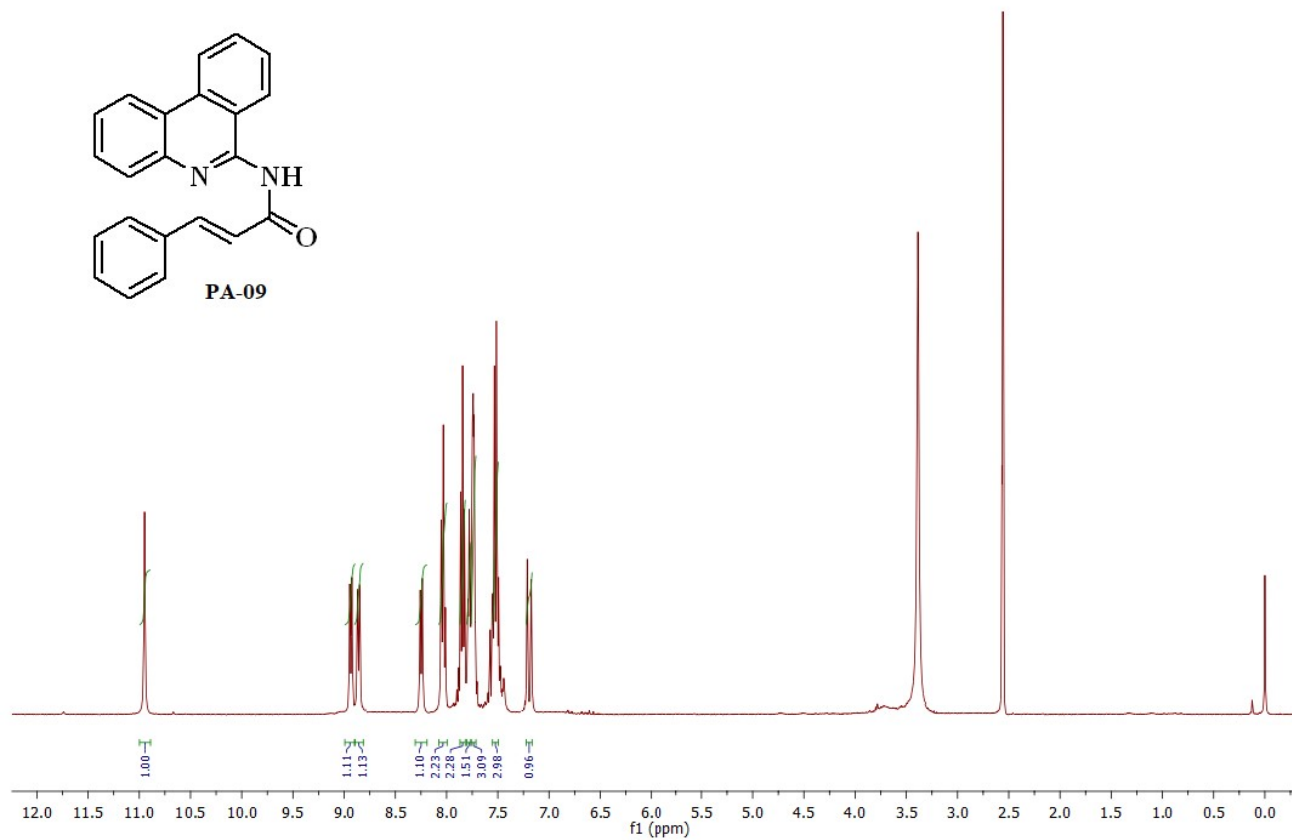
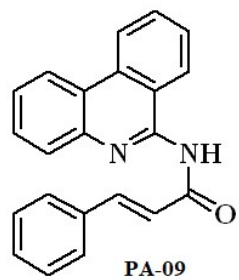
¹H NMR (400 MHz, DMSO-*d*₆) of PA-08



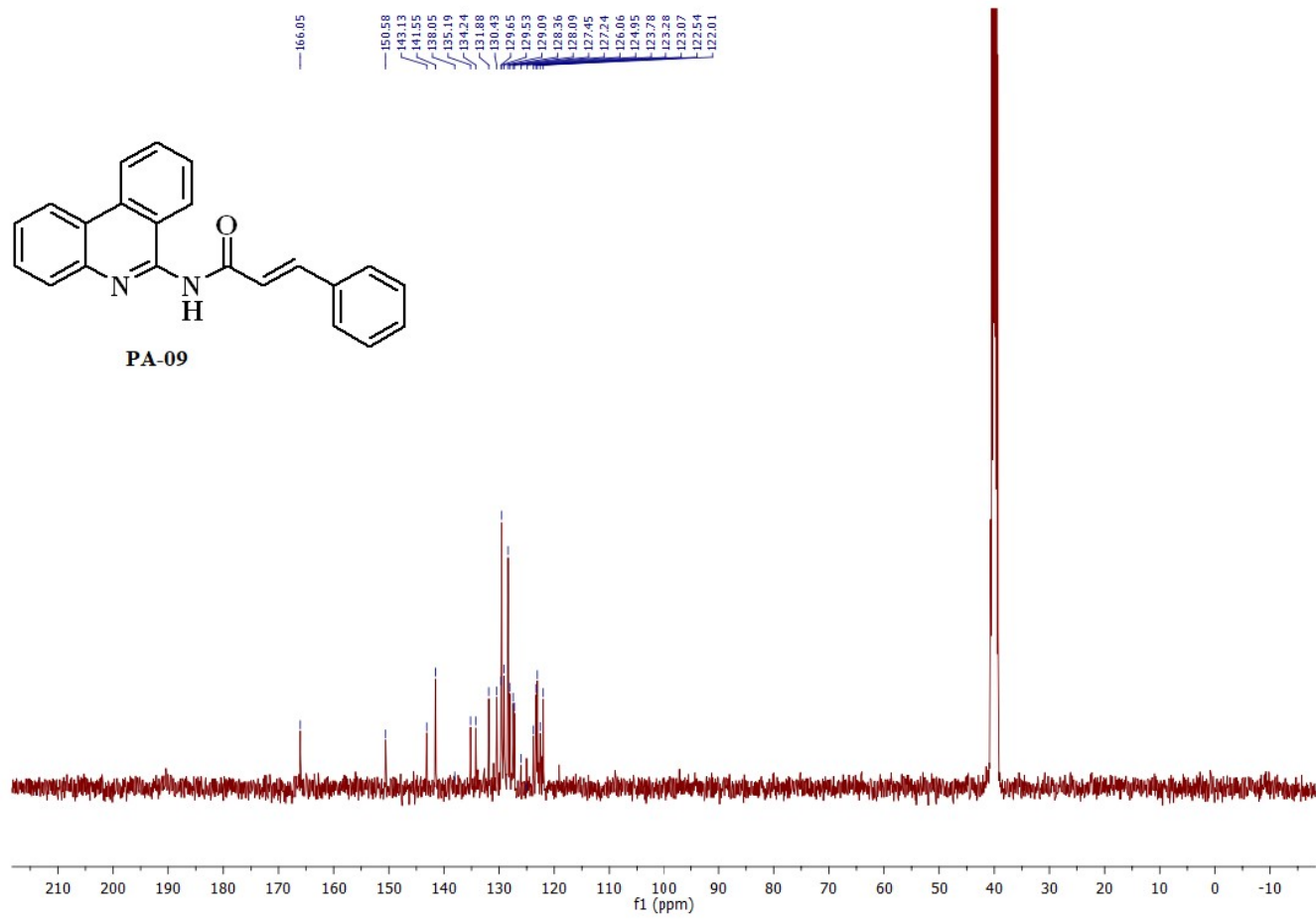
RawMode:Averaged 0.15-0.50(67-223) BasePeak:425(11293392)
BG Mode:Averaged 0.50-2.00(223-889) Segment 1 - Event 1



Mass spectra of compound PA-08

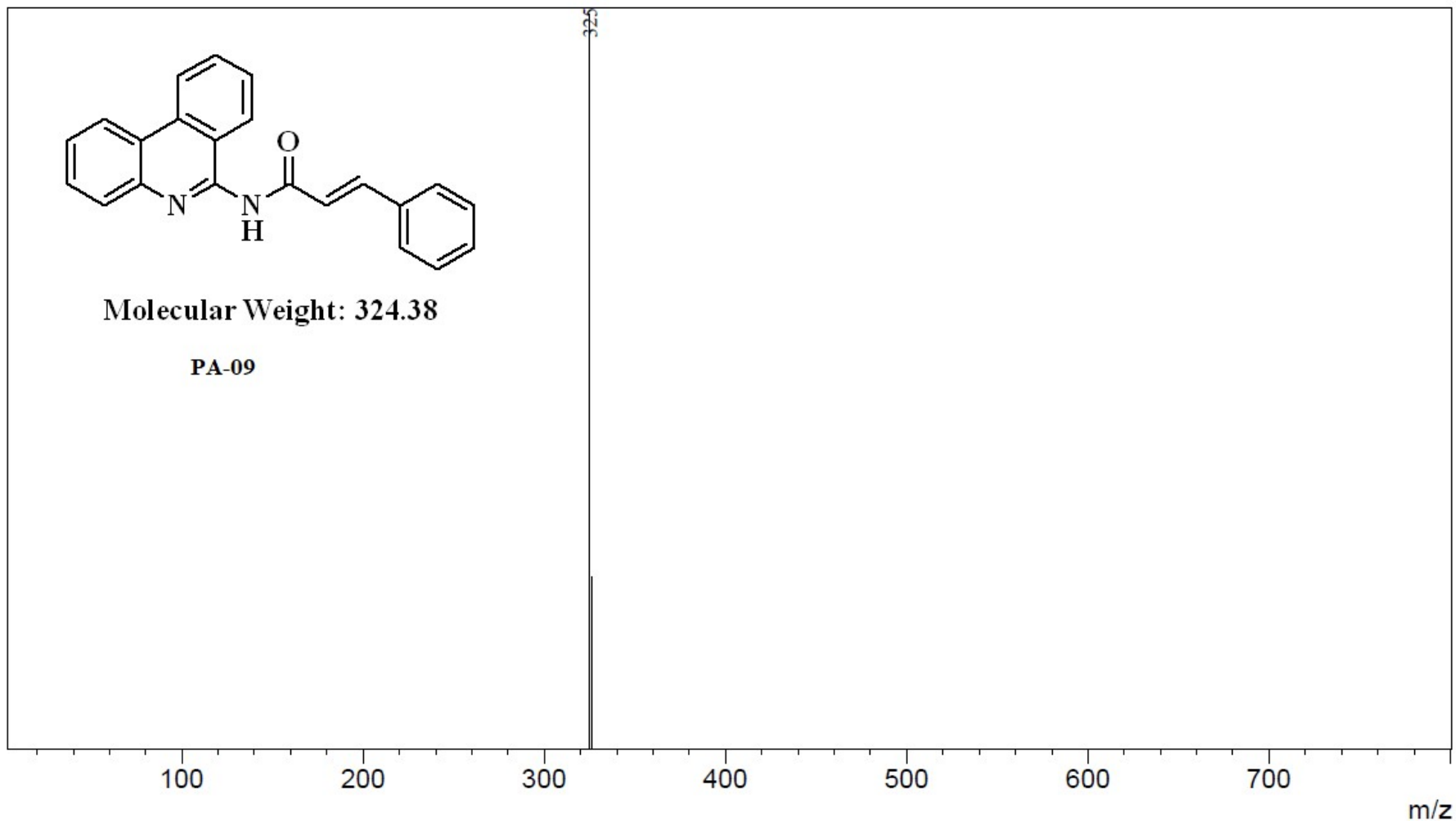


¹H NMR (400 MHz, DMSO-*d*₆) of PA-09

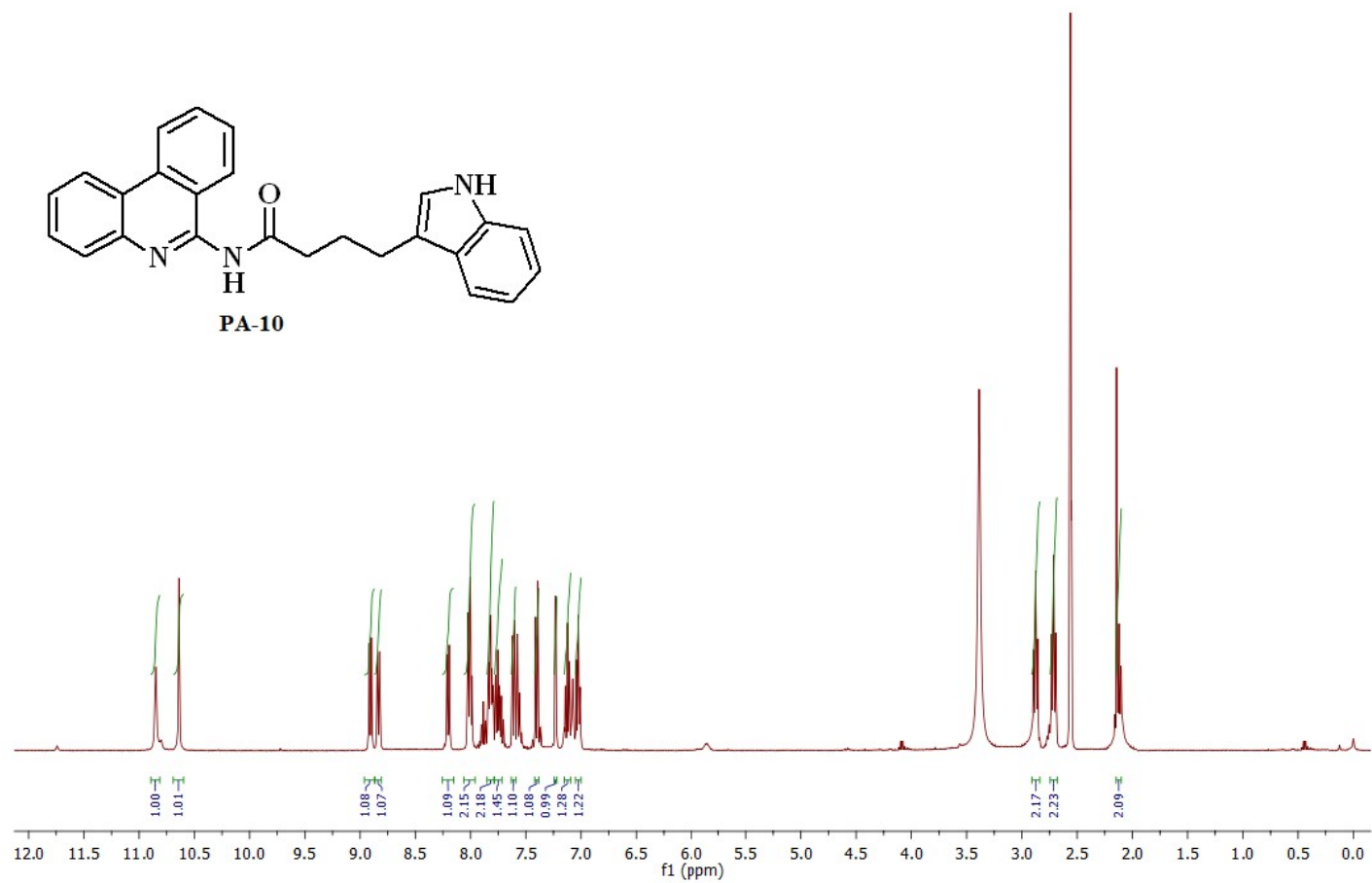


¹³C NMR (101 MHz, DMSO-*d*₆) of PA-09

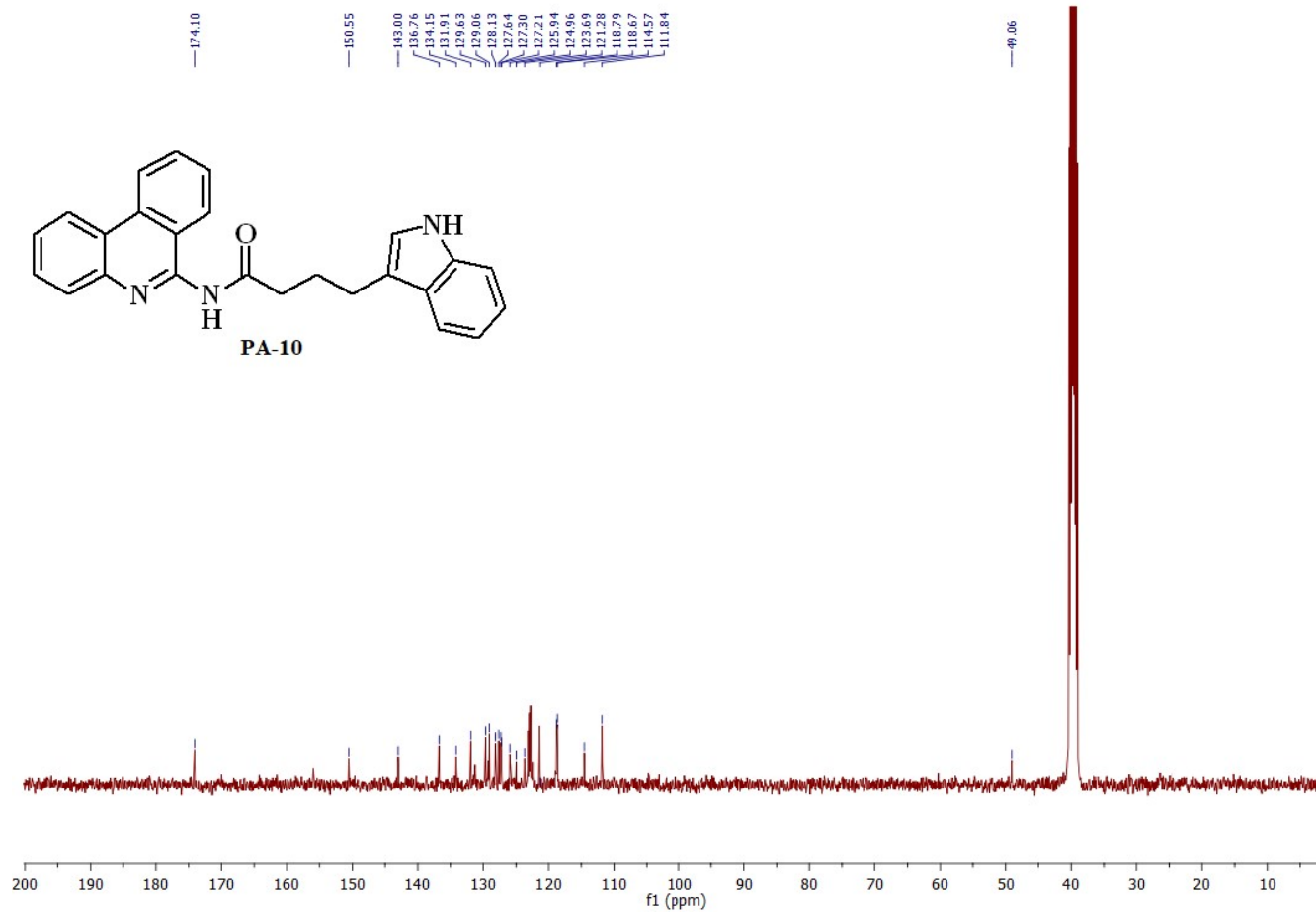
RawMode:Averaged 0.16-0.50(71-223) BasePeak:325(8992613)
BG Mode:Averaged 0.00-0.13(1-59) Segment 1 - Event 1



Mass spectra of compound PA-09

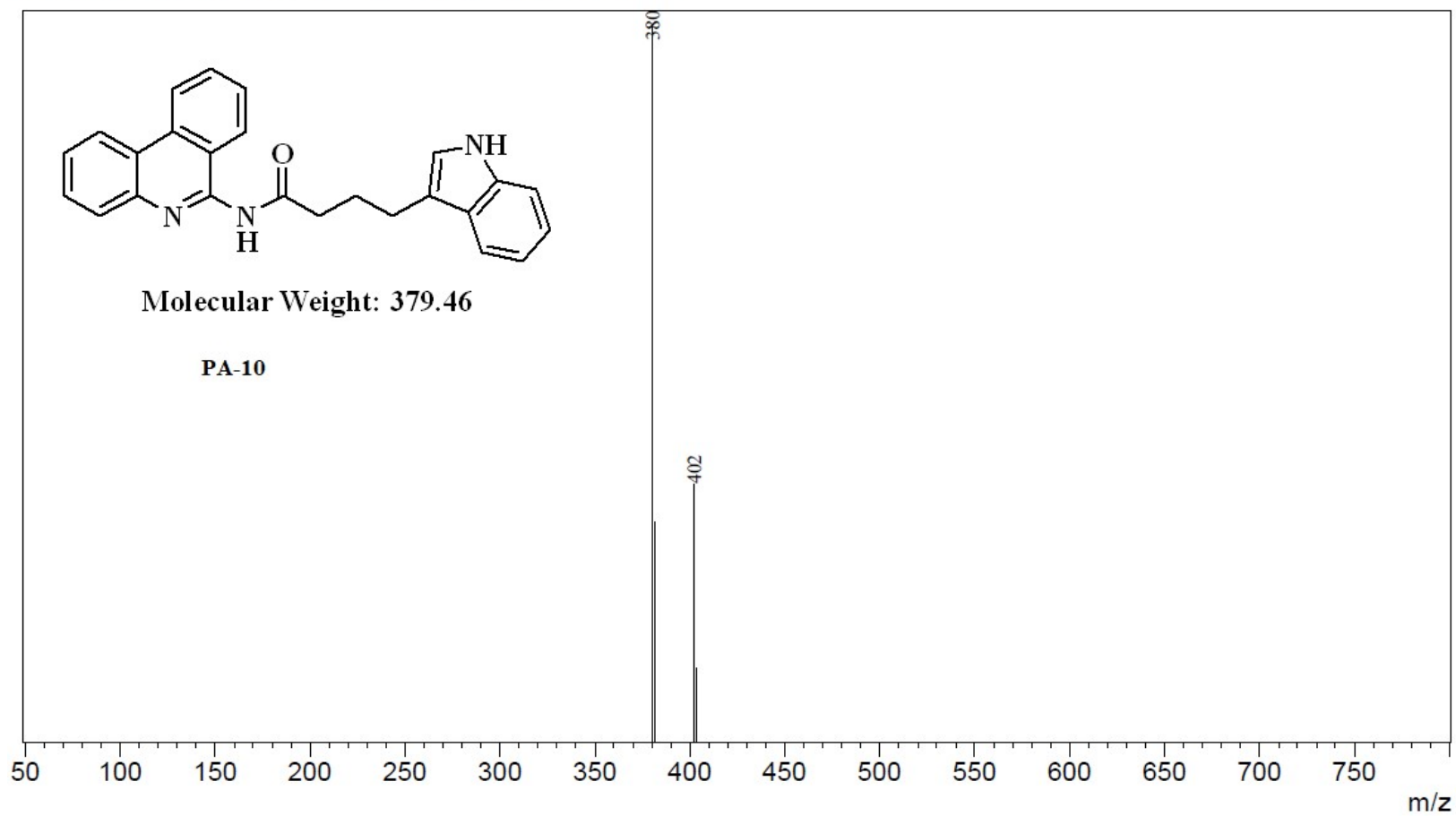


^1H NMR (400 MHz, DMSO- d_6) of PA-10

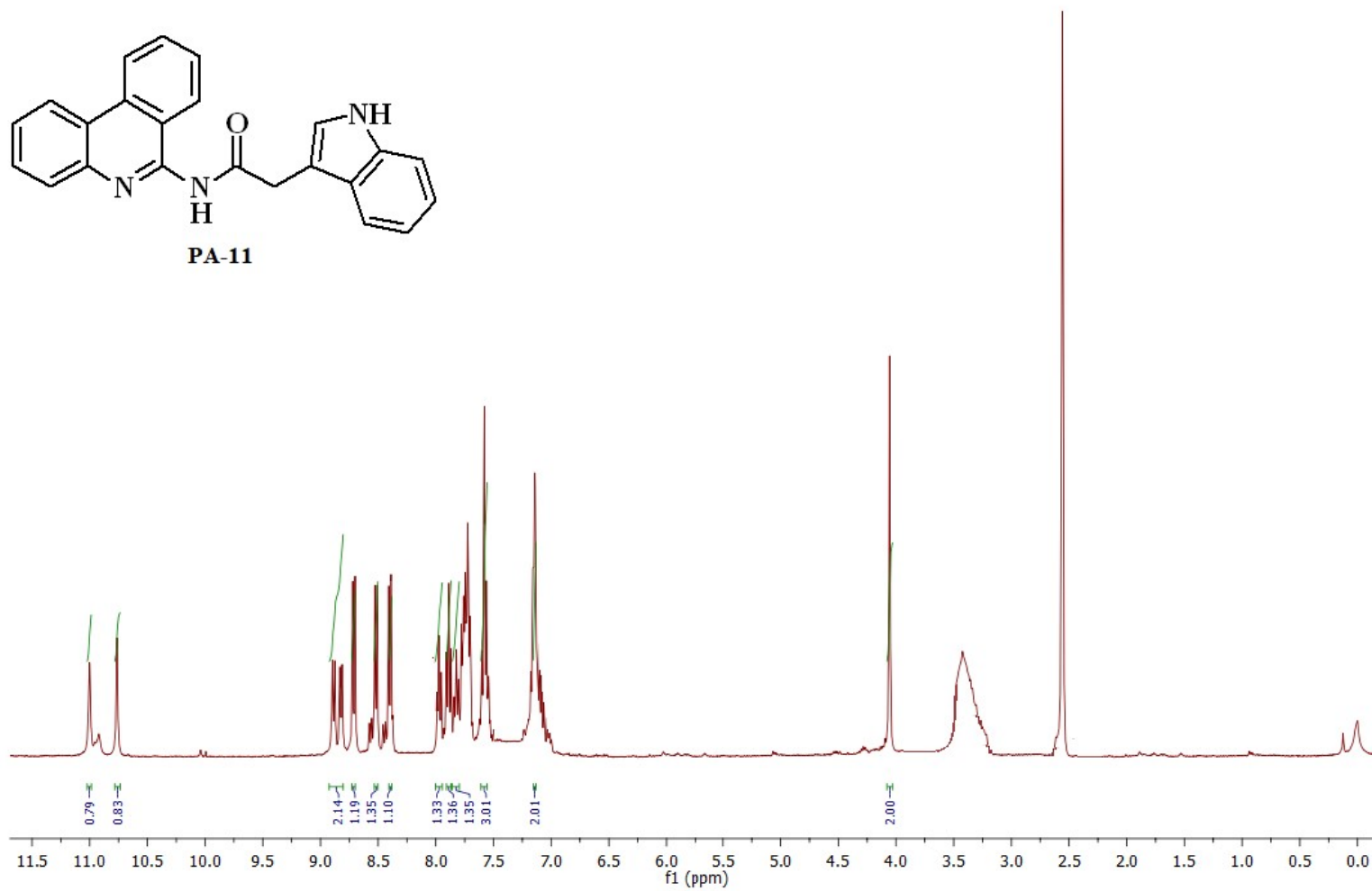
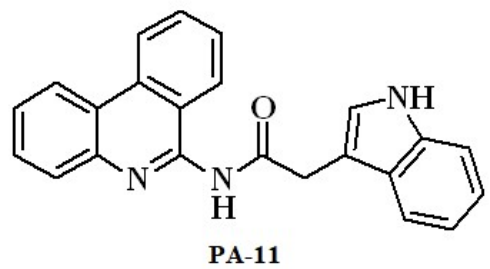


¹³C NMR (101 MHz, DMSO-*d*₆) of PA-10

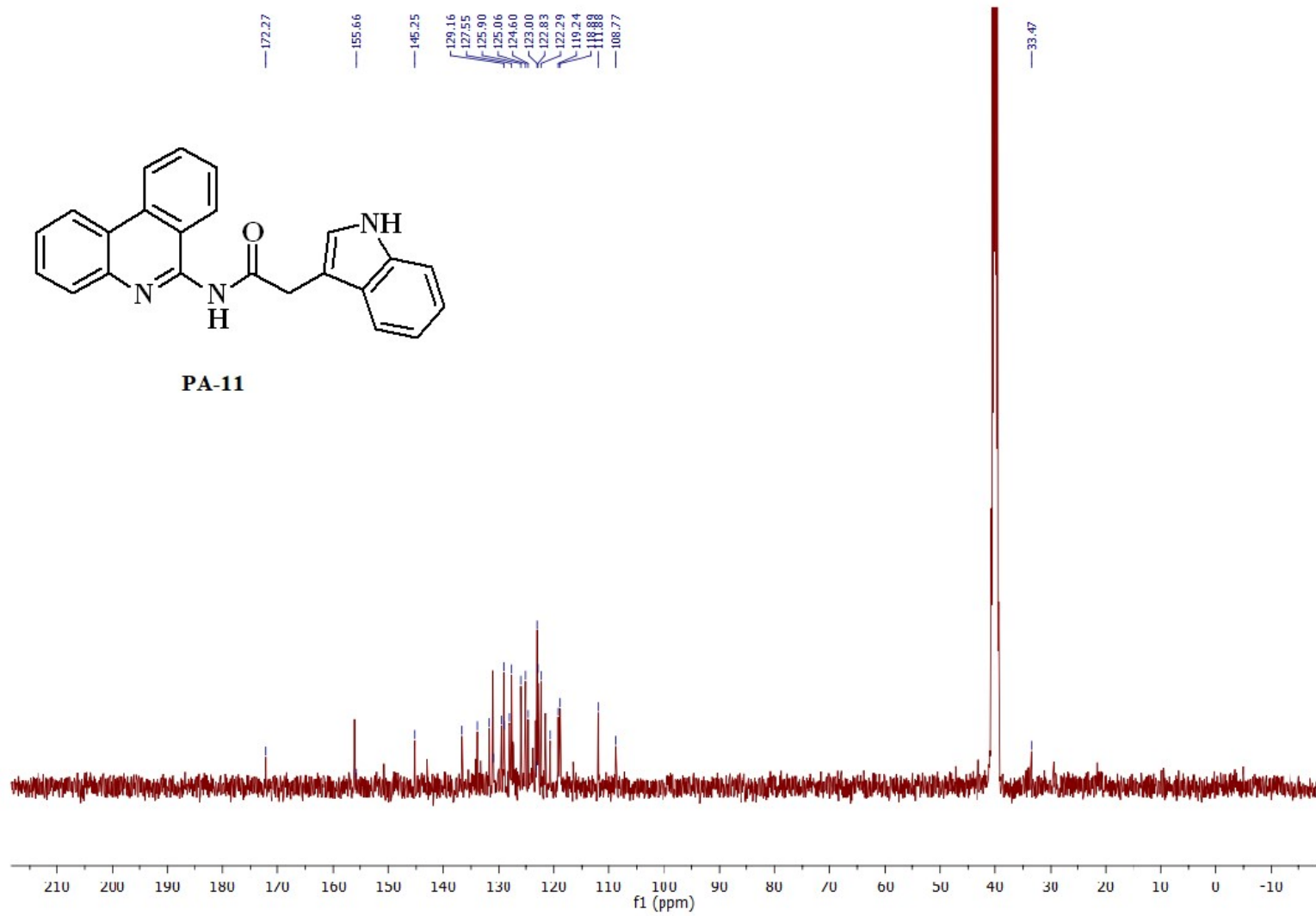
RawMode:Averaged 0.13-0.51(53-211) BasePeak:380(3293119)
BG Mode:Averaged 0.00-0.12(1-51) Segment 1 - Event 1



Mass spectra of compound PA-10

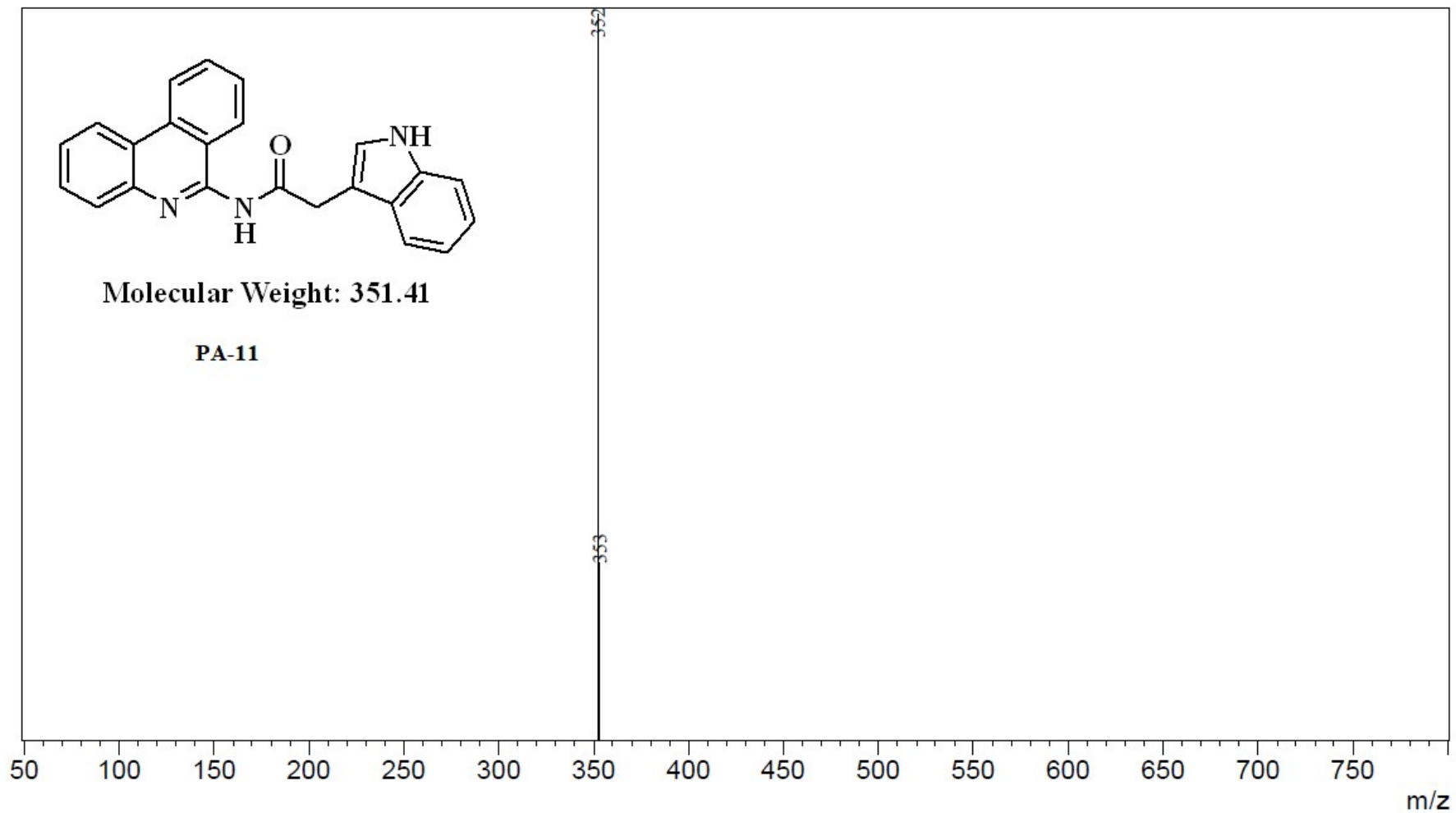


¹H NMR (400 MHz, DMSO-*d*₆) of PA-11

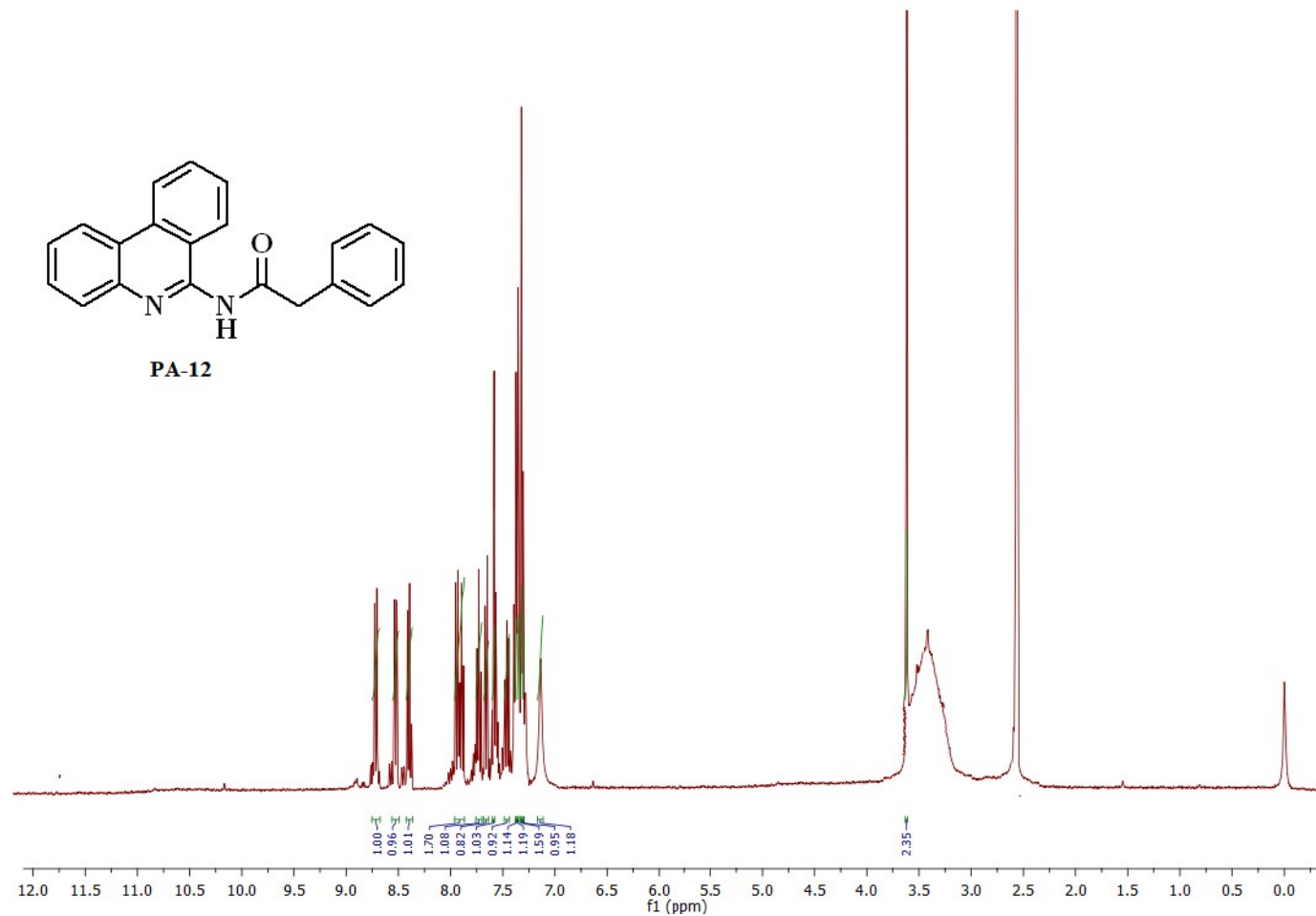


¹³C NMR (101 MHz, DMSO-*d*₆) of PA-11

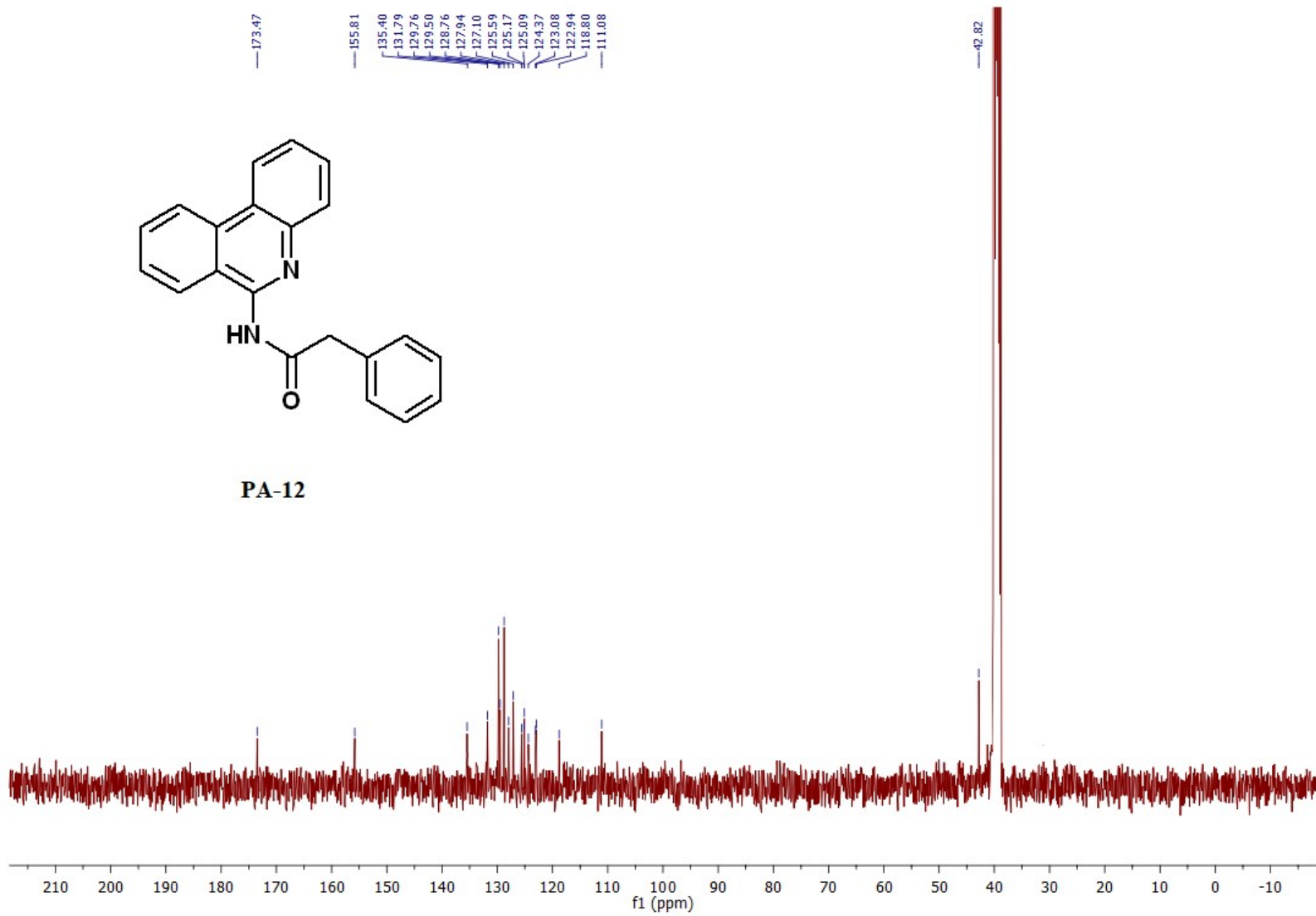
RawMode:Averaged 0.12-0.50(51-209) BasePeak:352(3481387)
BG Mode:Averaged 0.00-0.13(1-55) Segment 1 - Event 1



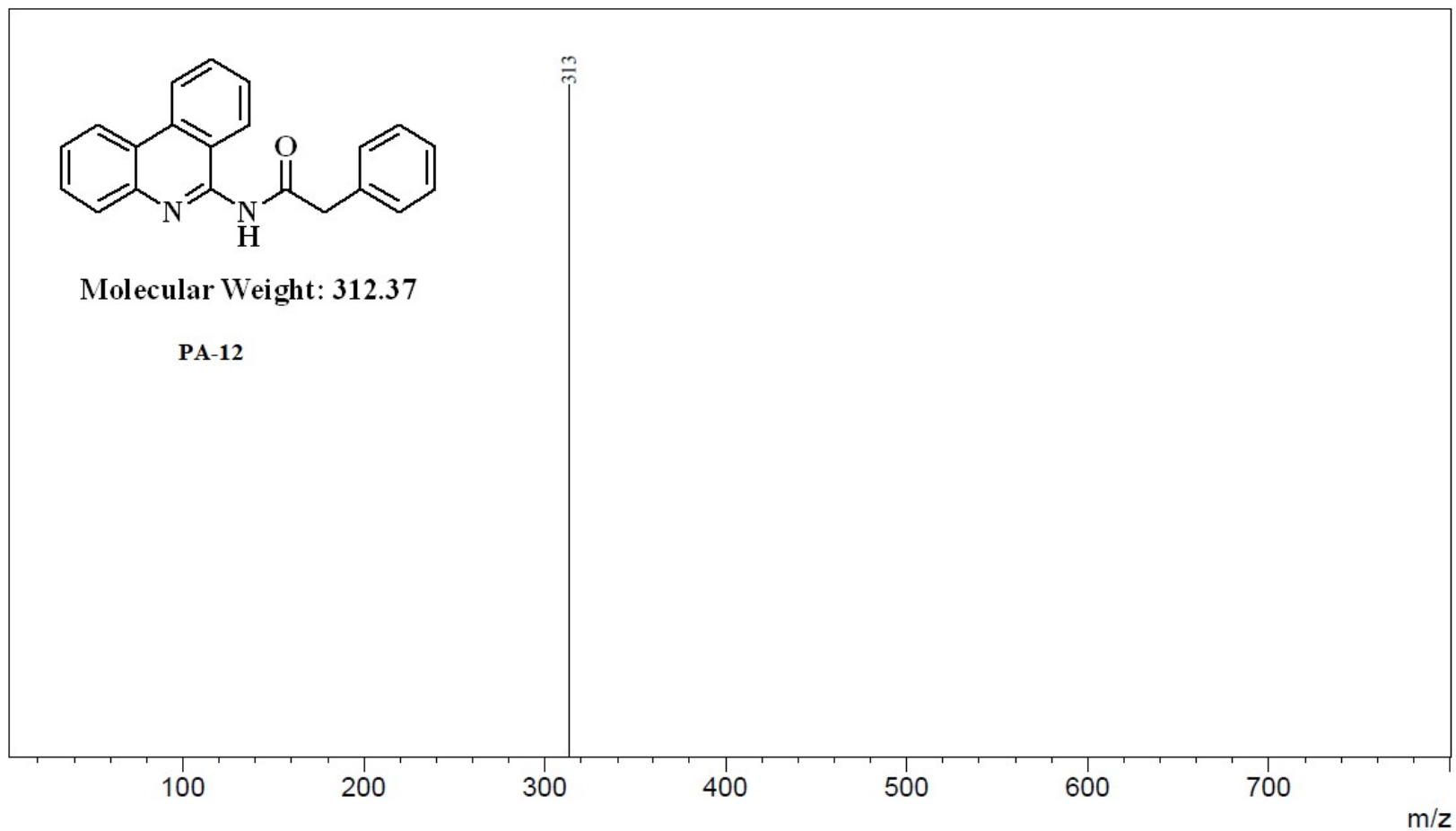
Mass spectra of compound PA-11



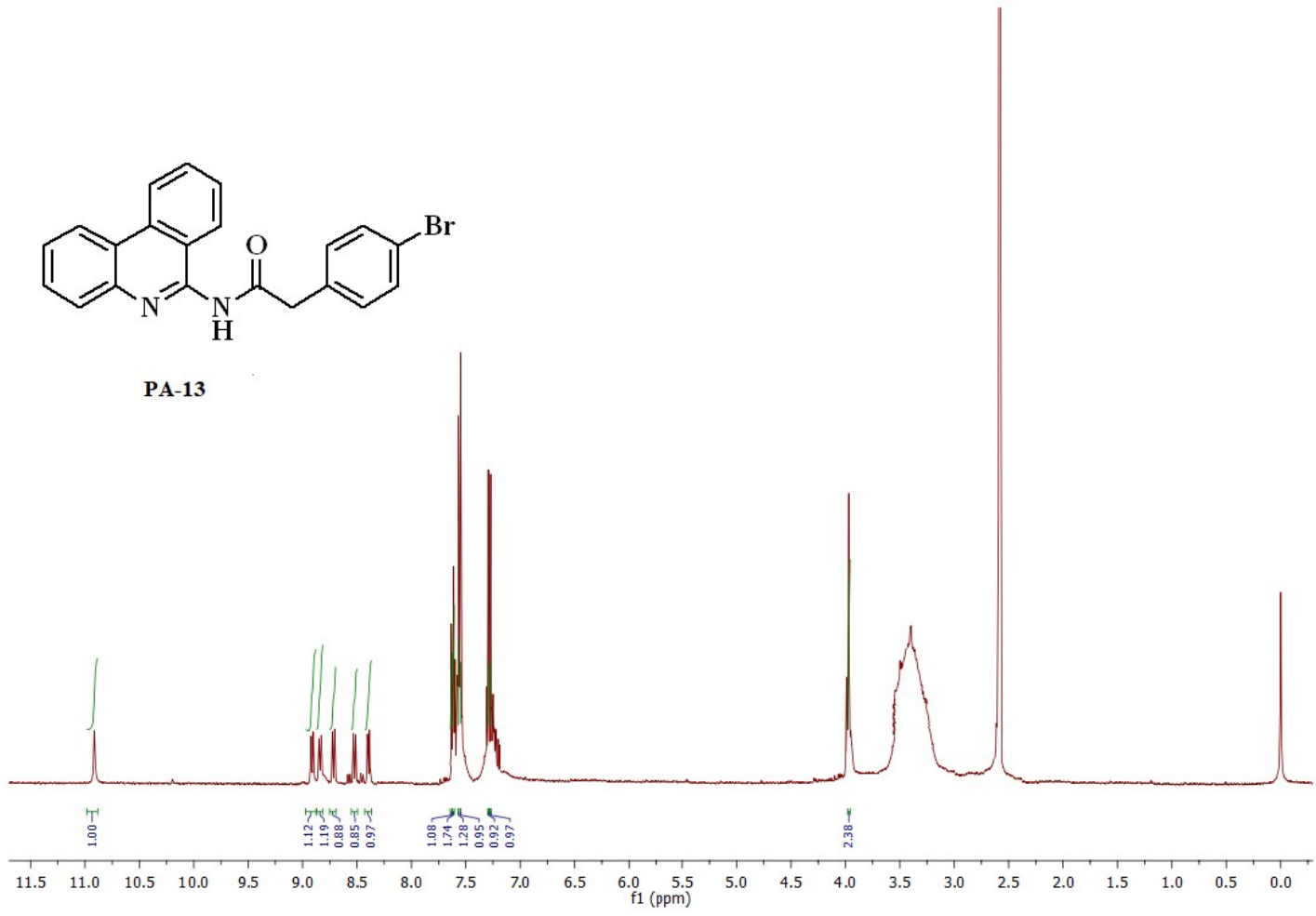
¹H NMR (400 MHz, DMSO-*d*₆) of PA-12



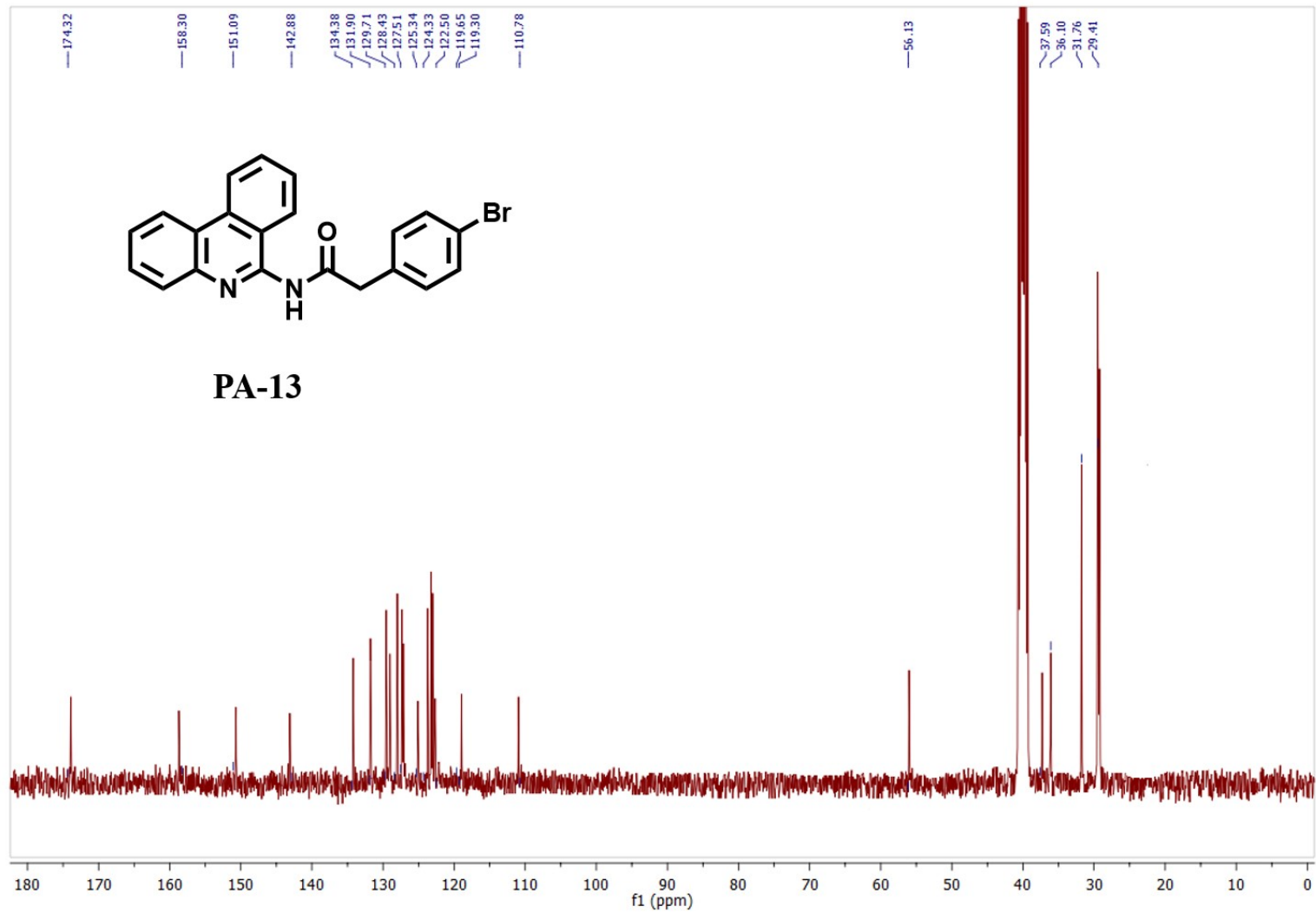
RawMode:Averaged 0.15-0.50(67-223) BasePeak:313(13263507)
BG Mode:Averaged 0.00-0.15(1-67) Segment 1 - Event 1



Mass spectra of compound PA-12

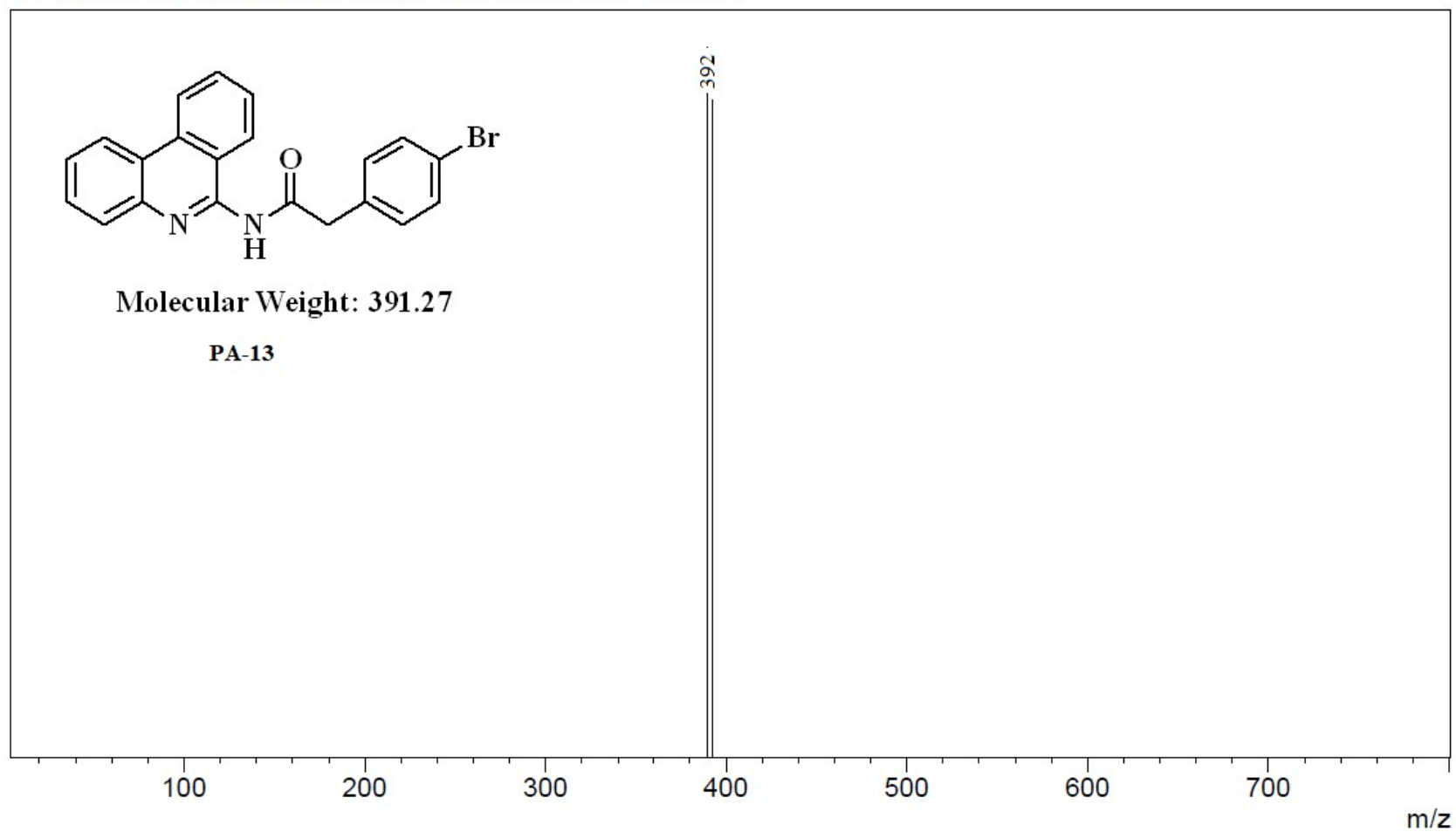


¹H NMR (400 MHz, DMSO-*d*₆) of PA-13

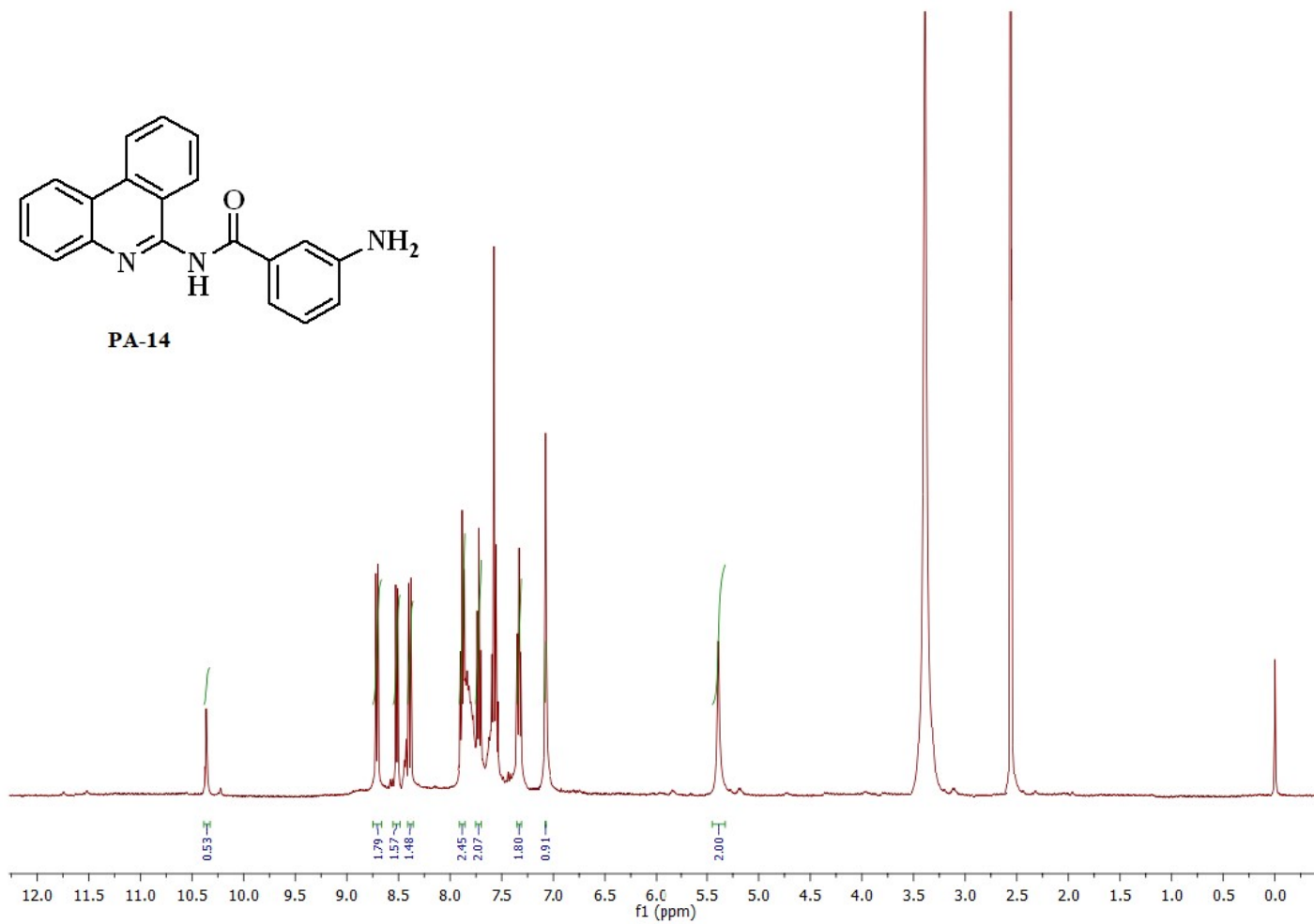


¹³C NMR (101 MHz, DMSO-*d*₆) of PA-13

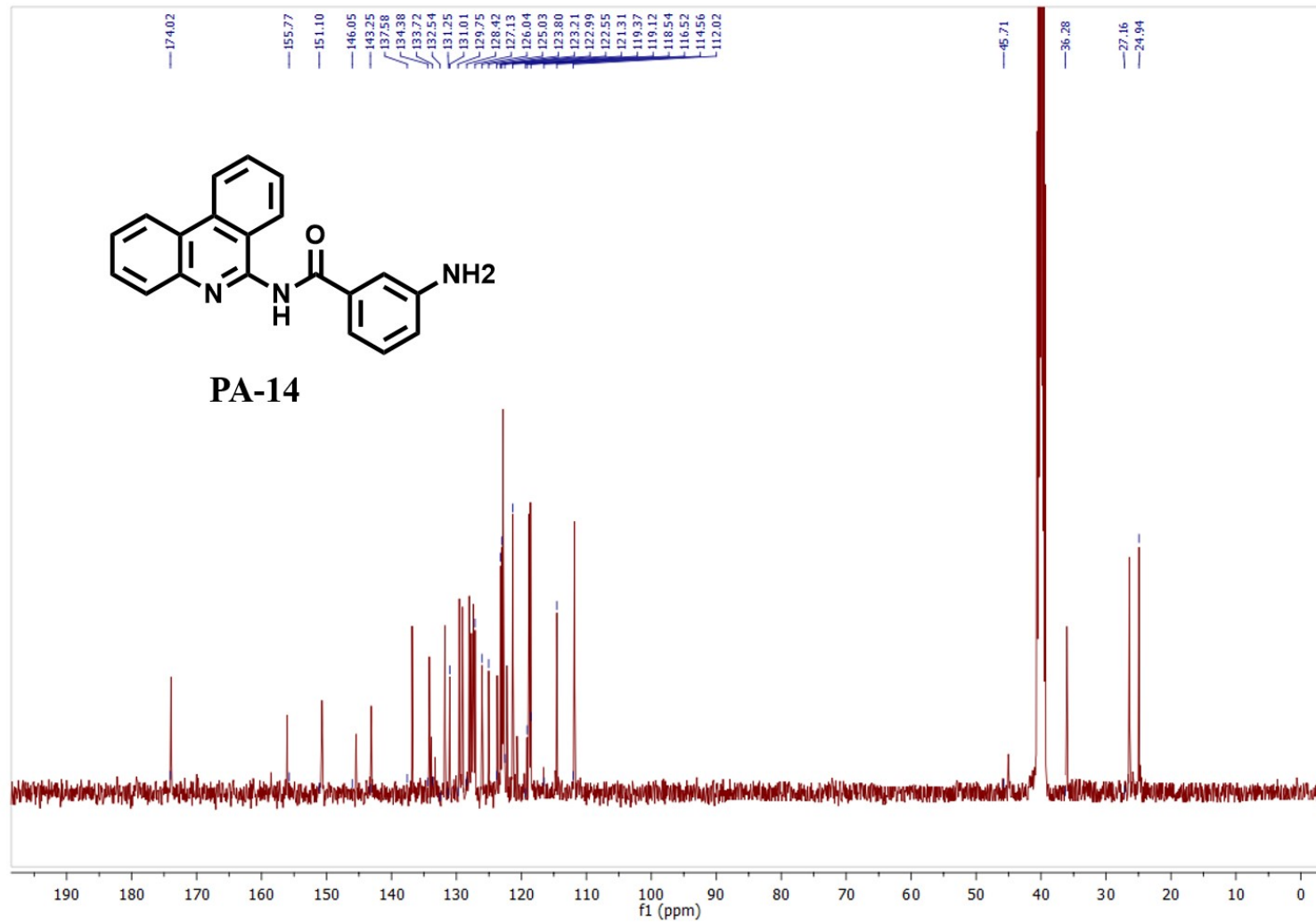
RawMode:Averaged 0.14-0.50(63-223) BasePeak:392(9999698)
BG Mode:Averaged 0.50-2.00(223-889) Segment 1 - Event 1



Mass spectra of compound PA-13

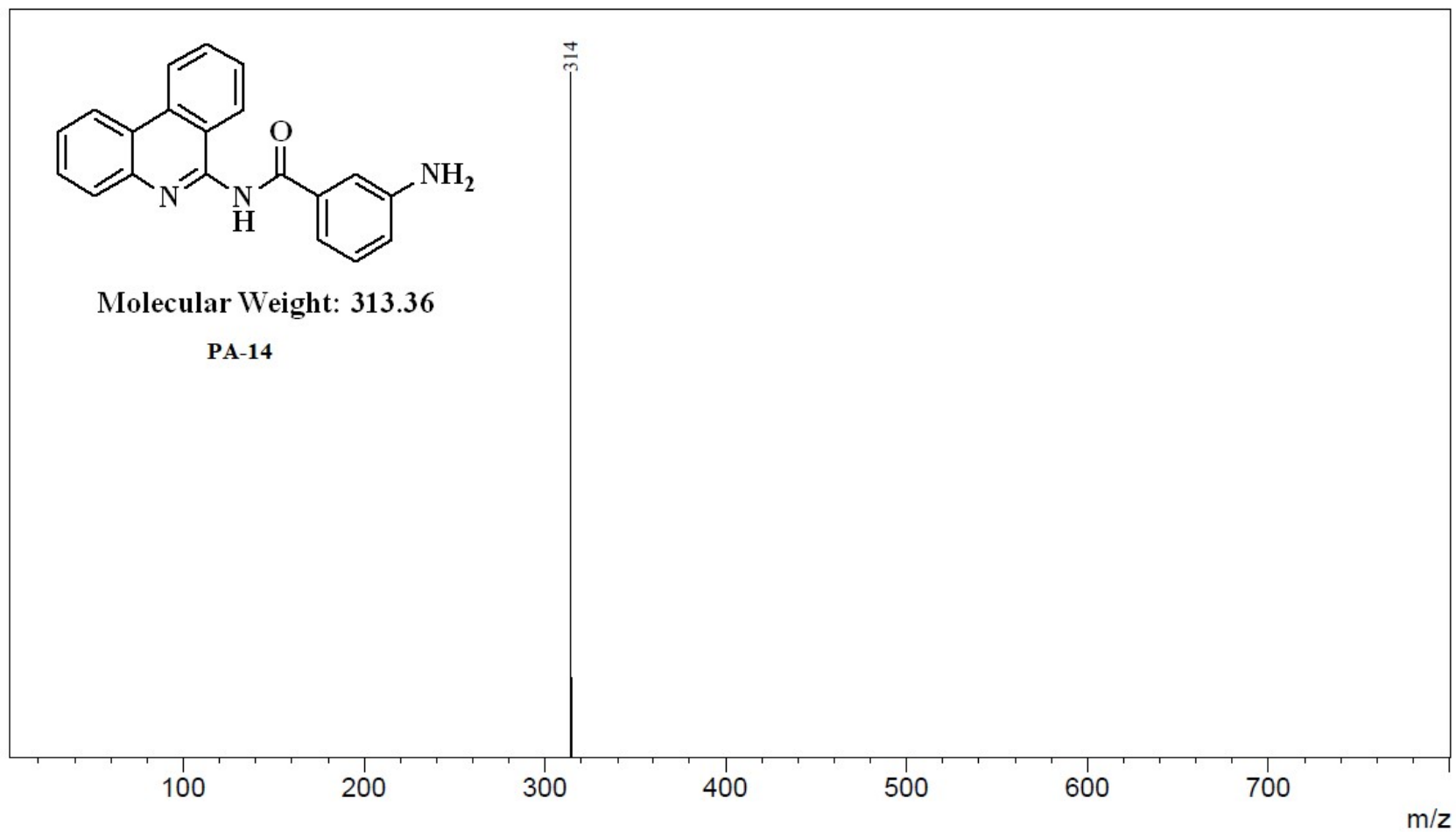


¹H NMR (400 MHz, DMSO-*d*₆) of PA-14

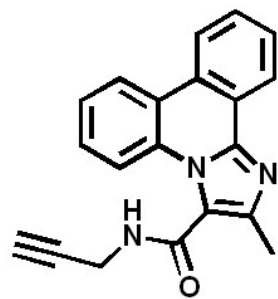


^{13}C NMR (101 MHz, $\text{DMSO-}d_6$) of PA-14

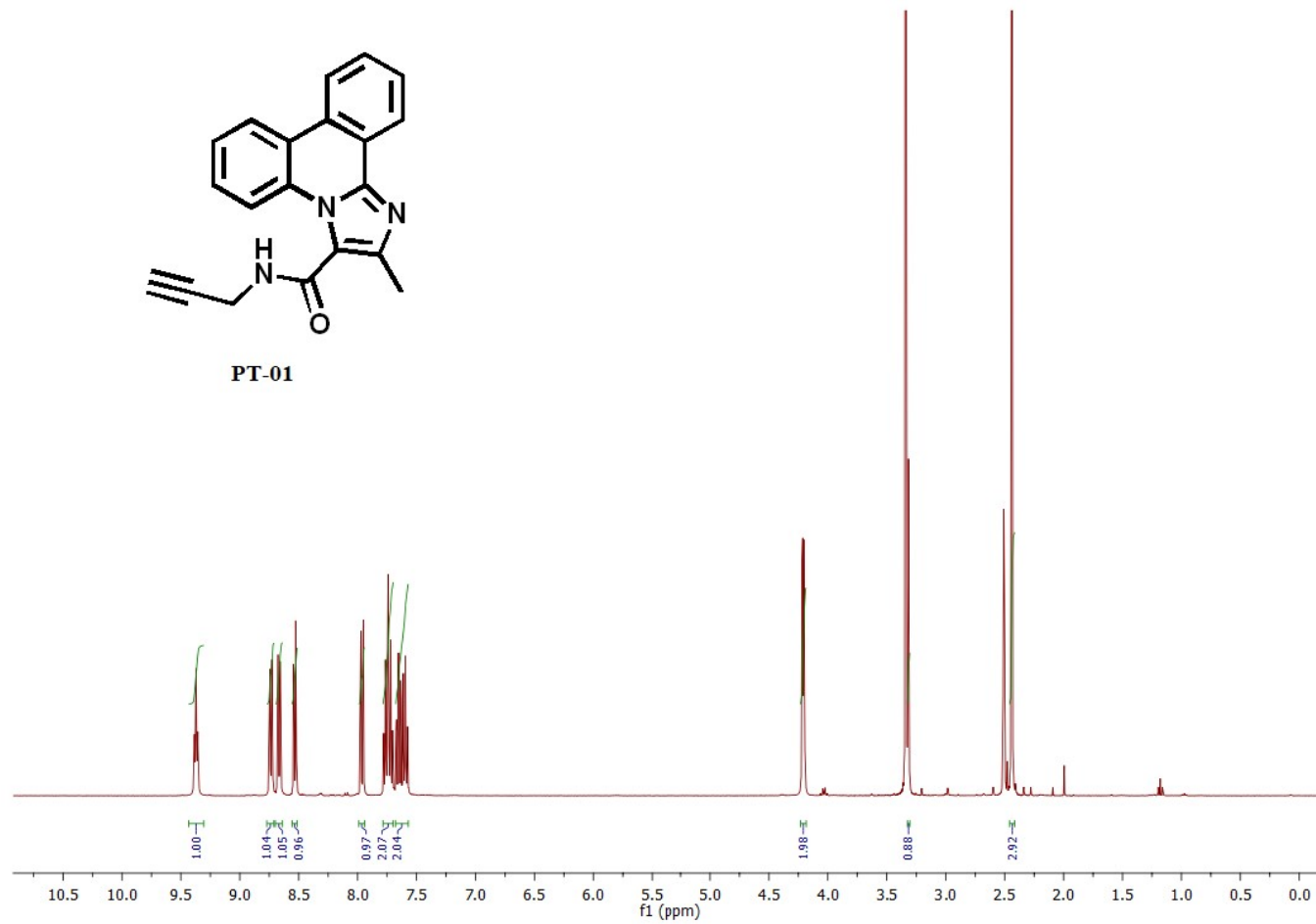
RawMode:Averaged 0.15-0.51(67-229) BasePeak:314(9986437)
BG Mode:Averaged 0.00-0.14(1-63) Segment 1 - Event 1



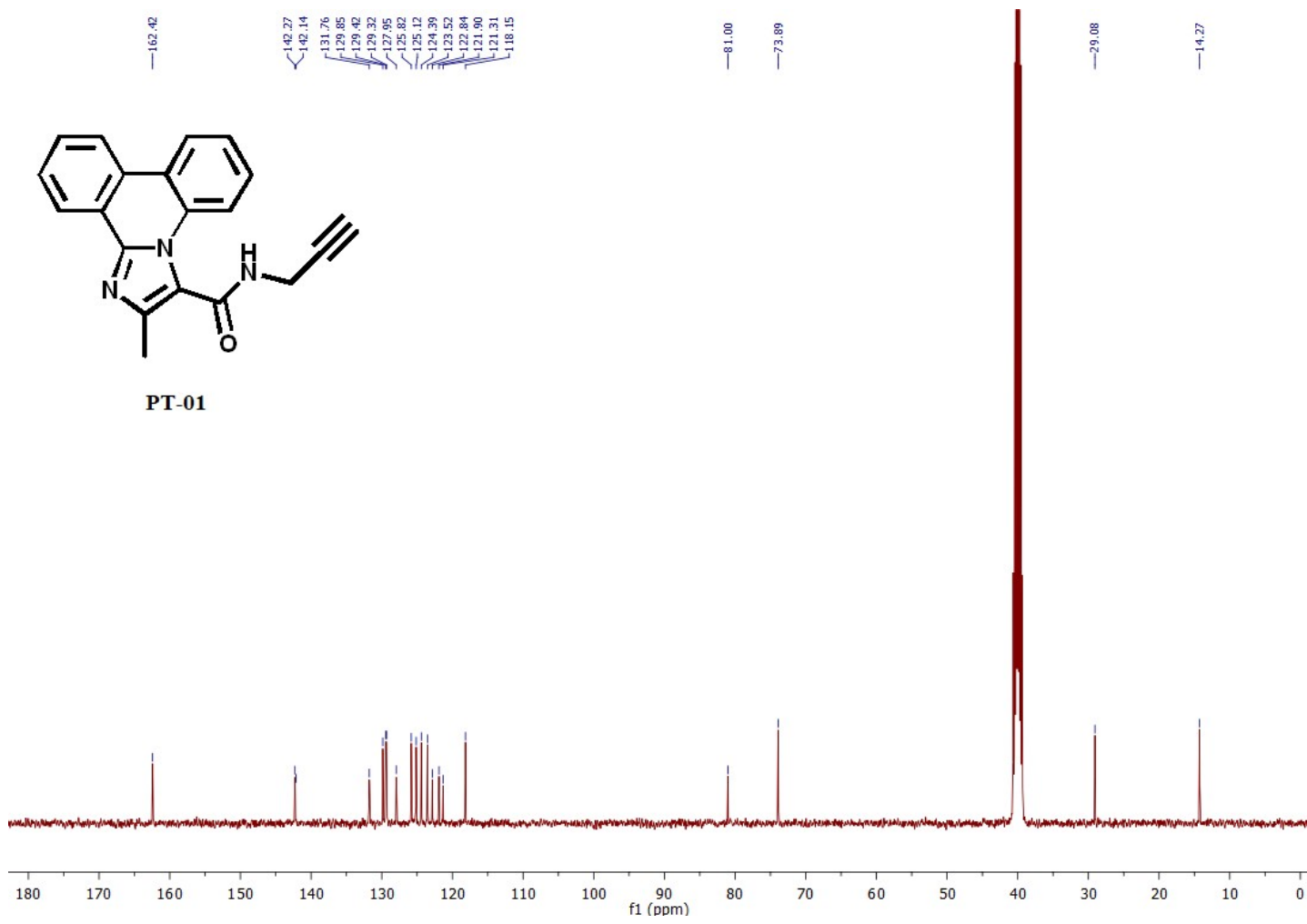
Mass spectra of compound PA-14

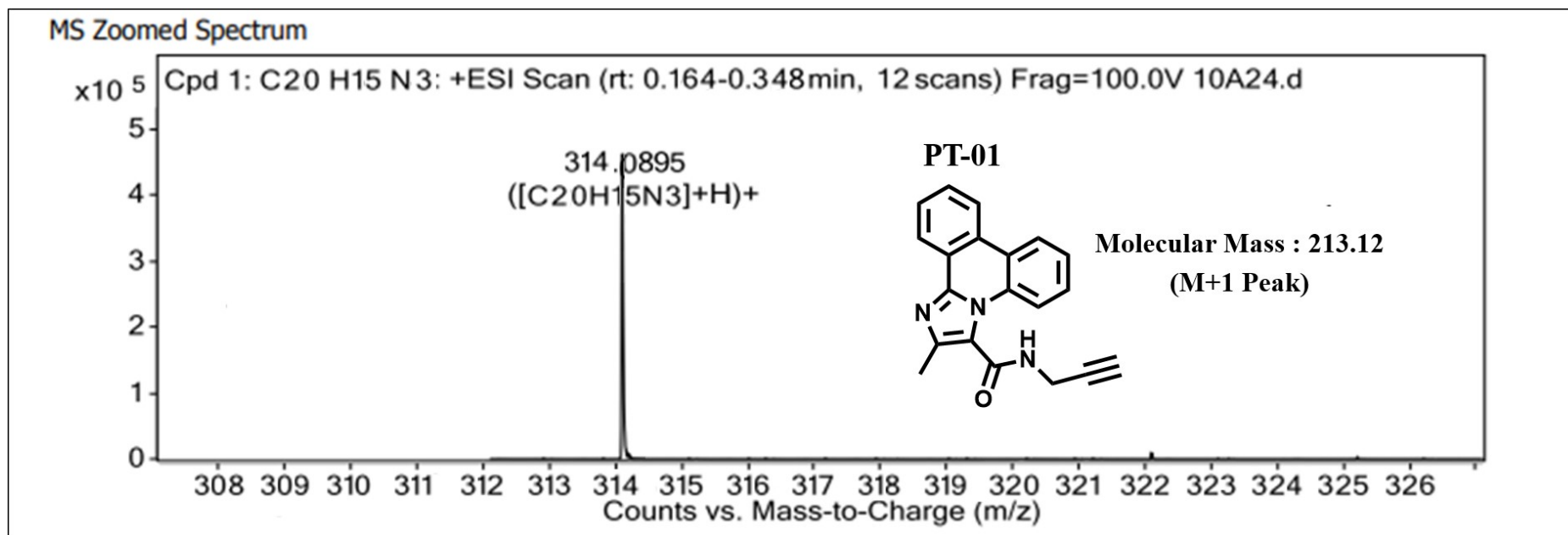


PT-01

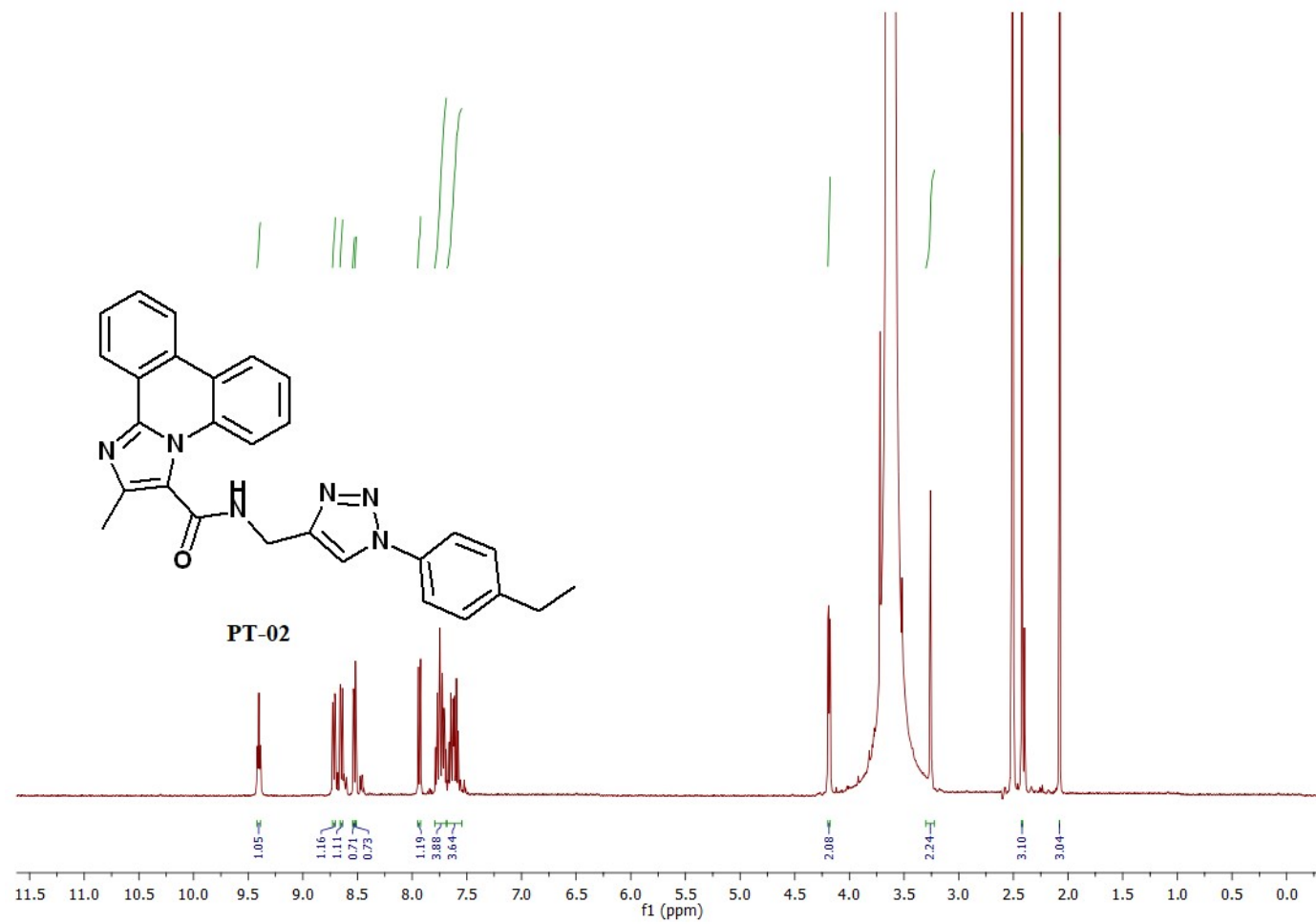


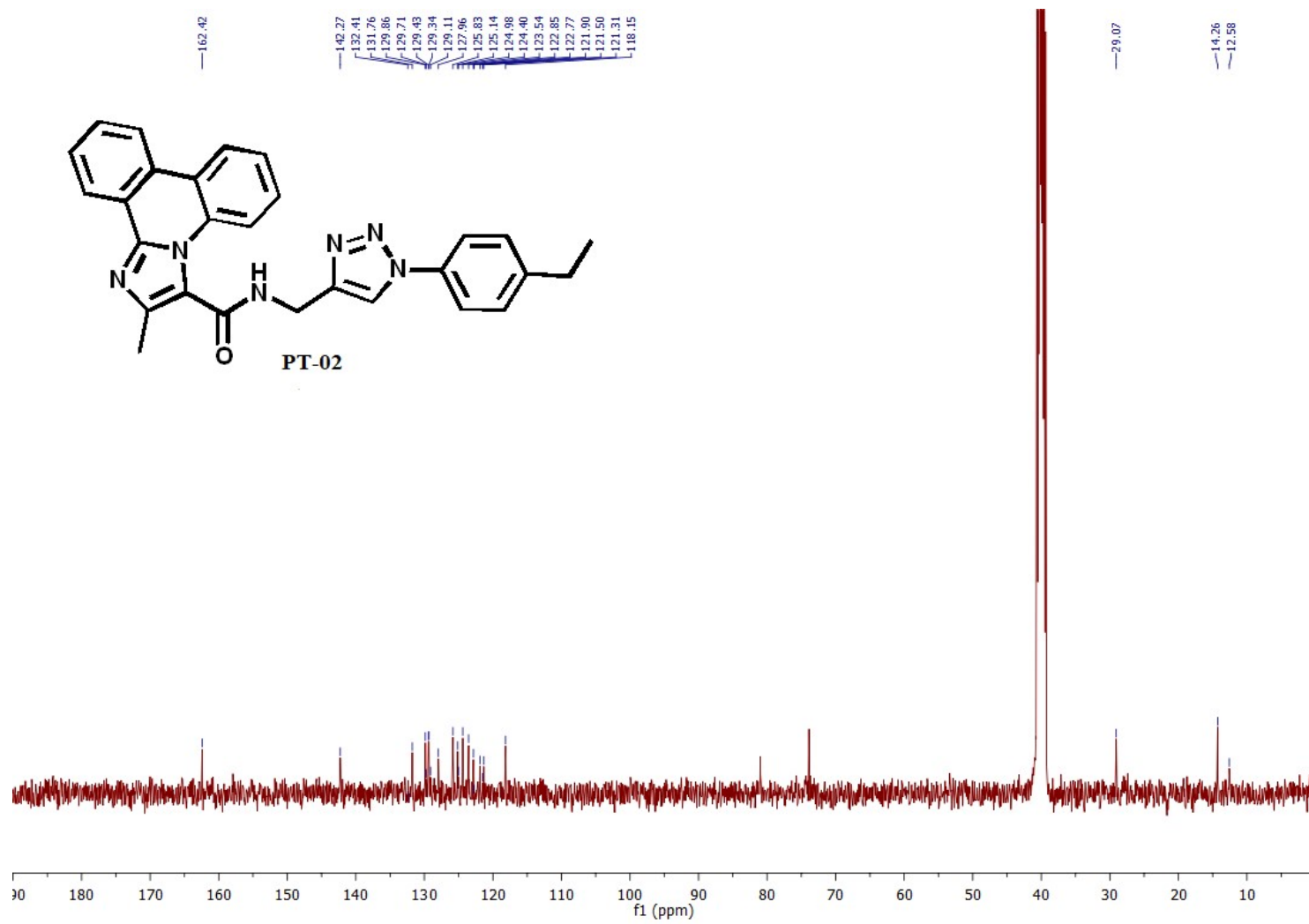
^1H NMR (400 MHz, $\text{DMSO-}d_6$) of PT-01



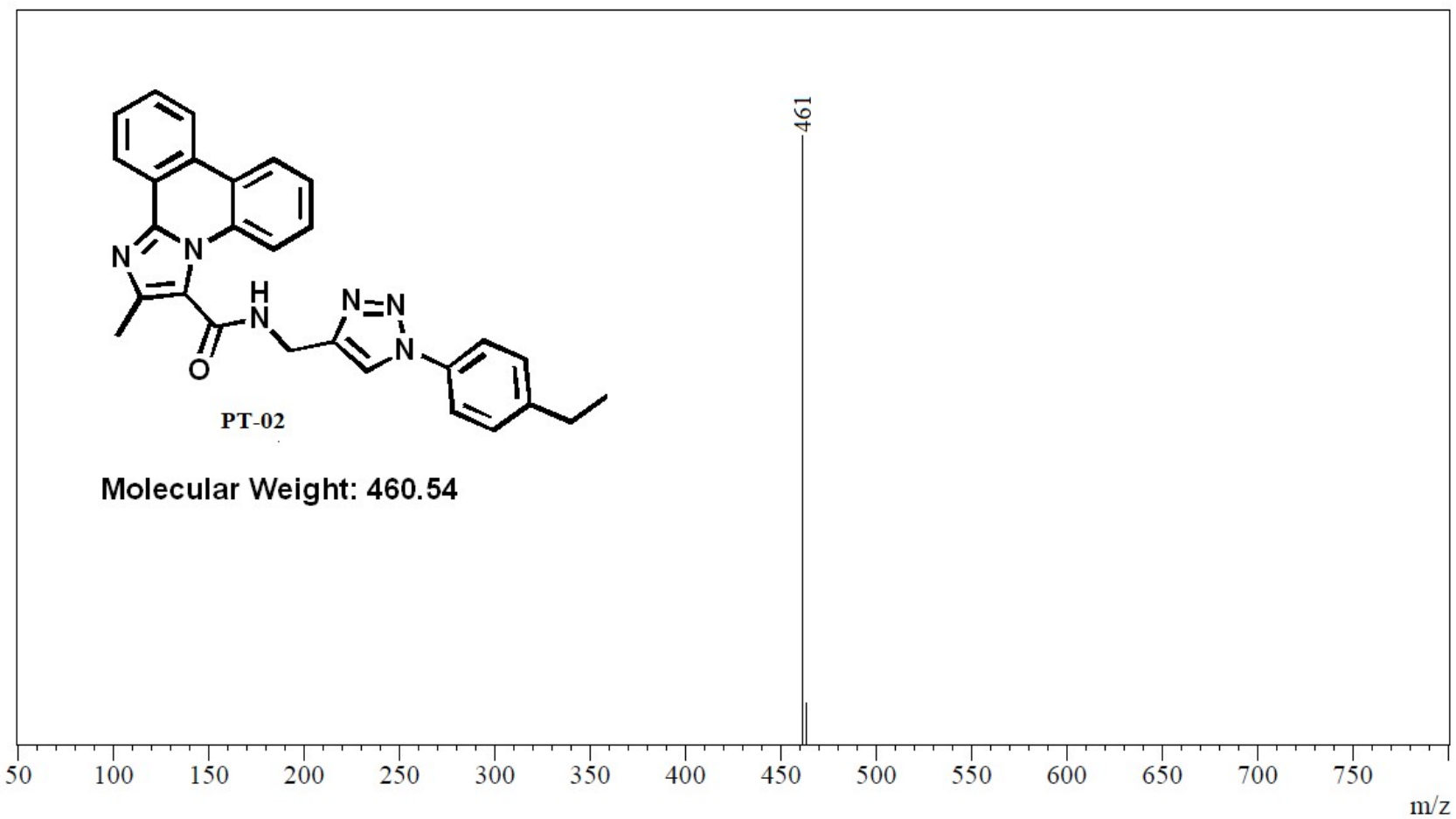


HRMS Mass spectra of compound PT-01

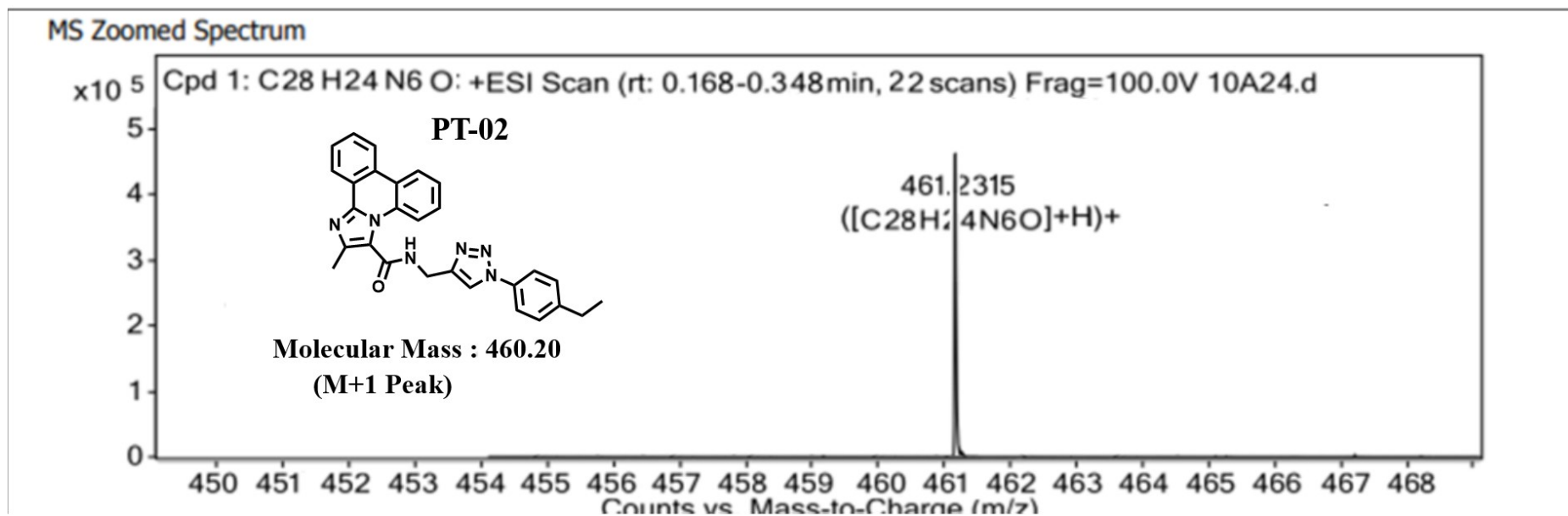




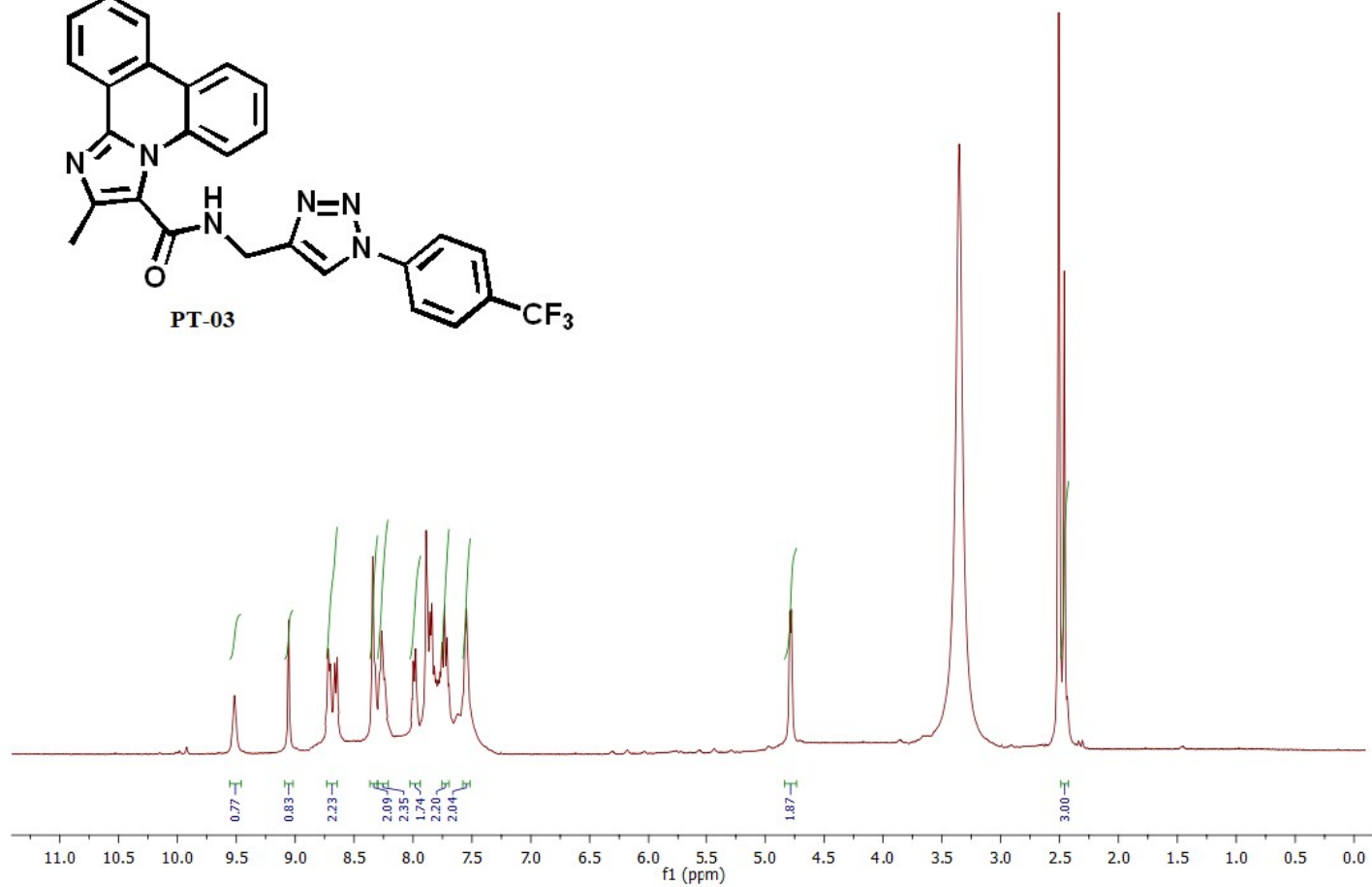
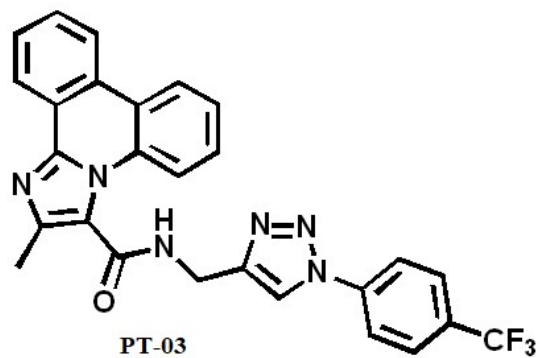
¹³C NMR (101 MHz, DMSO-d₆) of PT-02



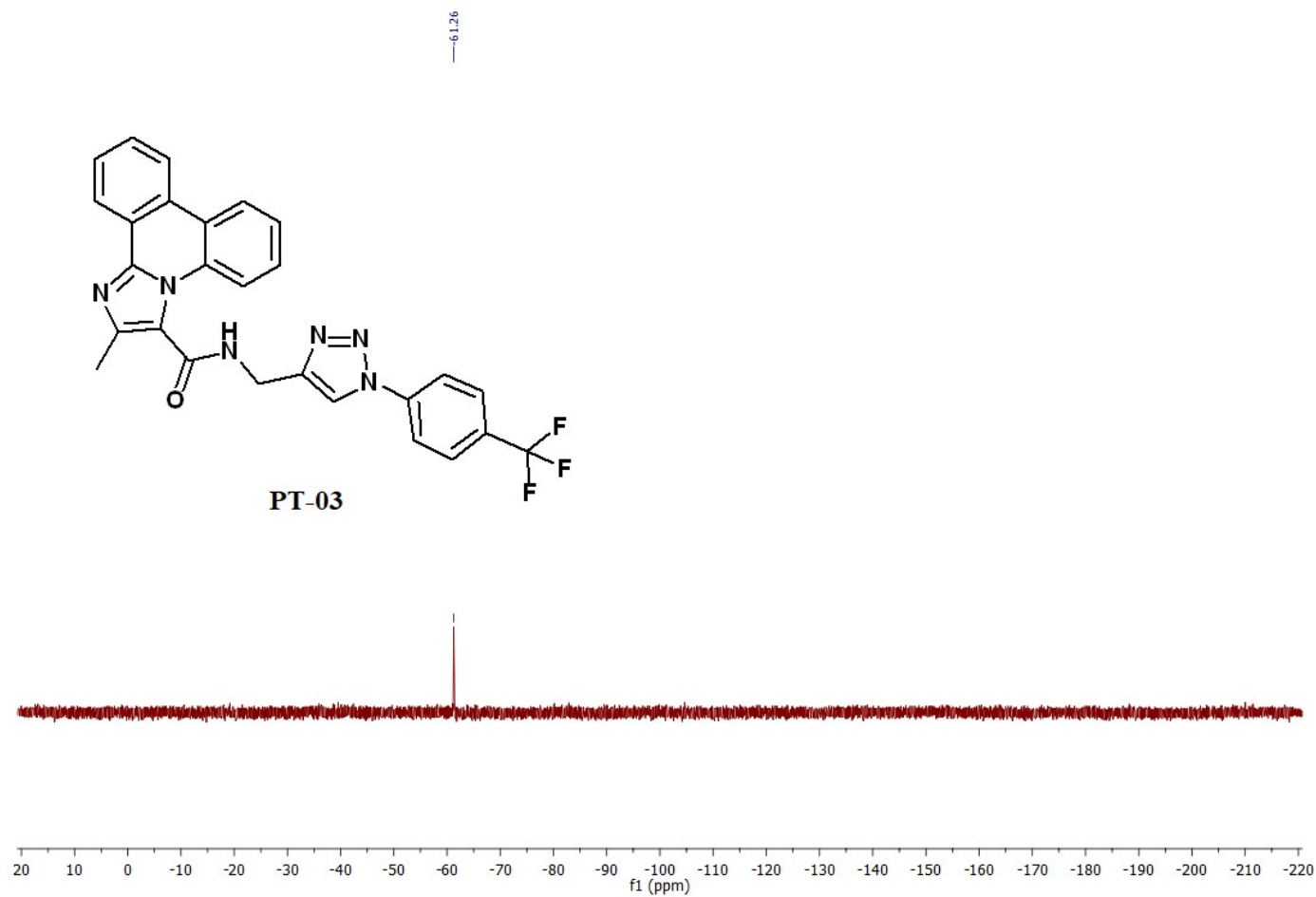
Mass spectra of compound PT-02

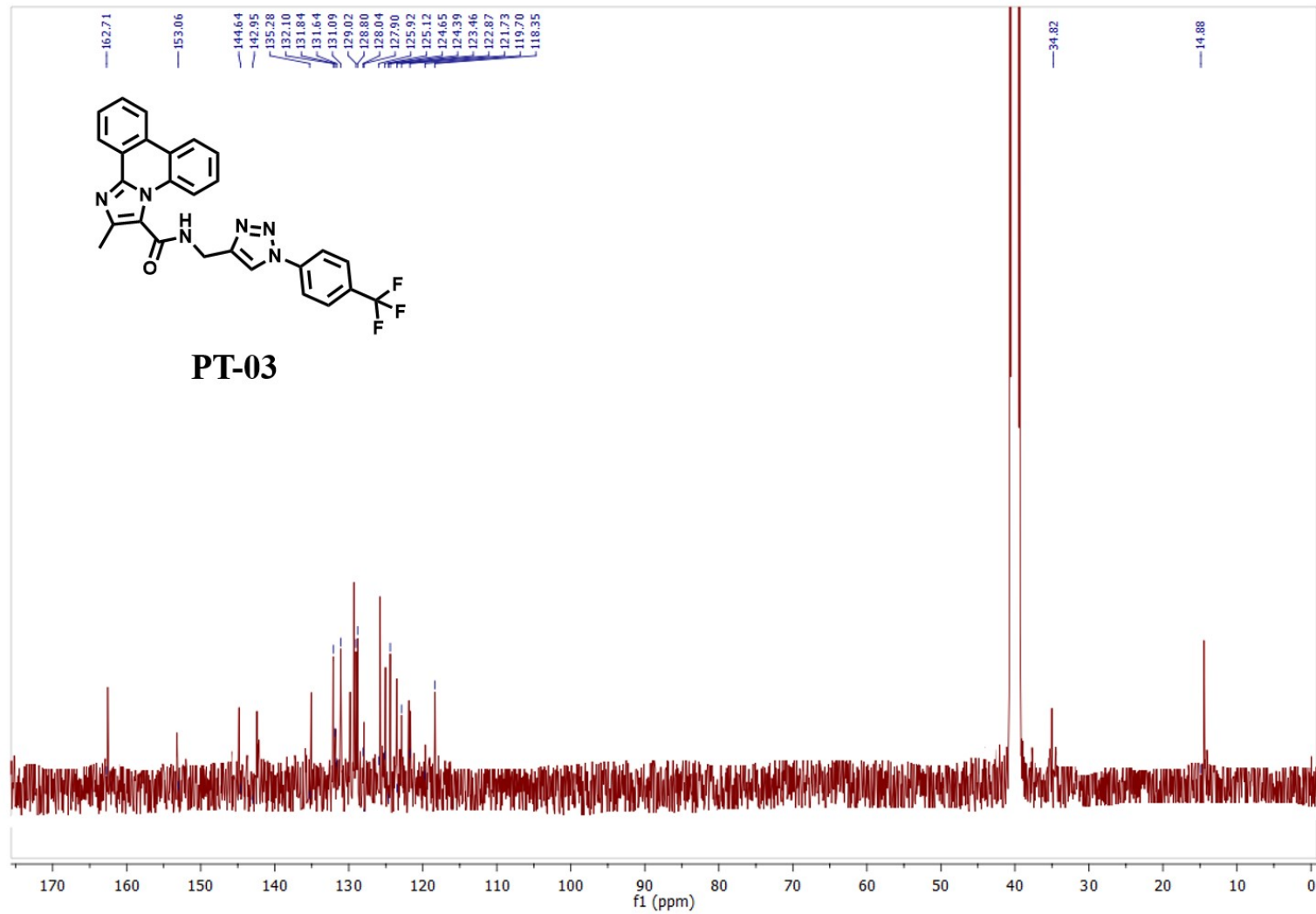


HRMS Mass spectra of compound PT-02

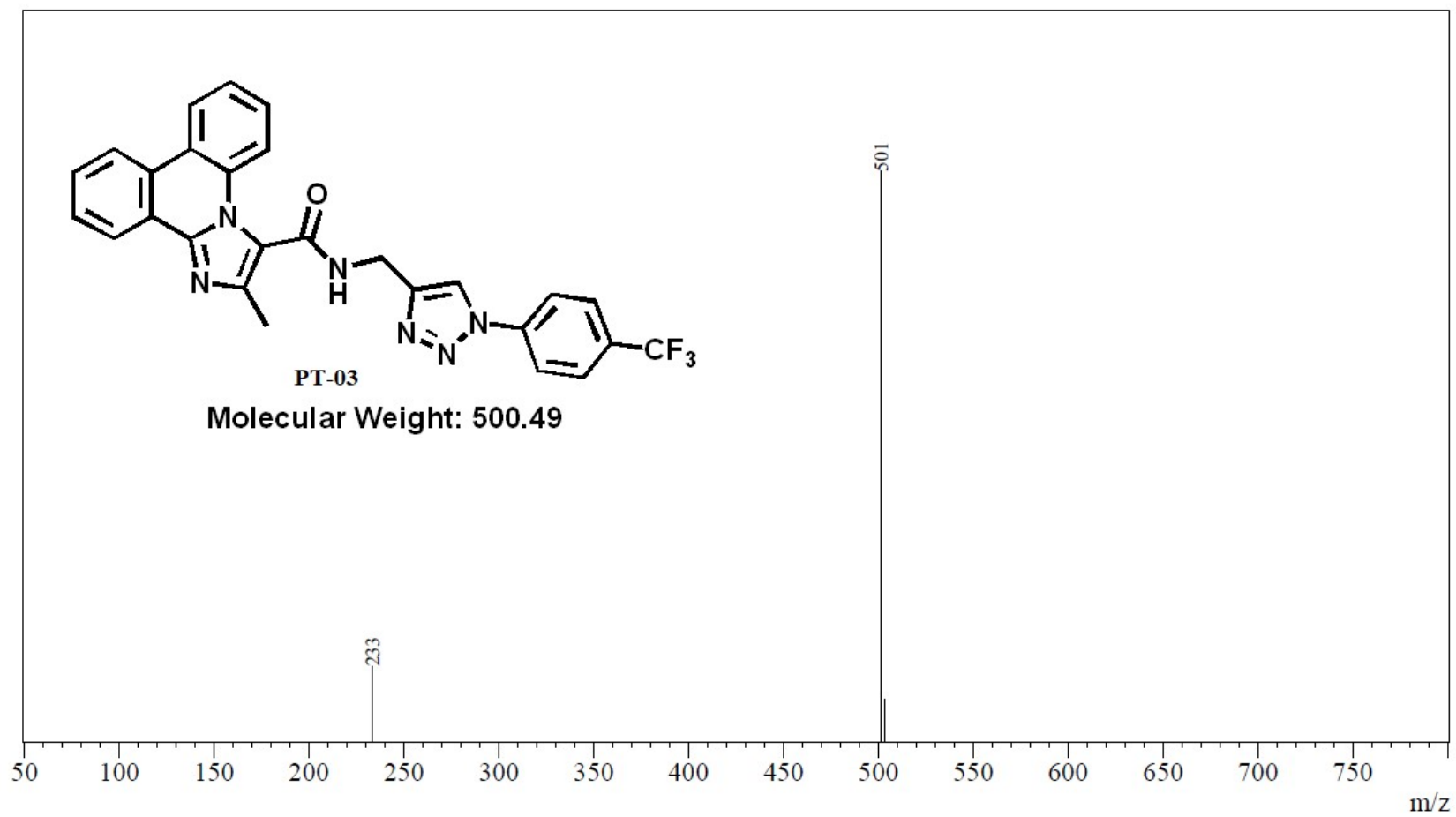


¹H NMR (400 MHz, DMSO-*d*₆) of PT-03

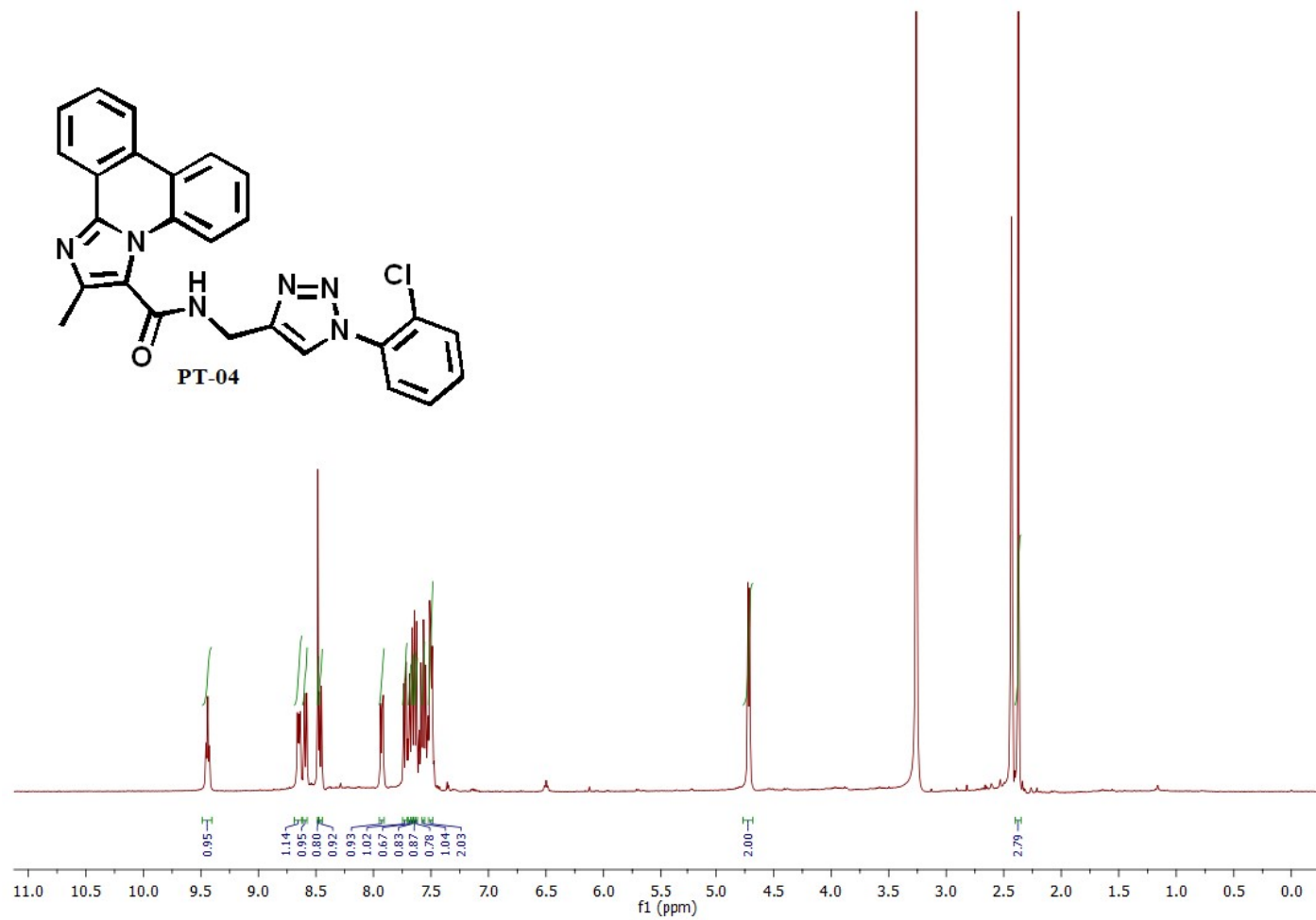




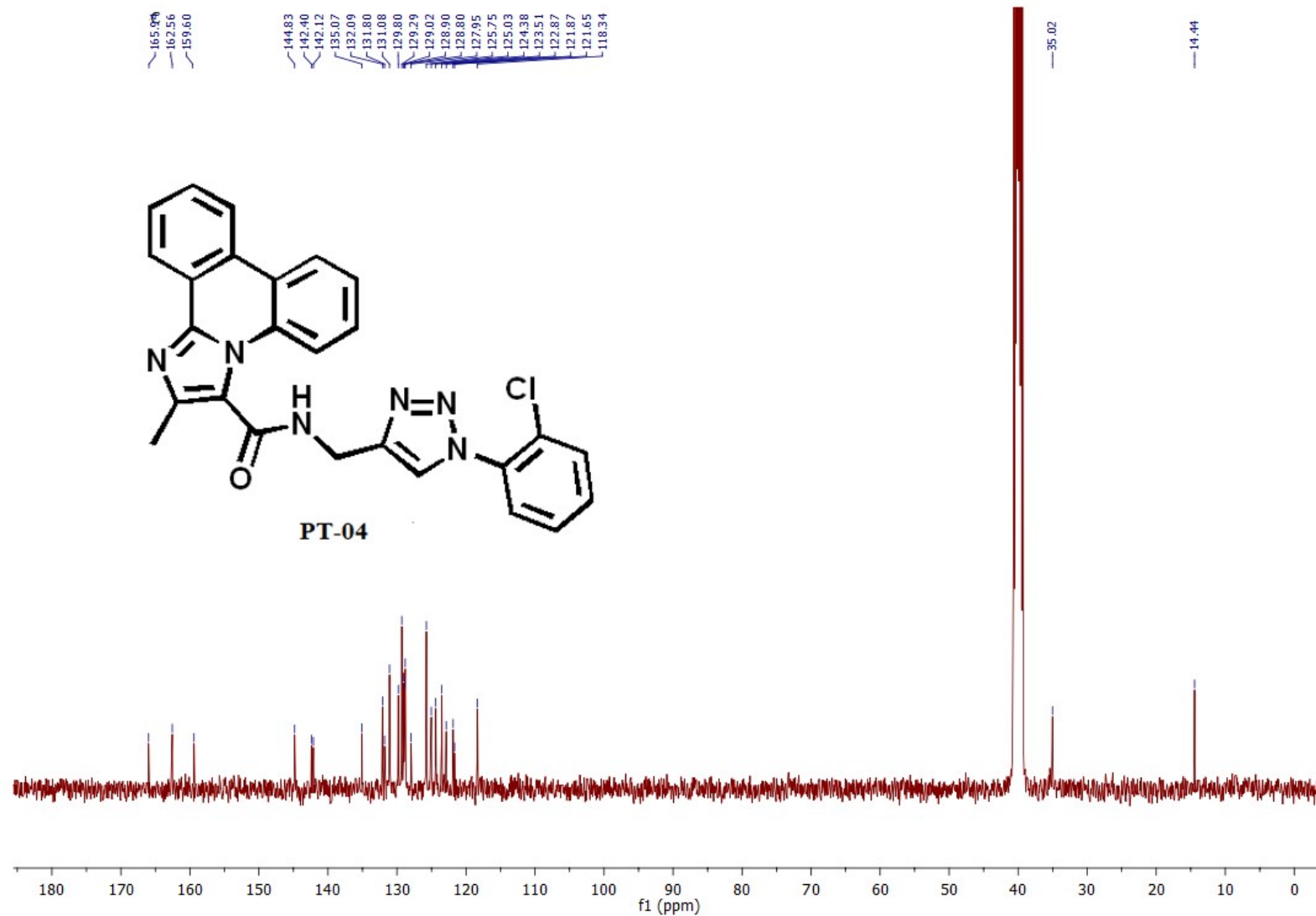
¹³C NMR (101 MHz, DMSO-*d*₆) of PT-03

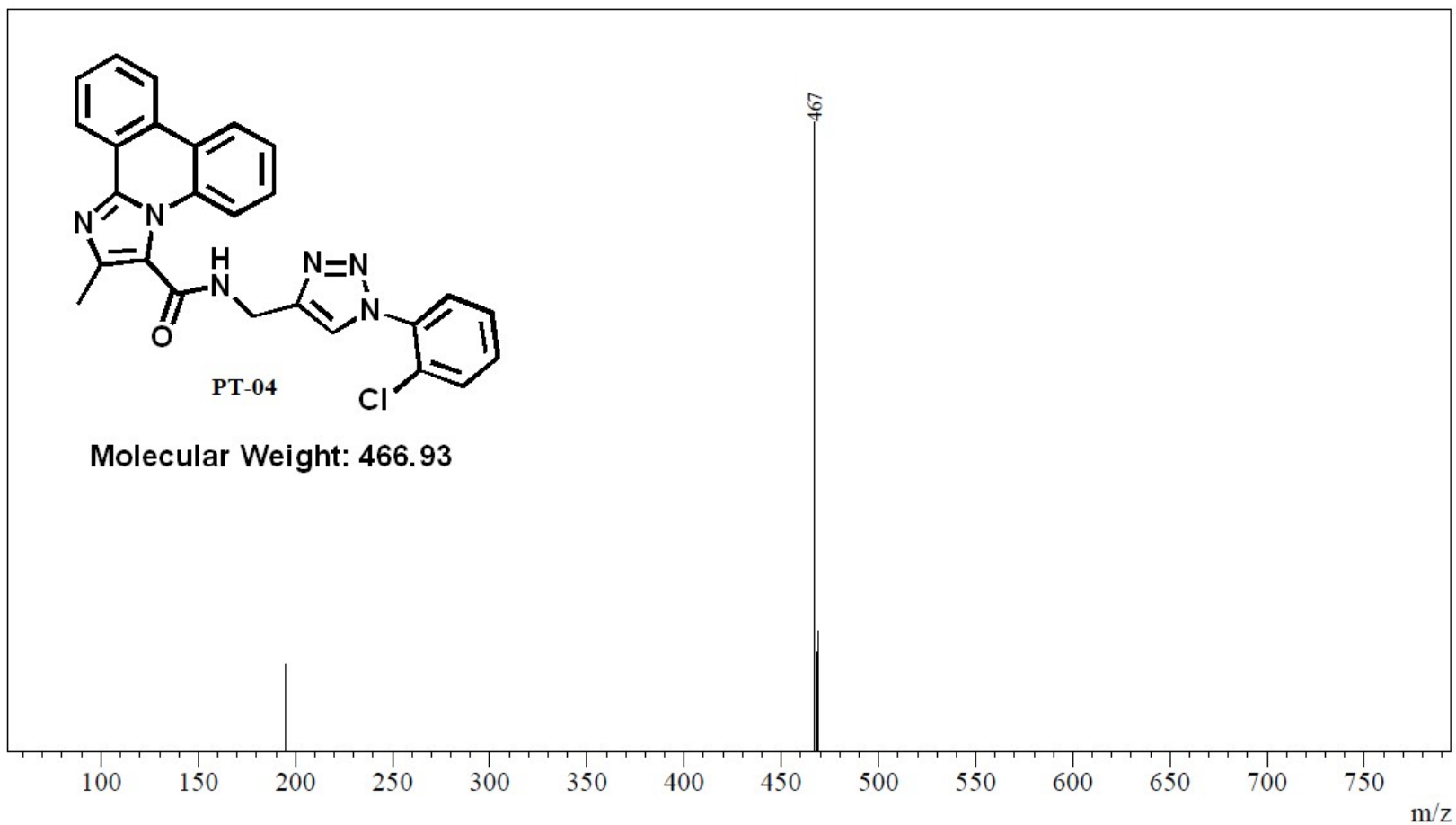


Mass spectra of compound PT-03

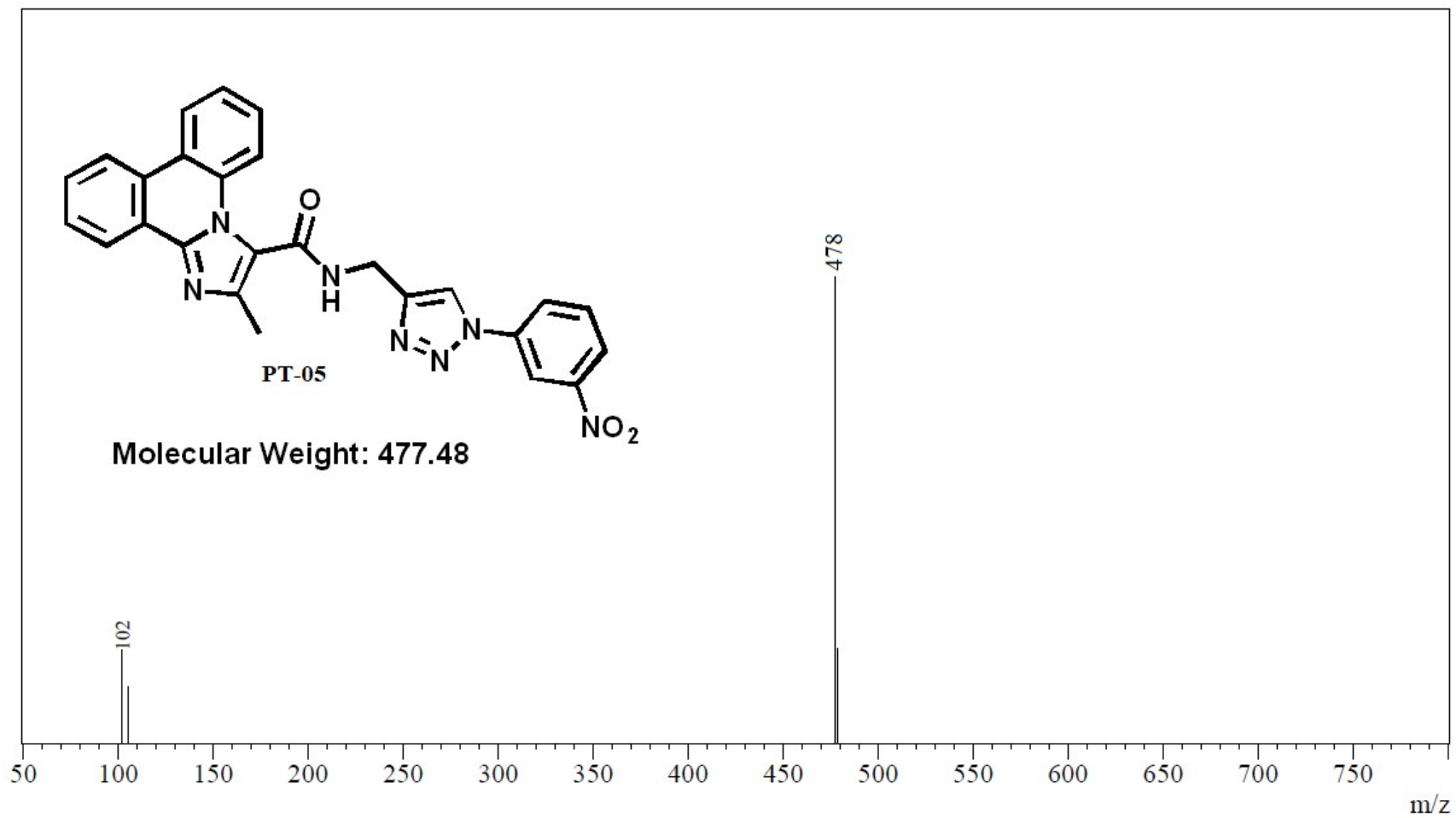


¹H NMR (400 MHz, DMSO-*d*₆) of PT-04

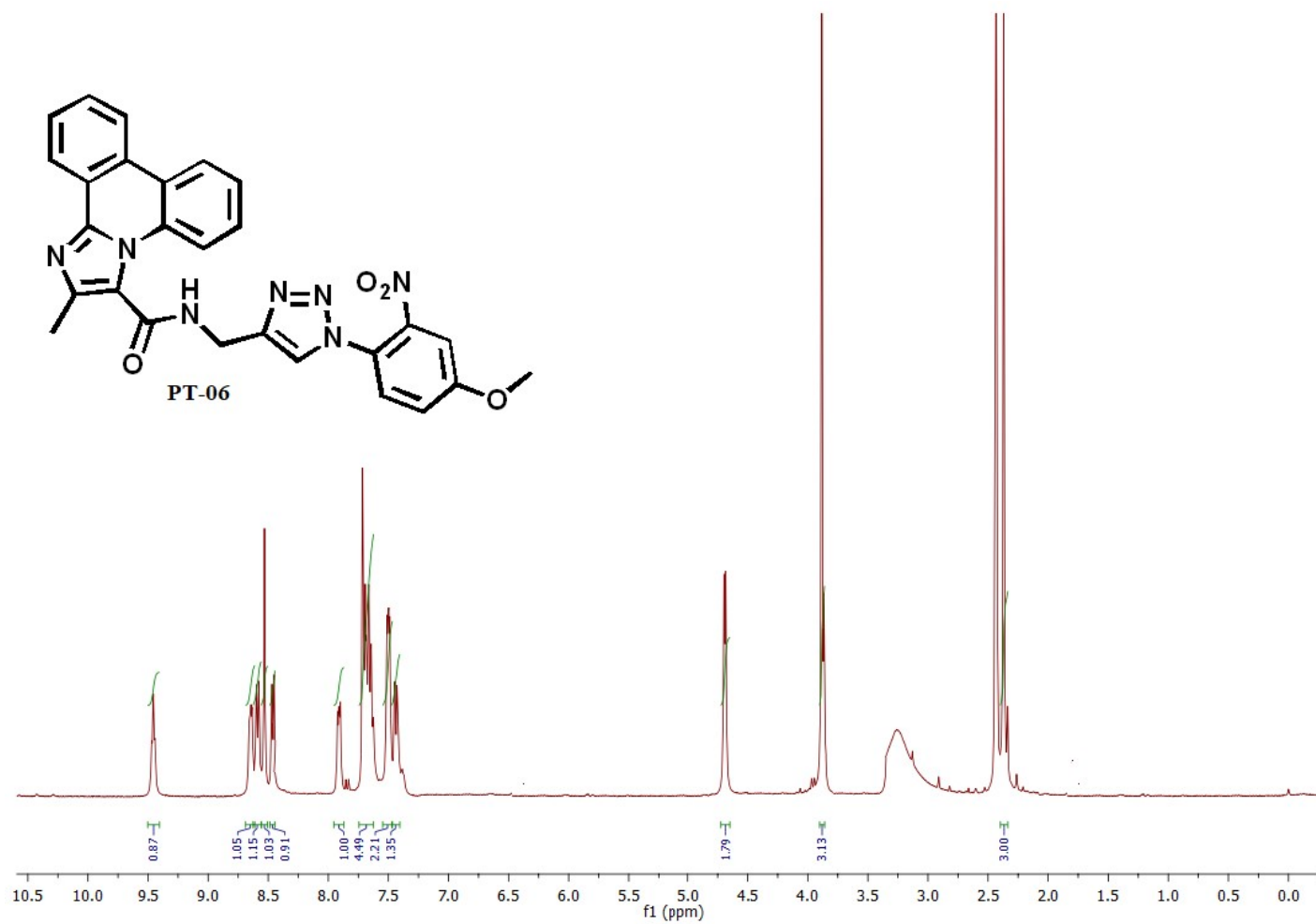




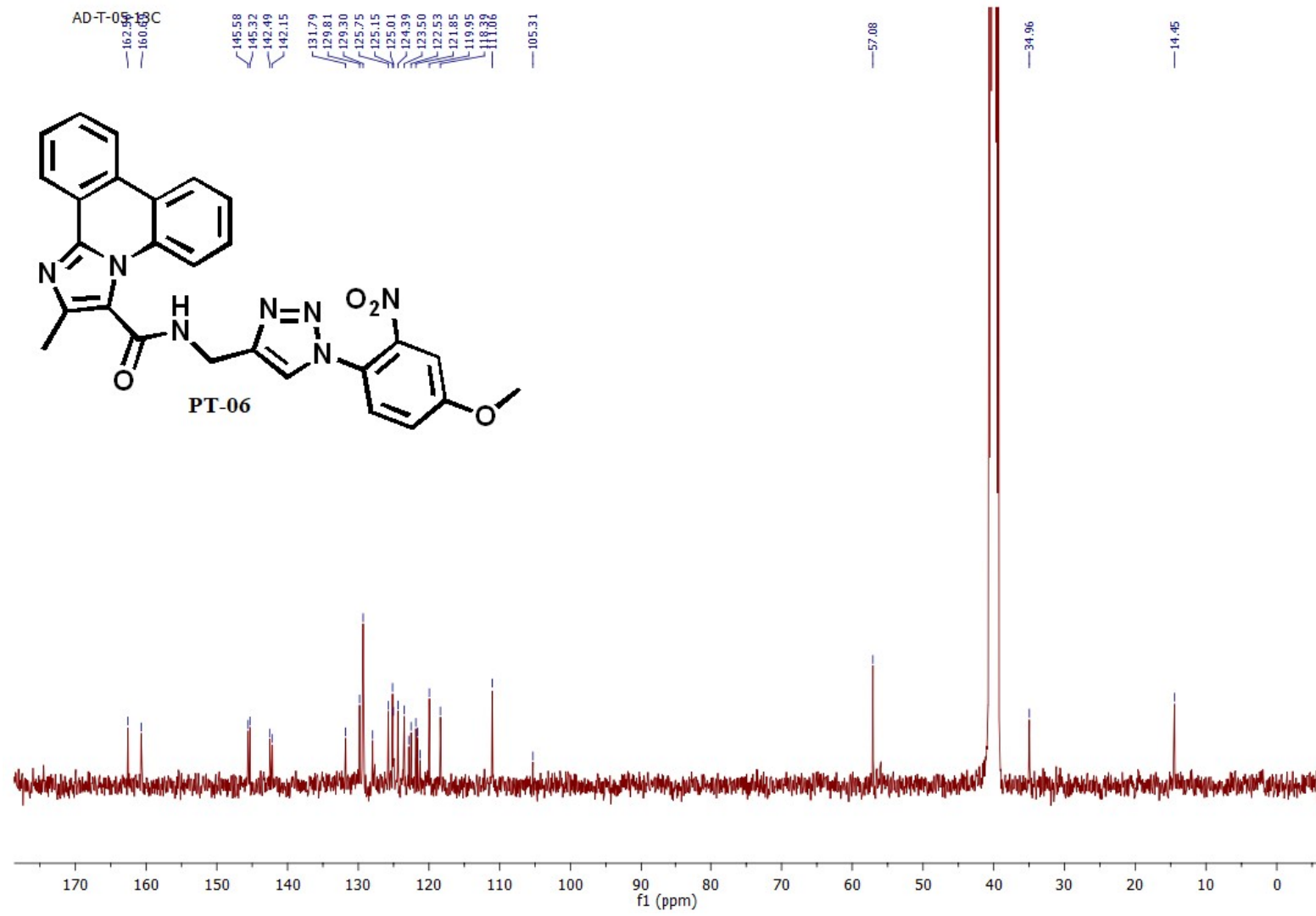
Mass spectra of compound PT-04



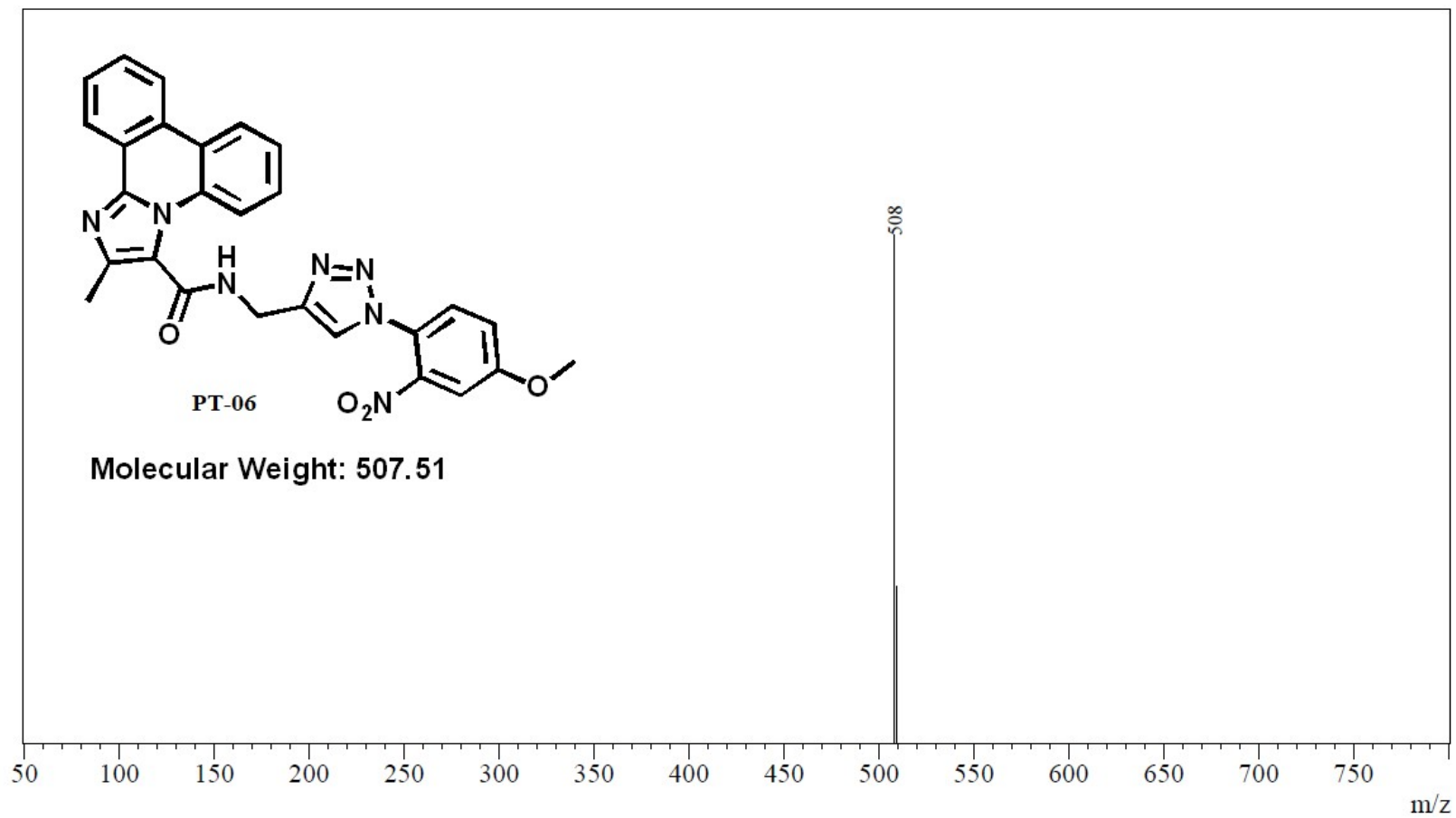
Mass spectra of compound PT-05



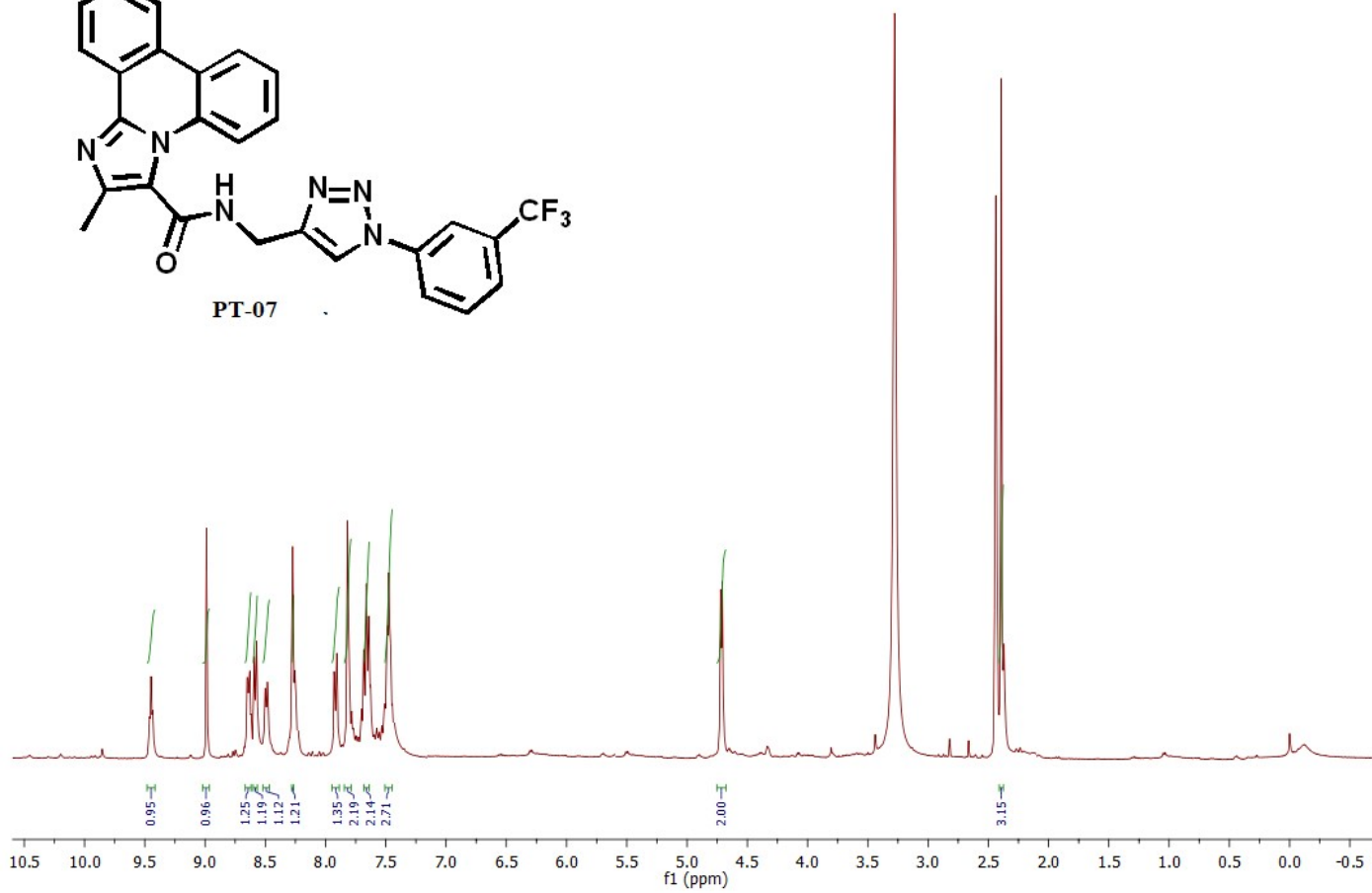
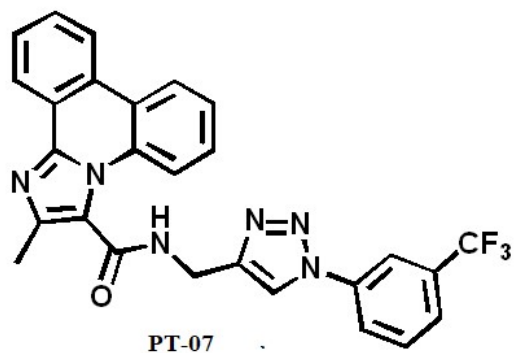
¹H NMR (400 MHz, DMSO-*d*₆) of PT-06



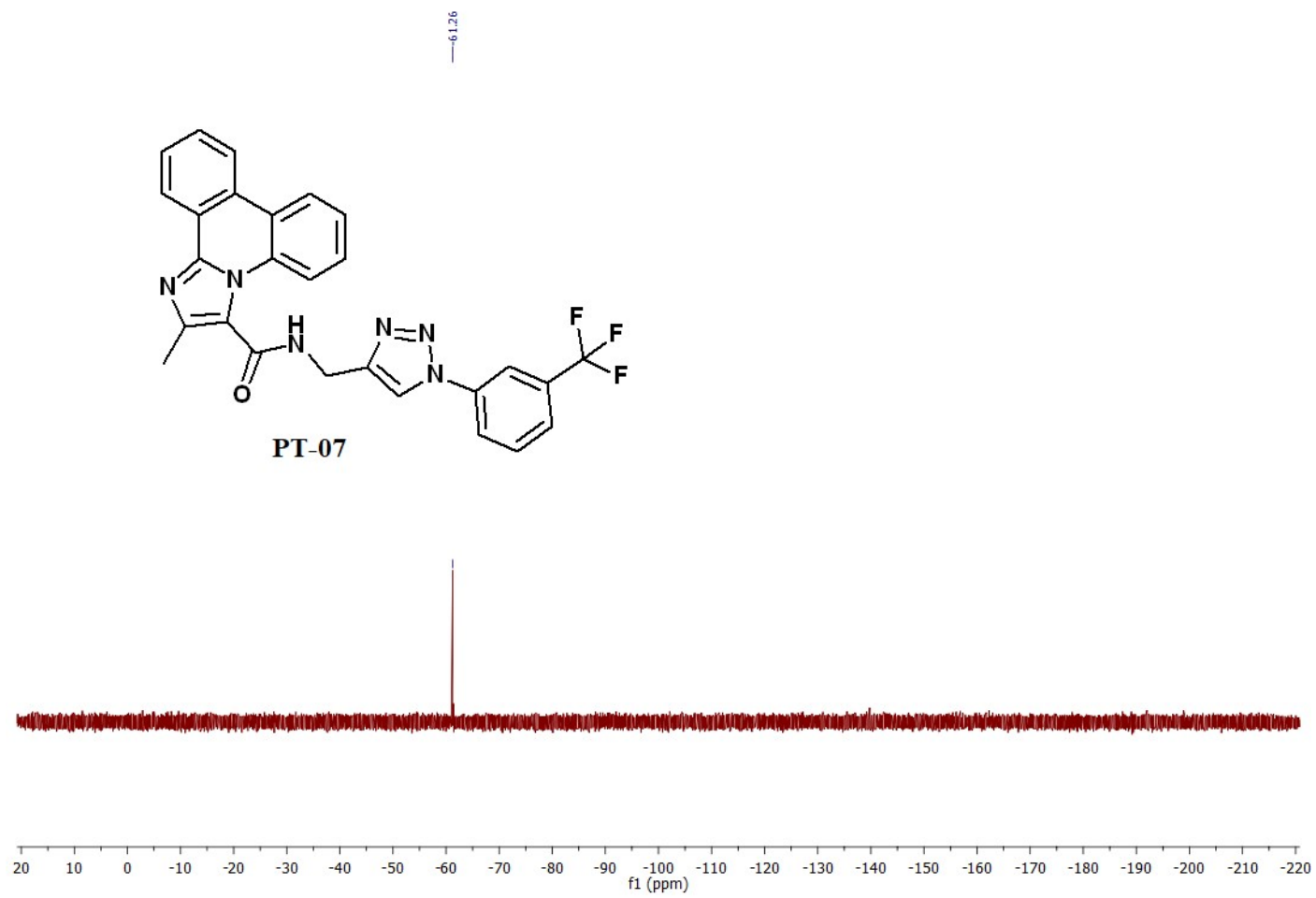
¹³C NMR (101 MHz, DMSO-*d*₆) of PT-06



Mass spectra of compound PT-06

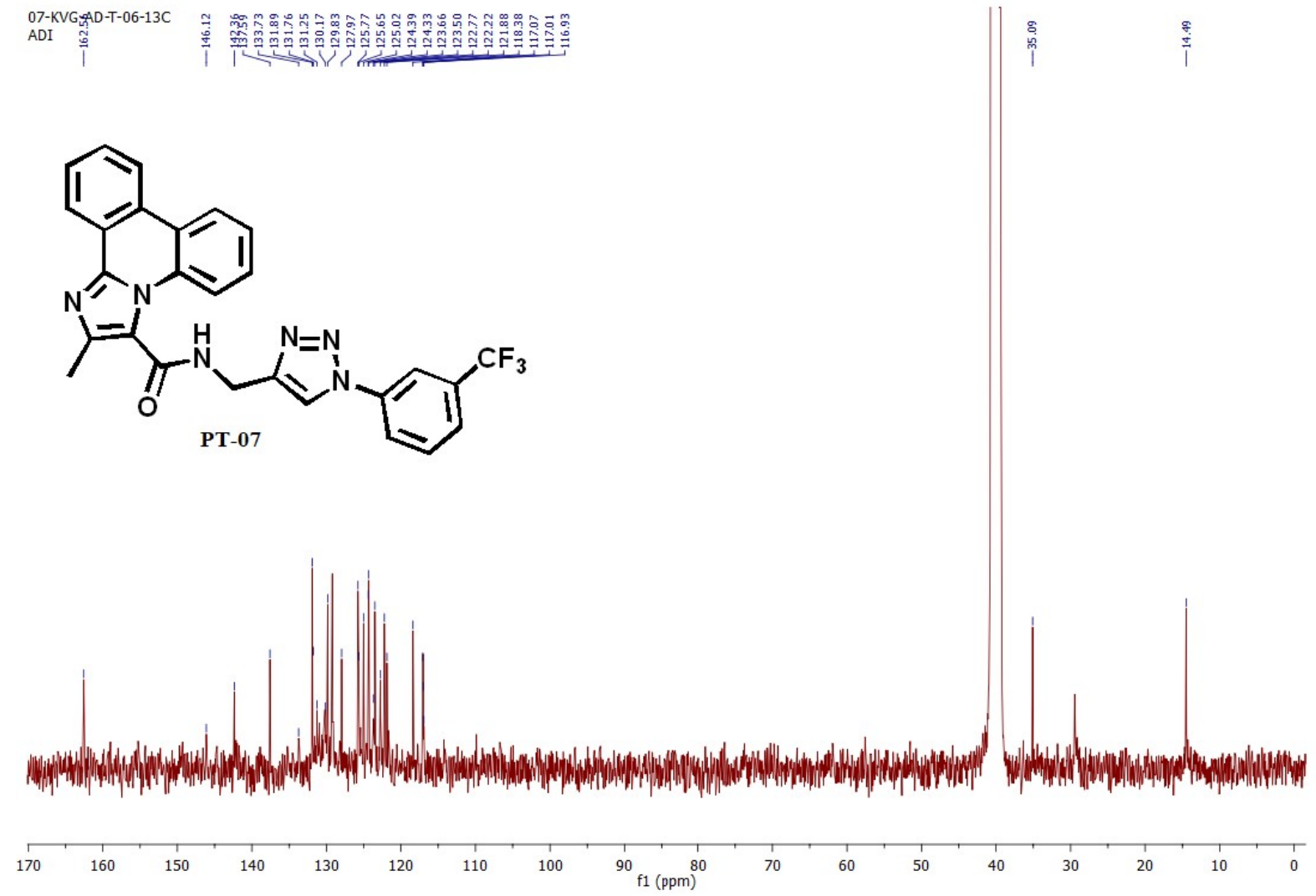
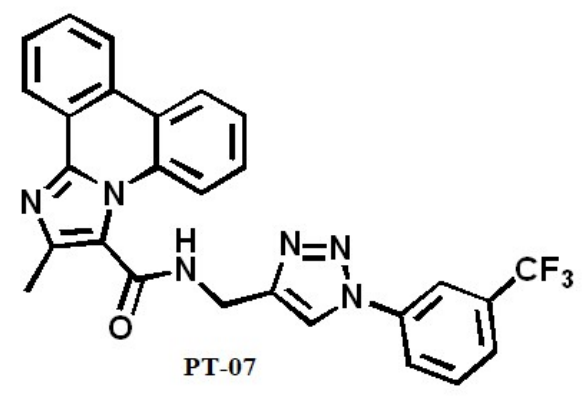


¹H NMR (400 MHz, DMSO-*d*₆) of PT-07

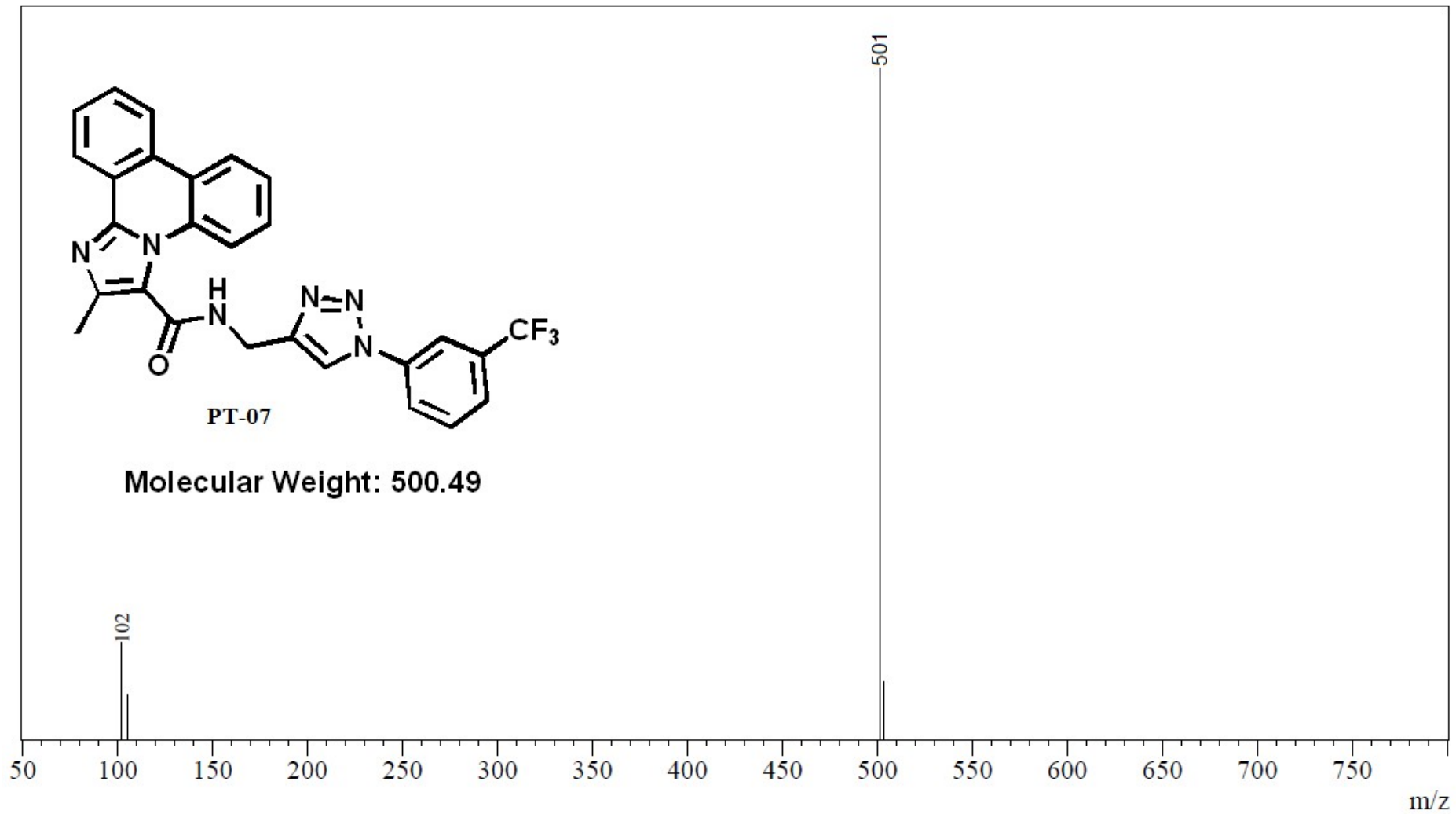


07-KVG AD-T-06-13C
ADI

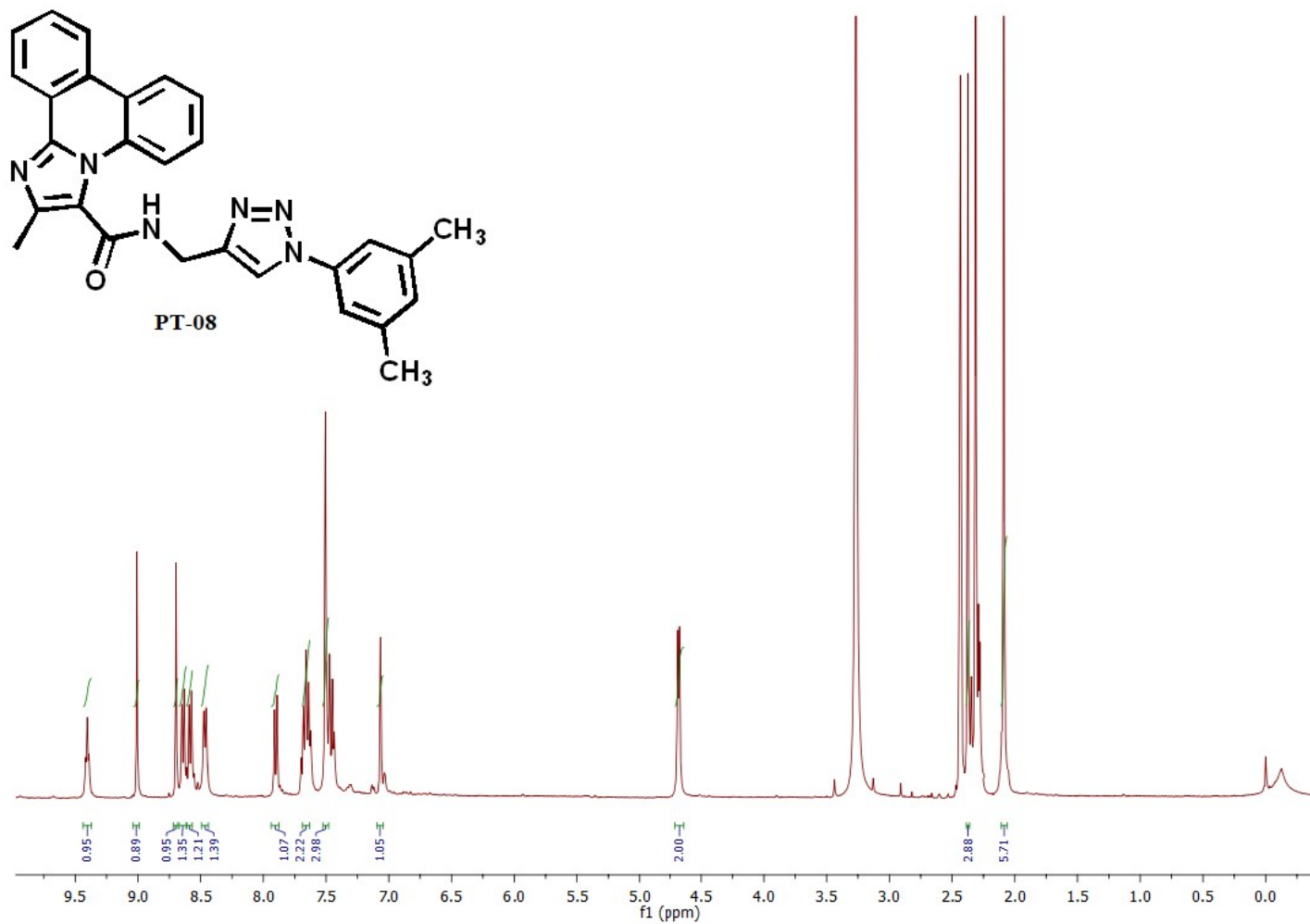
162.55
146.12
137.56
133.73
131.89
131.76
131.25
130.17
129.83
127.97
125.77
125.65
125.02
124.39
124.33
123.66
123.50
122.77
122.22
121.88
118.38
117.07
116.93



¹³C NMR (101 MHz, DMSO-*d*₆) of PT-07



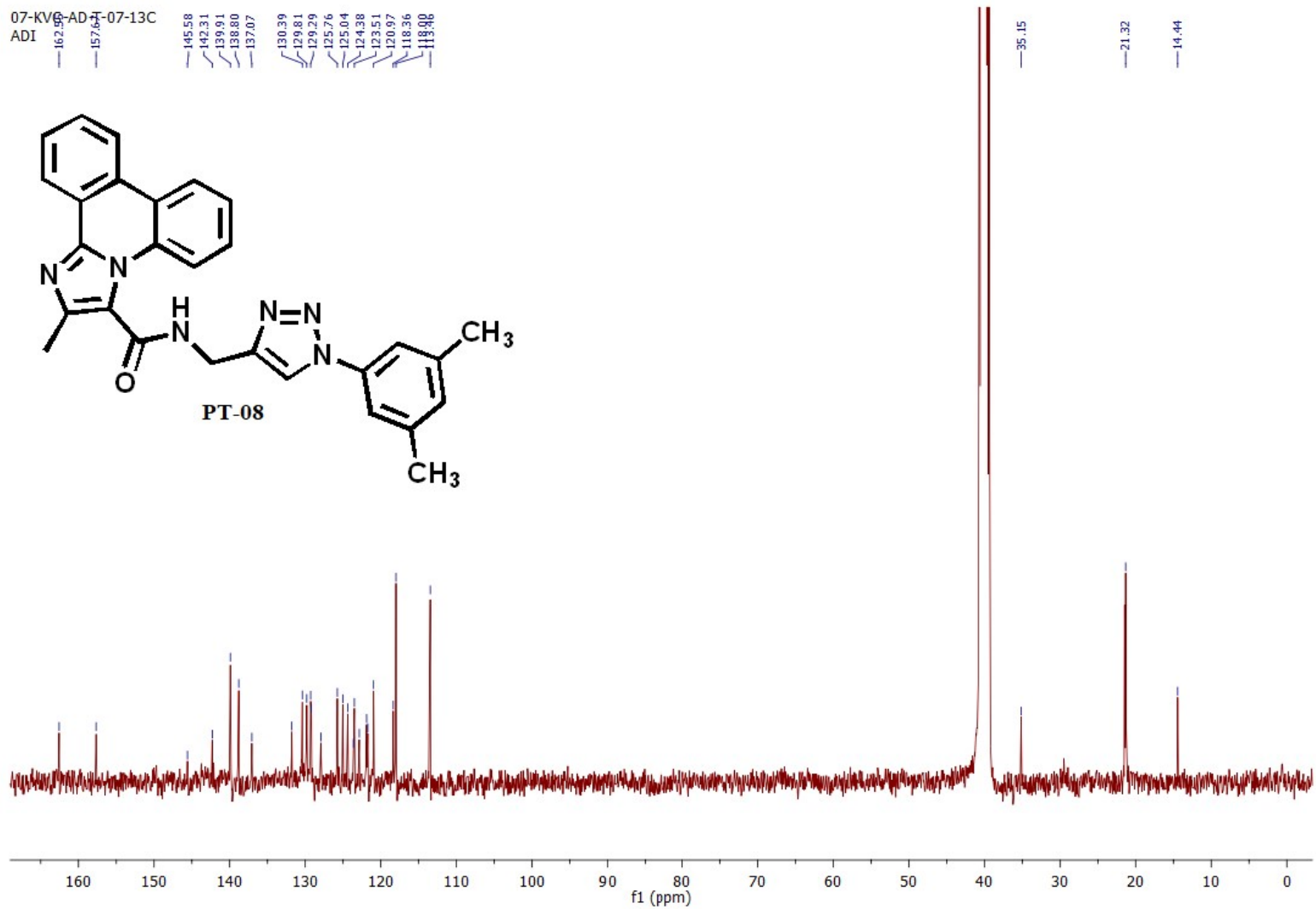
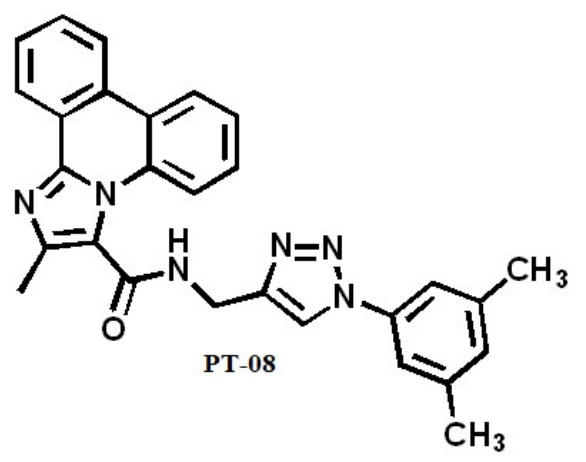
Mass spectra of compound PT-07



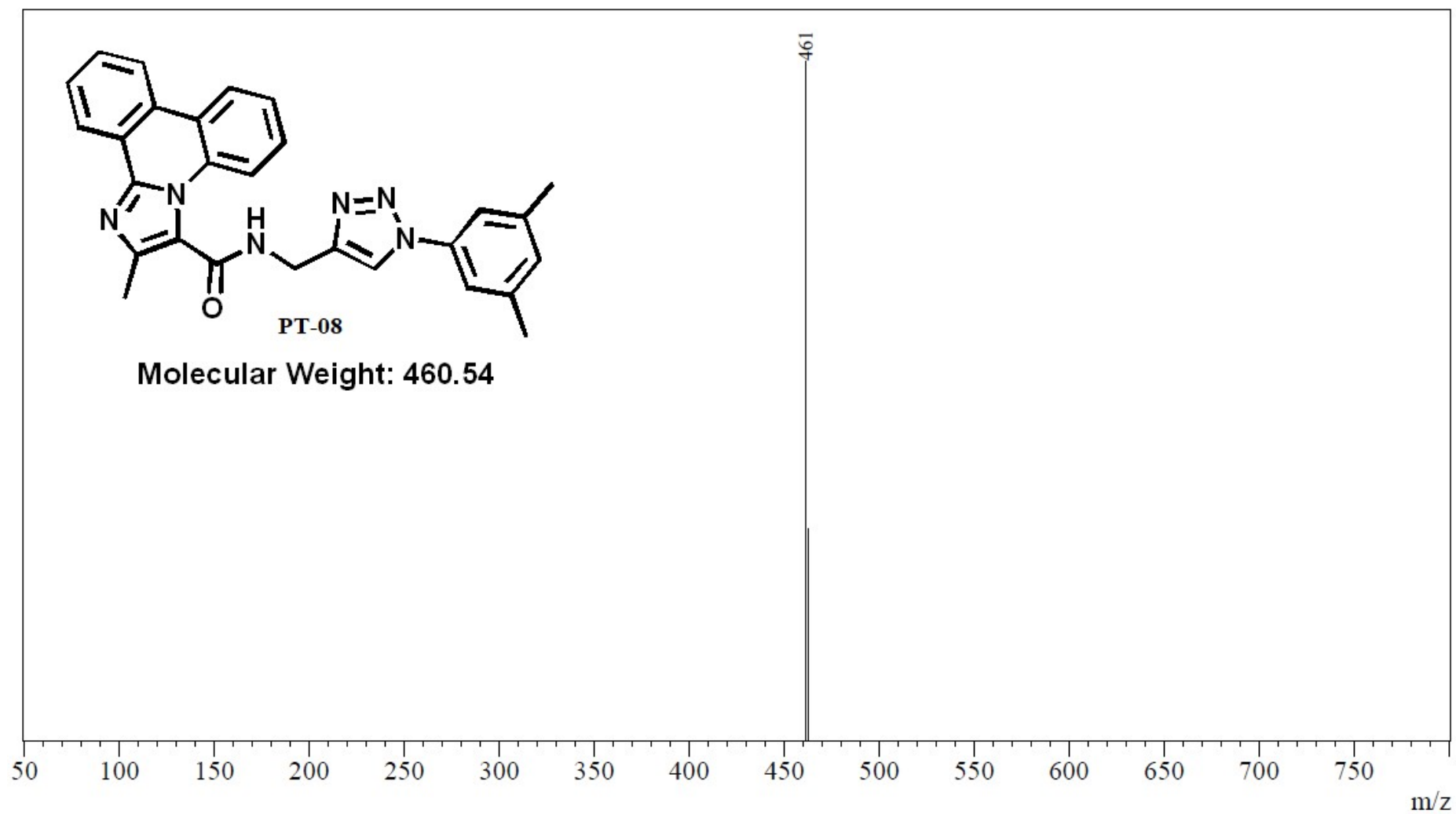
¹H NMR (400 MHz, DMSO-*d*₆) of PT-08

07-KV6-AD-07-13C
ADI

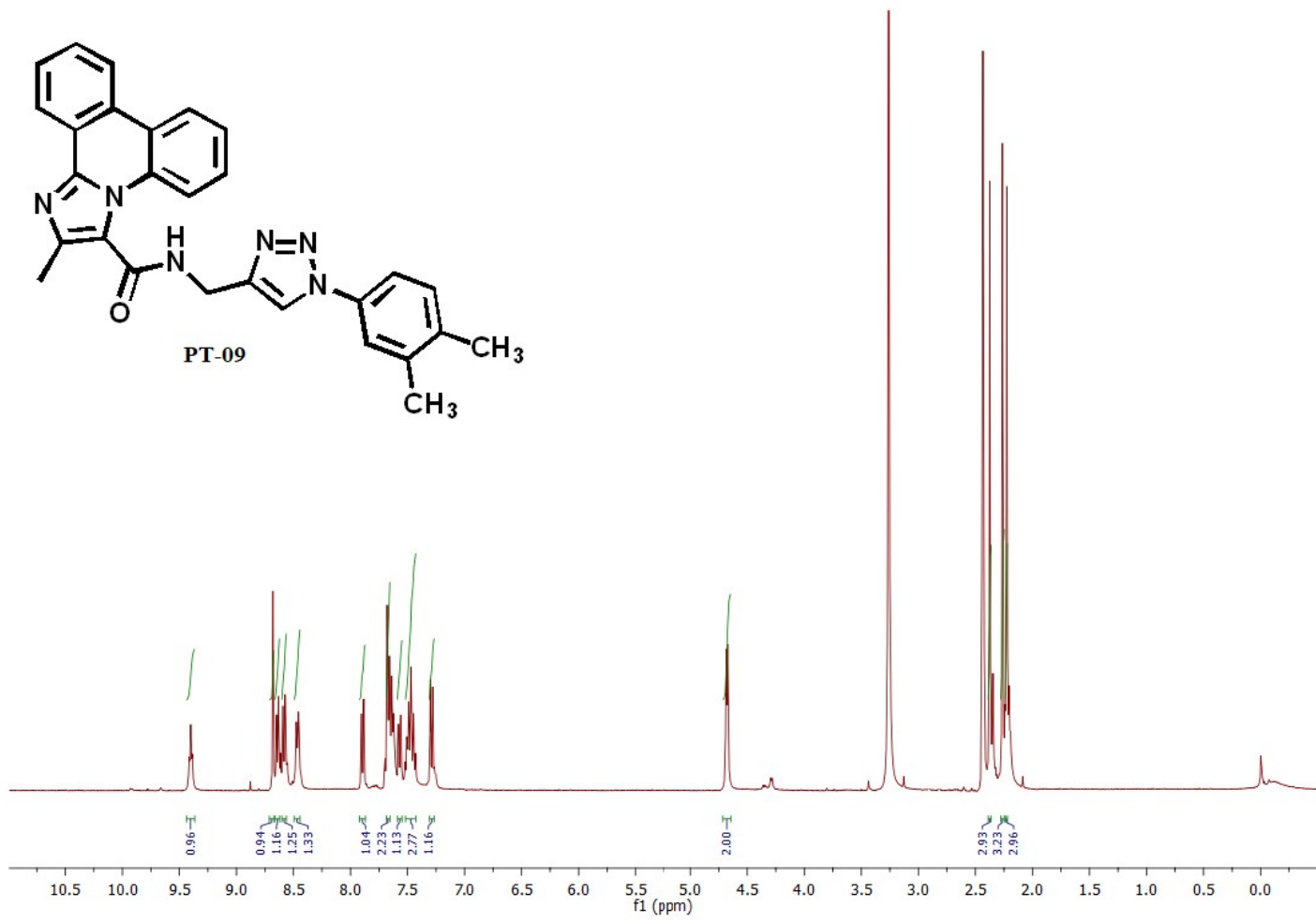
- 162.99
- 157.64
- 145.58
- 142.31
- 139.81
- 138.80
- 137.07
- 130.39
- 129.81
- 129.29
- 125.76
- 125.04
- 124.38
- 123.51
- 120.97
- 118.36
- 118.06



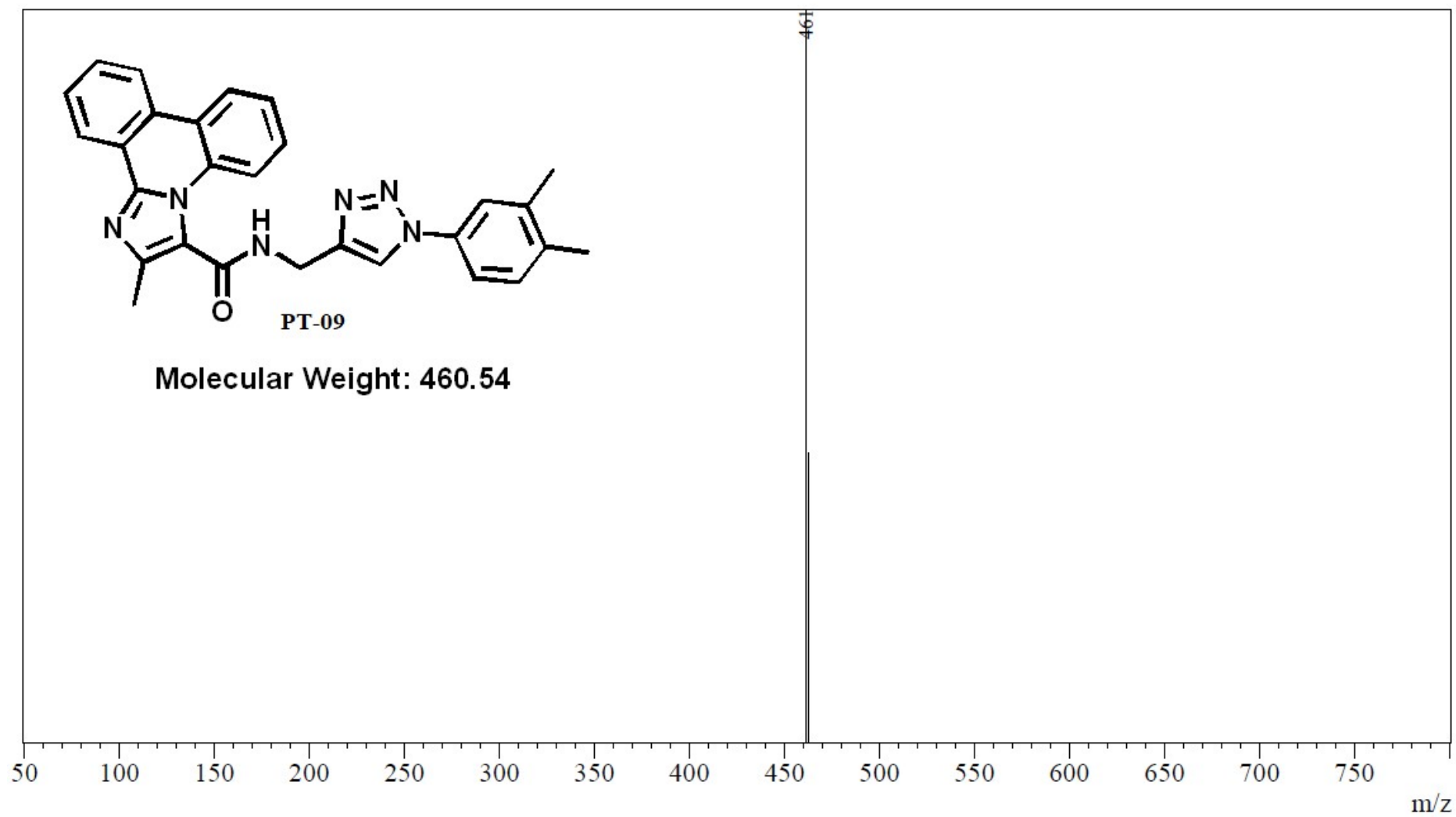
¹³C NMR (101 MHz, DMSO-*d*₆) of PT-08



Mass spectra of compound PT-08

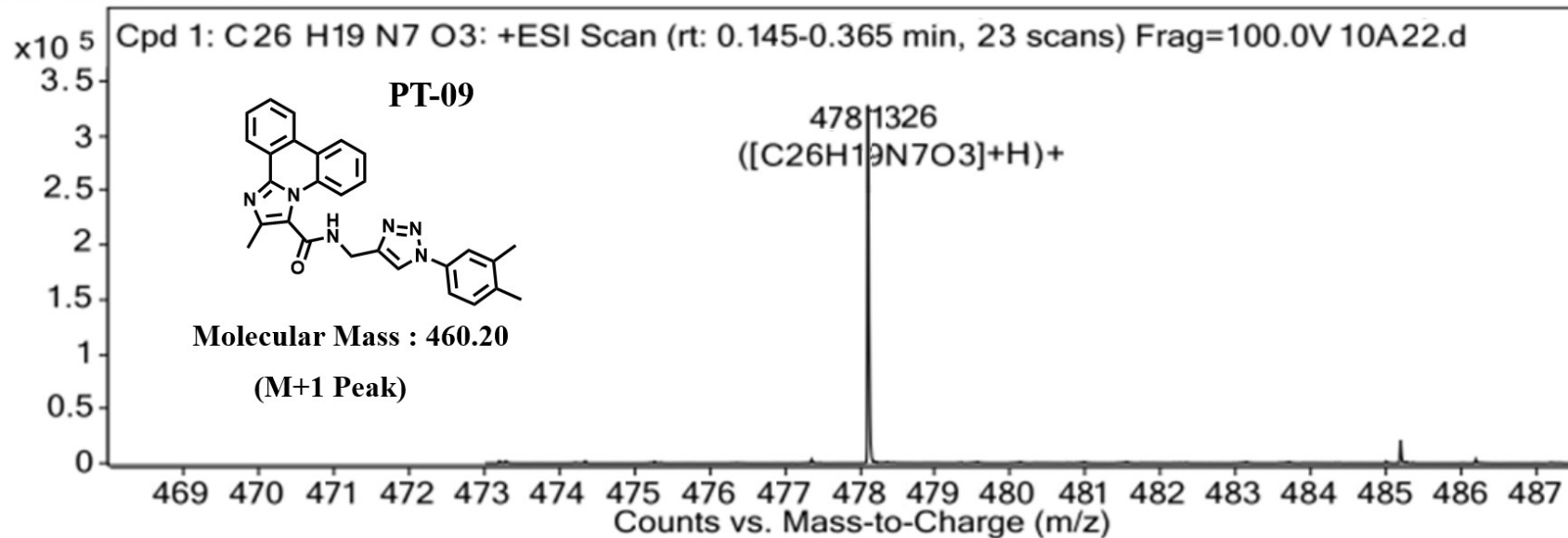


¹H NMR (400 MHz, DMSO-*d*₆) of PT-09

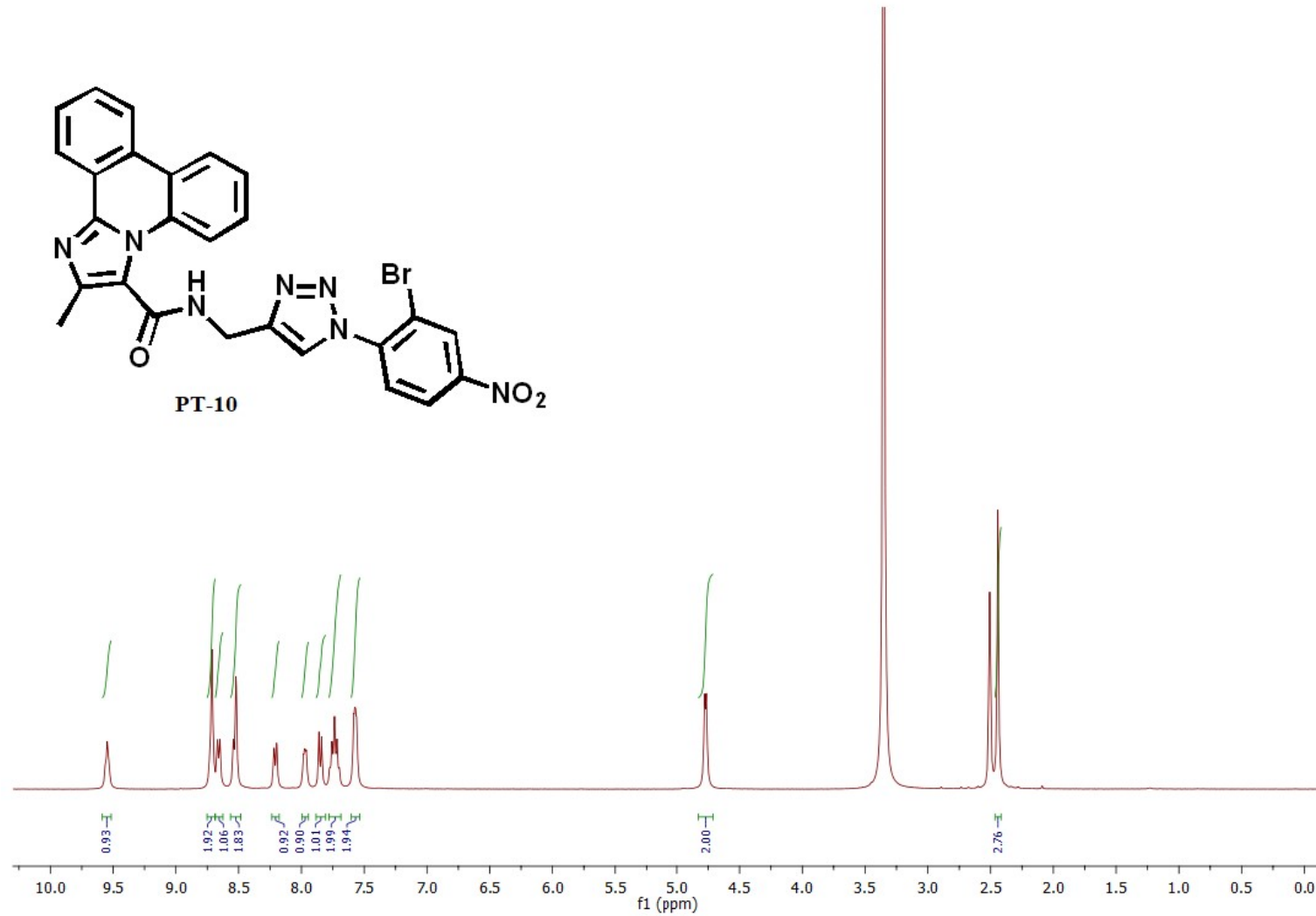


Mass spectra of compound PT-09

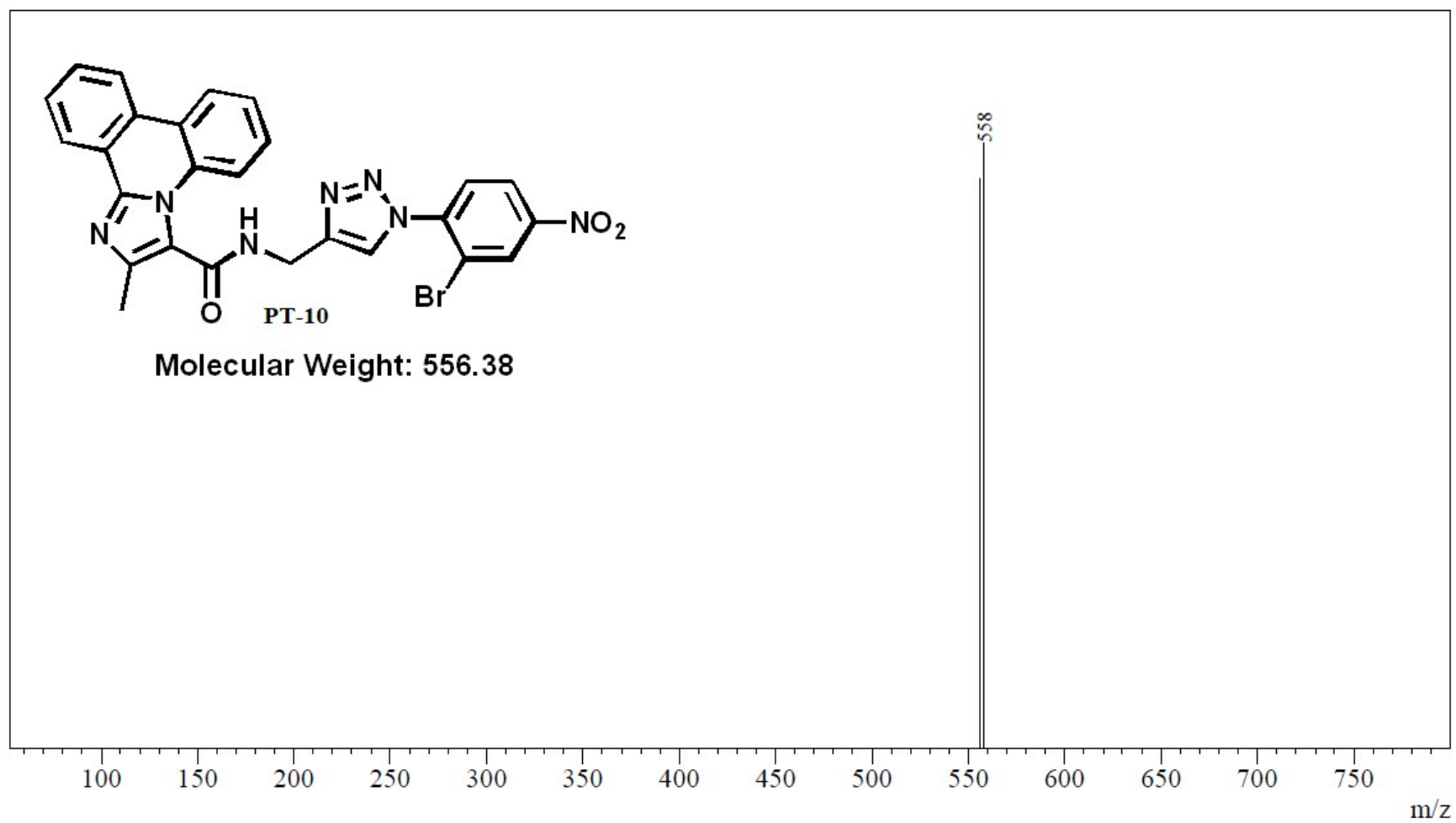
MS Zoomed Spectrum



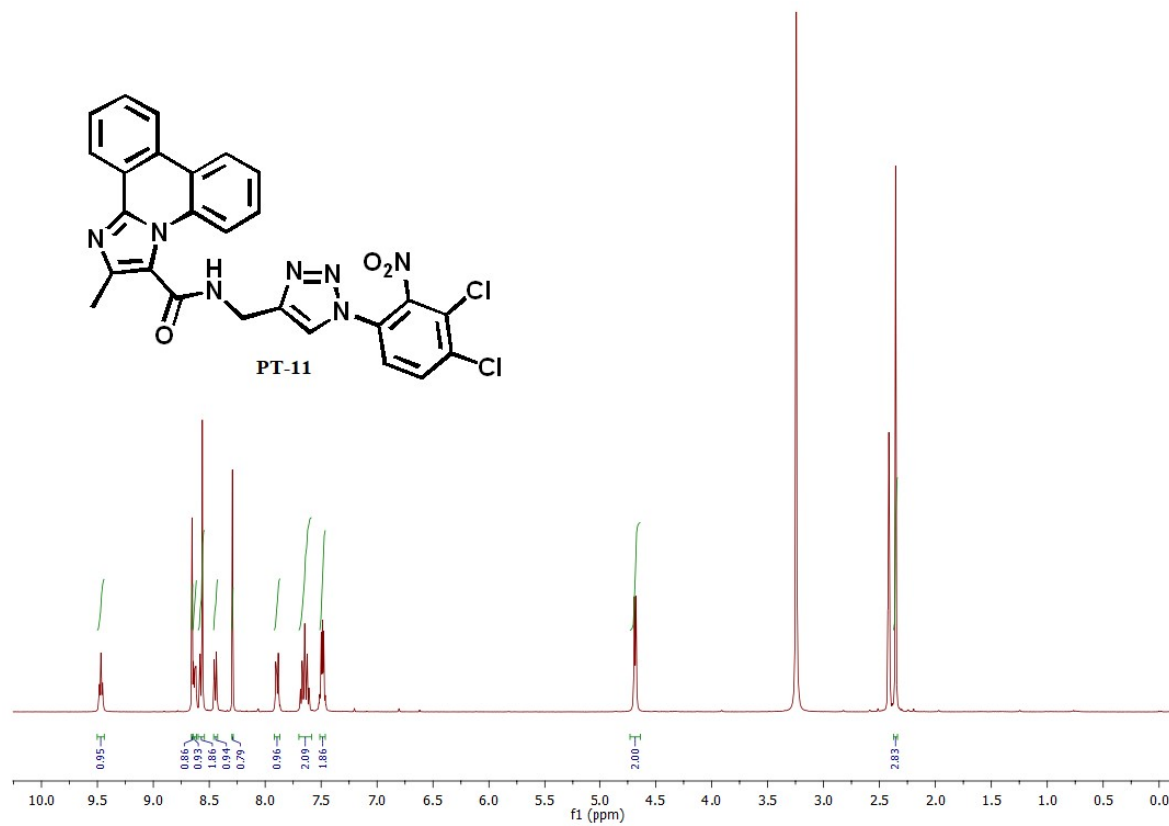
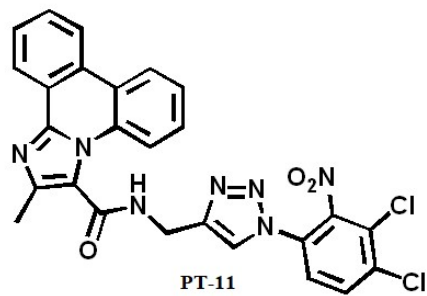
HRMS Mass spectra of compound PT-09



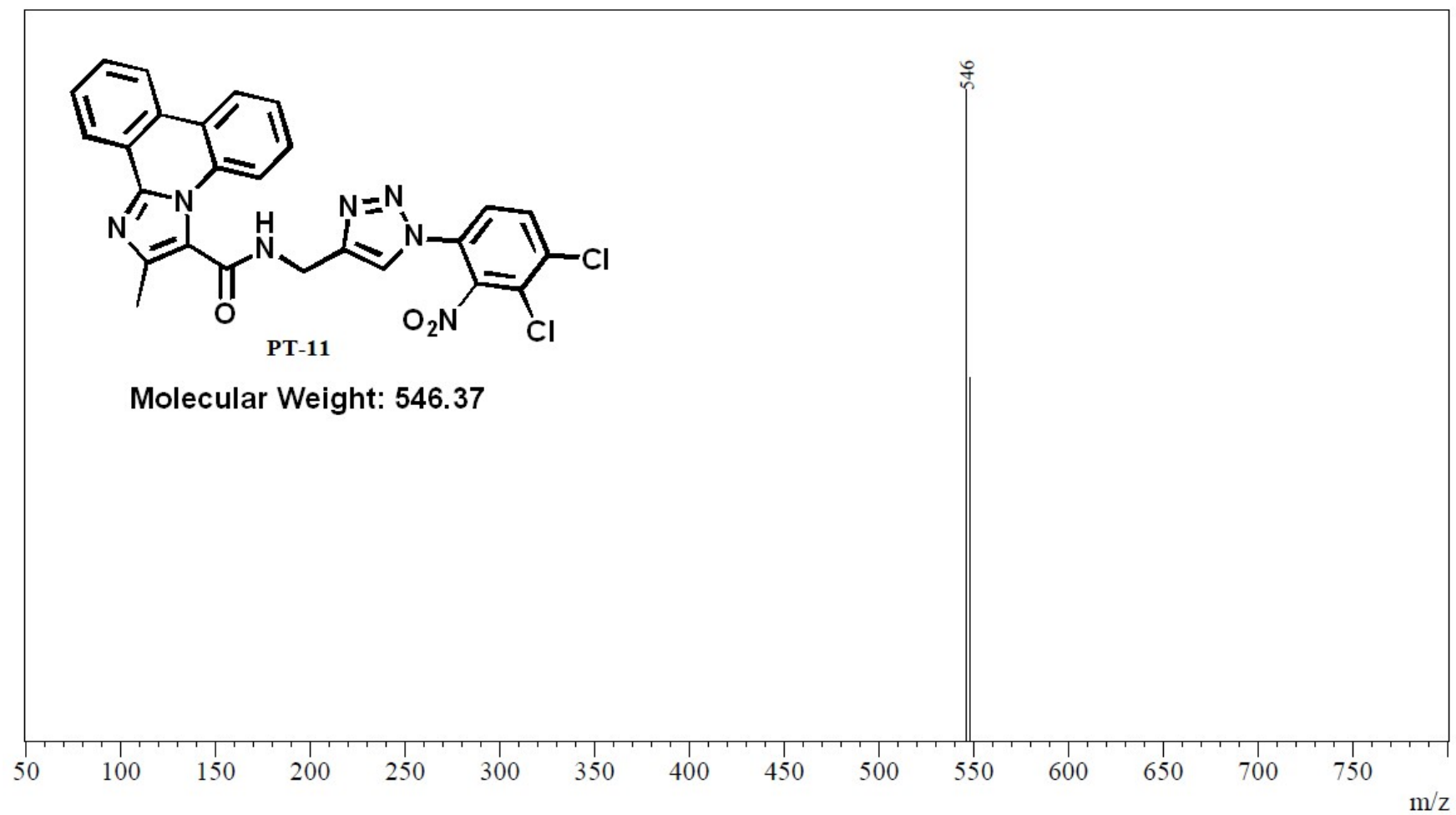
¹H NMR (400 MHz, DMSO-*d*₆) of PT-10



Mass spectra of compound PT-10



^1H NMR (400 MHz, $\text{DMSO-}d_6$) of PT-11



Mass spectra of compound PT-11

References:

1. Schrodinger, 2019-1. (n.d.). *Schrödinger Release 2019-1: LigPrep, Schrödinger, LLC, New York, NY, 2019.*
2. Burley, S. K., Berman, H. M., Bhikadiya, C., Bi, C., Chen, L., Di Costanzo, L., Christie, C., Dalenberg, K., Duarte, J. M., Dutta, S., Feng, Z., Ghosh, S., Goodsell, D. S., Green, R. K., Guranović, V., Guzenko, D., Hudson, B. P., Kalro, T., Liang, Y., Zardecki, C. (2019). *Nucleic Acids Research*, **47(D1)**, D464–D474.
3. *Schrödinger Release 2019-1: LigPrep, Schrödinger, LLC, New York, NY, 2019.*, n.d..
4. Mark, P., & Nilsson, L. (2001). *Journal of Physical Chemistry A*, **105(43)**, 9954–9960.
5. Jorgensen, W. L., Maxwell, D. S., Tirado-Rives, J. (1996). *Journal of the American Chemical Society*, **118(45)**, 11225–11236.
6. Berne, M. T. and B. J. G. J. M. (1993). Reversible multiple time scale molecular dynamics. *The Journal of Physical Chemistry*, **97(51)**, 13429–13434.
7. Cheng, A., & Merz, K. M. (1996). Application of the Nosé–Hoover Chain Algorithm to the Study of Protein Dynamics. *The Journal of Physical Chemistry*, **100(5)**, 1927–1937.
8. Karan Kumar, B., Faheem, Balana Fouce, R., Melcon-Fernandez, E., Perez-Pertejo Yolanda, Y., Reguera, R. M., Adinarayana, N., Chandra Sekhar, K. V. G., Vanaparathi, S., & Murugesan, S. (2021). *Journal of Biomolecular Structure and Dynamics*, 1–16.
9. Kumar, B. K., Faheem, Sekhar, K. V. G. C., Ojha, R., Prajapati, V. K., Pai, A., & Murugesan, S. (2020). *Journal of Biomolecular Structure and Dynamics*, 1–24.
10. Ejalonibu, M. A., Ogundare, S. A., Elrashedy, A. A., Ejalonibu, M. A., Lawal, M. M., Mhlongo, N. N., & Kumalo, H. M. (2021). In *International Journal of Molecular Sciences*, **22**, 13259.
11. Jeankumar, V. U., Reshma, R. S., Vats, R., Janupally, R., Saxena, S., Yogeeswari, P., & Sriram, D. (2016). *European Journal of Medicinal Chemistry*, **122**, 216–231.